ISTANBUL TECHNICAL UNIVERSITY ★ GRADUATE SCHOOL OF SCIENCE ENGINEERING AND TECHNOLOGY

CATALYTIC DEPOLYMERIZATION OF SCOTCH PINE AND LIGNIN IN SUPERCRITICAL ETHANOL

M.Sc. THESIS

CEYLANPINAR ATAY

Department of Chemical Engineering

Chemical Engineering Programme

JUNE 2015

ISTANBUL TECHNICAL UNIVERSITY ★ GRADUATE SCHOOL OF SCIENCE ENGINEERING AND TECHNOLOGY

CATALYTIC DEPOLYMERIZATION OF SCOTCH PINE AND LIGNIN IN SUPERCRITICAL ETHANOL

M.Sc. THESIS

CEYLANPINAR ATAY
(506131009)

Department of Chemical Engineering

Chemical Engineering Programme

Thesis Advisor: Prof. Dr. Filiz KARAOSMANOĞLU

JUNE 2015

İSTANBUL TEKNİK ÜNİVERSİTESİ ★ FEN BİLİMLERİ ENSTİTÜSÜ

SARIÇAM VE LİGNİNİN SÜPERKRİTİK ETANOLDE KATALİTİK DEPOLİMERİZASYONU

YÜKSEK LİSANS TEZİ

CEYLANPINAR ATAY
(506131009)

Kimya Mühendisliği Ana Bilim Dalı

Kimya Mühendisliği Programı

Tez Danışmanı: Prof. Dr. Filiz KARAOSMANOĞLU

HAZİRAN 2015

Ceylanpınar ATAY, a **M.Sc..** student of ITU **Graduate School of Science, Engineering and Technology** student ID **506131009**, successfully defended the thesis entitled **"Catalytic Depolymerization of Scotch Pine and Lignin in Supercritical Ethanol"**, which she prepared after fulling the requirements specified in the associated legislations, before the jury whose signatures are below.

Thesis Advisor :	**Prof. Dr. Filiz KARAOSMANOĞLU** Istanbul Technical University	……..
Jury Members :	**Prof. Dr. Güldem ÜSTÜN** Istanbul Technical University	……..
	Assoc. Prof. Dr. Gülnur MERTOĞLU ELMAS Istanbul University	……

Date of Submission: 4 May 2015
Date of Defense: 1 June 2015

To my dear mother,

FOREWORD

First of all, I would like to thank to my supervisor Prof. Dr. Filiz KARAOSMANOĞLU leads me to step on this road. Without her support, patience and trust, I would not accomplish my graduate thesis. She always encouraged me and enwidened my perspective not only in the academic career but also in professional and social life. I've learned so much from her since I ever met her during my undergraduate study at Istanbul Technical University. More than a supervisior, she has been one of the most important persons in my life. Besides, I would like to thank to Dr. Aslı İŞLER, M.Sc. Güner EKŞİ and M.Sc. Merve Nazlı ERDÖNMEZ BORAND for their endless support and contributions to my thesis.

I would like to express my gratitude and thanks to Prof. Dr. Ir. Emiel J. M. HENSEN accepting me to his biomass research group in Molecular Catalysis (SMK) of Chemistry and Chemical Engineering Department at Eindhoven University of Technology (TU/e). During my thesis research at TU/e, he has always been helpful to me and shared his precious knowledge with me besides creating a comfortable and warm working environment for me both in laboratory and the office. In addition, I would like to thank to my coach Xiaoming HUANG facilitating my research in the laboratory. He has been nice to convey all his knowledge to me specifically on my research topic. I would like to thank all researchers in SMK who were always kind, open-hearted and helpful to me.

I would like to express my gratitude in particular to TUBITAK Marmara Research Center Energy Institute Deputy Director Dr. Osman OKUR, M.Sc. Berrin Engin and Solid Fuel Laboratory staff, facilitating my laboratory studies.

Moreover, I owe Assoc. Prof. Dr. Gülnur ELMAS MERTOĞLU providing my laboratory studies in Faculty of Forestry Products Chemistry and Technology Department at Istanbul University.

At last, I would like to thank to my lovely family, my dear mother Pharmacist Neriman ATAY and my sister İpeknur ATAY. They always stand behind me in good and bad times. I would not be where I am now, without their unquestionable love, encourage and faith on my success.

April 2015

Ceylanpınar ATAY
Chemical Engineer

TABLE OF CONTENTS

Page

TABLE OF TABLES

Page

TABLE OF FIGURES

Page

ABBREVIATIONS

ACS	**:**American Chemical Society
Ag	**:**Silver
Al	**:**Aluminium
BCD	**:**Base Catalyzed Depolymerization
BTX	**:**The mixture of Benzene, Toluene and Xylene
C3	**:**Three Carbon
C5	**:**Five Carbon
C6	**:**Six Carbon
C7	**:**Seven Carbon
C8	**:**Eight Carbon
C9	**:**Nine Carbon
C10	**:**Ten Carbon
C11	**:**Eleven Carbon
C12	**:**Twelve Carbon
C_2H_4	**:**Ethene
C_2H_6	**:**Ethane
C_3H_6	**:**Propane
C_3H_8	**:**Propane
CF	**:**Carbon Fiber
CH_4	**:**Methane
CHP	**:**Combined Heat and Power
Co	**:**Cobalt
CO	**:**Carbon monoxide
CO_2	**:**Carbon dioxide
CO_2-TPD	**:**Carbon dioxide-Temperature Programmed Desorption
Cr	**:**Chromium
Cu	**:**Copper
DOE	**:**The United States Department of Energy
EERE	**:**Energy Office of Biomass
EJ	**:**Exajoules
Fe	**:**Iron
FT-IR	**:**Fourier Transform-Infrared Spectroscopy
GSC	**:**Gas-Solid Chromatography
GC-MS	**:**Gas Chromatography-Mass Spectroscopy
GWh	**:**Gigawatt Hour
H_2	**:**Hydrogen
Ha	**:**Hectare
He	**:**Helium
HDO	**:**Hydrodeoxygenation
IEA	**:**International Energy Agency
IPCC	**:**Intergovernmental Panel on Climate Change
IRENA	**:**International Renewable Energy Agency
ISTD	**:**Internal Standard

ISO **:**International Organization for Standardization
KCl **:**Potassium Chloride
LCF **:**Lignocellulosic Feedstock
LR **:**Lignin Residue
Mg **:**Magnesium
Mo **:**Molybdenum
Mtoe **:**Million tonnes of oil equivalent
NMR **:**Nuclear Magnetic Resonance
NREL **:**National Renewable Energy Laboratory
O **:**Oxygen
OGM **:**The Republic of Turkey General Directorate of Forestry
Pd **:**Palladium
PNNL **:**Pacific Northwest National Laboratory
Pt **:**Platinum
REN21 **:**Renewable Energy Policy Network for the 21st Century
RES **:**Renewable Energy Sources
Rh **:**Rhodium
RSC **:**The Royal Society of Chemistry
Ru **:**Ruthenium
S **:**Sulfur
SEM **:**Scanning Electron Microscopy
SiO_2 **:**Silicon dioxide
SP **:**Scotch Pine
SPR **:**Scotch Pine Residue
TAPPI **:**Technical Association of Pulp and Paper Industry
TCD **:**Thermal Conductivity Detector
THF **:**Tetrahydrofuran
TPES **:**Total Primary Energy Supply
TurkStat **:**Turkish Statistical Institute
UNDP **:**United Nations Development Programme
USDA **:**The United States Department of Agriculture
WBA **:**World Bioenergy Association
WEC **:**World Energy Council
WGBN **:**Wisconsin Grasslands Bioenergy Network
XRD **:**X-Ray Diffraction

CATALYTIC DEPOLYMERIZATION OF SCOTCH PINE AND LIGNIN IN SUPERCRITICAL ETHANOL

SUMMARY

Lignocellulosic biomass is an abundant, renewable and worldwide available source that can be valorized into a wide range of biofuels, biochemicals and biomaterials. Lignocellulosic feedstock (LCF) biorefineries can utilize lignocellulosic biomass by means of various conversion technologies. Of them, catalytic conversion is an efficient technology moves forward with the development of new heterogeneous catalysts. As the technology emerges, not only lignocellulosic biomass but also lignin has been realized as a promising future feedstock for the production of value-added products. Although lignin has been an undervalued component compared to cellulose and hemicellulose and utilized only as a fuel source, the huge potential of its valorization has been a center of attraction. Lignin can be effectively valorized in LCF biorefineries taking the advantage of largely available lignin sourced from the existing industrial processing such as paper and pulp production. As numerous biofuels, biochemicals and biomaterials can be produced from lignocellulosic biomass, particularly lignin is the future green feedstock for the production of aromatics being produced from fossil-based sources. Direct and effective valorization of lignocellulosic biomass as well as lignin is an ideal strategy for the transition from fossil-based chemical industry to a bio-based on in the future.

One-pot catalytic depolymerization is a recent and advancing technology for the valorization of lignocellulosic biomass and lignin. Multifunctional catalysts and supercritical solvents are the key factors for an effective depolymerization. In this study, the depolymerization of Scotch Pine and Protobind 1000 lignin over CuMgAl metal mixed oxides in supercritical ethanol were studied. Effects of CuMgAl metal mixed oxides on catalytic lignin depolymerization were examined by the synthesis of the catalysts with different Cu content and (Cu+Mg)/Al ratio by the calcination of Layered Double Hydroxides (LDHs). CuMgAl metal mixed oxides and their precursors, LDHs were characterized by N_2 physisorption, XRD, CO_2-TPD and SEM techniques. Based on the results, the optimum catalysts for catalytic lignin depolymerization in supercritical ethanol was $Cu_{20}MgAlO_4$ catalyst. Catalytic depolymerization of Scotch Pine was carried out over $Cu_{20}MgAlO_4$ at two different temperature. The effect of temperature on catalytic depolymerization of Scotch Pine was targeted. Also, cellulose as a model compound of lignocellulosic biomass and glucose as a model compound of glucose were catalytically depolymerized over $Cu_{20}MgAlO_4$ at the same operating conditions with Scotch Pine in order to better understand depolymerization mechanism. Depolymerization products of each catalytic depolymerization reactions were analyzed according to gas, liquid and solid phase products. Satisfactory monomer yields were obtained with numerous liquid phase products as the candidates or precursors of various biofuels and/or biochemicals.

SARIÇAM VE LİGNİNİN SÜPERKRİTİK ETANOLDE KATALİTİK DEPOLİMERİZASYONU

ÖZET

Günümüzde artan dünya nüfusuna paralel olarak toplumsal refahın sürekliliğinin sağlanması için dünyada enerji ihtiyacı artmıştır ve artmaya devam edeceği de öngörülmektedir. Fosil kaynakların tükenme tehdidi ile karşı karşıya gelmesi ve iklim değişikliği ile artan çevresel kaygılar, tüm dünyayı yenilenebilir ve sürdürülebilir enerji kaynakları arayışına itmiştir. Tam bu noktada yenilenebilir enerji kaynakları ön plana çıkmıştır. Yenilenebilir enerji kaynakları; güneş, rüzgar, su ve biyokütledir. Özellikle biyokütle doğada bol miktarda bulunan, dünyanın her yerinde kolayca erişilebilen emre amade bir kaynak olması bakımından diğerlerinin arasından sıyrılmıştır. Lignoselülozik biyokütle, sürdürülebilir ve temiz teknolojilerle enerji üretimine olanak veren bir yenilenebilir kaynaktır. İnsanlar ve hayvanlar tarafından yenmemesi bakımından gıda ve yem endüstrileri ile rekabet etmemektedir. Lignoselülozik biyokütle; selüloz, hemiselüloz ve lignin olmak üzere başlıca üç önemli bileşeni içermektedir. Selüloz, glukozların kovalent bağlarla bağlanması ile meydana gelmiş bir karbonhidrattır. Hemiselüloz, beş karbonlu şekerler (pentoz) ve altı karbonlu şekerler (heksoz) ile pektinden oluşan dallanmış bir yapıdadır. Lignin ise; p-kumaril alkol, koniferil alkol ve sinapil alkol olarak adlandırılan üç temel monomerden oluşan karmaşık yapılı, amorf ve üç boyutlu bir polimerdir. Lignin, biyokütleye yapısal destek, sağlamlık ve hidrofobik özellik katan biyokütle bileşenidir.

Lignoselülozik biyokütlenin değerlenmesi, varolan teknolojilerle fosil kaynaklardan elde edilen biyoyakıtların, biyokimyasalların ve biyomateryallerin biyokütleden üretilebilmesi nedeniyle büyük önem kazanmıştır. Biyorafineriler, yukarıda sayılan ürünlerin sürdürülebilir ve eşzamanlı olarak birleşik ve entegre proseslerle biyokütleden üretilebileceği konseptlerdir. Geleneksel rafineriler, fosil yakıtlar kullanarak geniş bir yelpazede yakıt, kimyasal, materyal ve enerji üretirken biyorafinerilerde bunların eşdeğeri biyoyakıtlar, biyokimyasallar, biyorafineriler ve aynı zamanda biyogüç (ısı, soğuk ve biyoelektrik) biyokütleden üretilebilmektedir. Biyorafineriler geleneksel rafinerilerin üretemediği gıda ve yem gibi pek çok ürünü meydana getirebilir. Biyorafineler, geleneksel rafinerilere ve biyokütle kullanan diğer konseptlere kıyasla pek çok avantaja sahiptir.

Biyorafineriler, çeşitli yöntemlerle adlandırılıp sınıflandırılabilir. Örneğin; biyorafinerideki prosesler sonucu elde edilen son ürüne göre biyorafineriler, biyoetanol biyorafinerileri, biyodizel biyorafinerileri, biyogaz biyorafinerileri vb. isimler alabilir. Bunlardan biyoetanol biyorafineleri, biyorafinerilerin en önemlilerinden olup uzun yıllardır birinci kuşak biyoetanol (şekerli ve nişastalı kaynaklardan etanol) ve ikinci kuşak biyoetanol (lignoselülozik kaynaklardan etanol) üretiminde kullanılmaktadır. Modern biyorafineriler ise, dört farklı konsept altında değerlendirilmektedir. Bunlar; Bütün-ekin biyorafinerisi, Yeşil biyorafineri, İki platform biyorafinerisi ve Lignoselülozik hammadde biyorafinerileridir. Modern

biyorafineriler arasından Lignoselülozik hammadde biyorafinerileri, lignoselülozik biyokütlenin uygun dönüşüm teknolojileri ile en verimli ve etkin biçimde değerlendirilebileceği biyorafinerilerdir. Lignoselülozik hammadde biyorafinerilerinde çeşitli termokimyasal ve biyokimyasal yöntemlerle lignoselülozik biyokütle pek çok farklı ürüne dönüştürülebilir. Termokimyasal yöntemler, yakma, birlikte yakma, gazlaştırma, piroliz, karbonizasyon ve sıvılaştırma yöntemlerinden oluşurken biyokimyasal yöntemler fermantasyon, aerobik ve anaerobik sindirme ve enzimatik hidroliz yöntemlerini kapsamaktadır. Lignoselülozik biyokütlenin tüm bileşenlerinin bu yöntemlerle verimli bir biçimde değerlenmesi, biyorafinerilerde üretim maliyetlerinin dengelenmesi bakımından ideal bir strateji olarak karşımıza çıkmaktadır.

Lignoselülozik biyokütle bileşenlerinden selülozun ve hemiselülozun değerlenmesi çok uzun yıllardır bilinmekte ve günümüz biyorafinerilerinde başarılı ile uygulanmaktadır. Ancak lignin, selülozun ve hemiselülozun yanında karmaşık yapısından dolayı ihmal edilmiştir. Günümüz biyorafinerilerinde veya kağıt endüstrisi gibi çeşitli endüstrilerde selüloz ve hemiselülozdan ayrılarak yan ürün olarak elde edilen lignin yalnızca bir yakıt kaynağı olarak kullanılmıştır. Mevcut proseslerde büyük miktarda lignin açığa çıkmakta ve işlenmeden kalmaktadır. Ancak son yıllarda ligninde saklı potansiyel keşfedilmiş, ligninin de tıpkı lignoselülozik biyokütlenin diğer bileşenleri gibi biyoyakıtlara, biyokimyasallara ve biyomateryallere değerlenebileceği ortaya konmuştur. Böylelikle lignin, Lignoselülozik hammadde biyorafinerilerde etkili bir biçimde işlenebilecek önemli bir hammadde haline gelmiştir. Özellikle günden güne gelişen tekniklerle Lignoselülozik hammadde biyorafinerilerde ligninin karmaşık yapısını parçalabilmekte ve ligninden pek çok katma değerli ürün üretilebilmektedir. Bunlardan en önemlisi, halihazırda fosil kaynaklardan üretilmekte olan aromatiklerdir. Lignin, kimya endüstrisinde oldukça önemli bir yeri olan aromatiklerin üretiminde geleceğin yeşil kaynağı olarak nitelendirilmektedir. Ligninin ve lignoselülozik biyokütlenin değerlenmesi ile bu ve benzeri ürünler, fosil kökenli eşdeğerlerinin ikameleri olarak üretilebilmektedir. Böylelikle gelecekte fosil-tabanlı kimya endüstrisinden biyo-tabanlı kimya endüstrisine geçiş hedeflenmektedir.

Lignoselülozik hammadde biyorafinerileri, lignoselülozik biyokütle ve ligninin değerlenmesi amacıyla çok çeşitli dönüşüm yöntemleri kullanabilmektedir. Katalitik dönüşüm, günümüzde özellikle çok fonksiyonlu ve etkin heterojen katalizörlerin geliştirilmesi ile oldukça başarılı bir yöntem olarak karşımıza çıkmaktadır. Katalitik dönüşümle uygun katalizörler kullanılarak istenilen ürünlere daha kolay ulaşılabilmektedir. Katalitik dönüşüm yöntemlerden Tek aşamalı (tek kapta) katalitik depolimerizasyon, günümüz biyorafinerilerine kolaylıkla entegre edilebilecek yeni ve gelişmekte olan bir katalitik dönüşüm tekniğidir.

Tek aşamalı katalitik depolimerizasyonla, ligninin ve lignoselülozik biyokütlenin değerlenmesi doğrudan ve etkili bir biçimde gerçekleştirilebilir. Katalizör ve solvent seçimi, katalitik depolimerizasyona etki eden önemli faktörlerdendir. Poröz metal oksit katalizörler, hidrojenleme ve hidrojenoliz reaksiyonlarını yürüterek katalitik depolimerizasyonun verimliliğini artırmaktadır. Bakır tabanlı poröz metal oksitler, lignoselülozik biyokütleyi ve lignini süperkritik ortam koşullarında deoksijenize sıvı ürünlere dönüştürmekte etkili katalizörlerdendir. CuMgAl karma metal oksitler, doğada bol bulunur ve ucuz metallerden elde edilebilmeleri bakımından diğer karma metal oksitlerin yanında önem kazanmıştır ve katalitik depolimerizasyonda oldukça

yaygın olarak kullanılmaktadır. Bakır, alüminyum ve magnezyum elementleri ile birlikte kullanıldığında düşük molekül ağırlıklı alkollerin dehidrojenasyonu, alkollerin carbon-carbon birleşme reaksiyonları gibi reaksiyonları teşvik ettiği bilinmektedir.

Katalitik depolimerizasyonda bir diğer önemli nokta, uygun solvent seçimidir. Süperkritik etanol, CuMgAl karma metal oksitlerle depolimerizasyonda oldukça etkili bir solventtir. Etanol, yenilenebilir kaynaklardan elde edilebilmesi, göreceli olarak düşük kritik noktaya sahip olması açısından oldukça kullanışlı bir solventtir. Etanol, katalitik depolimerizasyon ortamına hidrojen veren bir solvent olmasının yanında, yüksek derecede reaktif olan fenolik ara ürünleri dengede tutarak bir kapama ajanı görevi üstlenmekte ve repolimerizasyonu baskılamaktadır. Sözü geçen bu avantajları nedeniyle süperkritik etanol, su, metanol vb. diğer solventlerden daha iyi sonuçlar ortaya koymuştur.

Bu çalışmada, Sarıçam ve Protobind 1000 ligninin CuMgAl karma metal oksit katalizörler üzerinde süperkritik etanolde katalitik depolimerizasyonu çalışılmıştır. Protobind 1000 ligninin süperkritik etanolde katalitik depolimerizasyonu deneylerinde CuMgAl karma metal oksit katalizörlerin katalitik depolimerizasyon üzerinde etkilerinin ortaya konulması amaçlanmıştır. Bu amaçla, iki farkı grup CuMgAl karma metal oksit katalizörler, bunların öncüleri olan Çift Tabakalı Hidroksitlerin kalsinasyonu yoluyla sentezlenmiştir. İlk grupta farklı bakır içeriklerine ve ikinci grupta farklı (Cu+Mg)/Al oranlarına sahip CuMgAl karma metal oksit katalizörler üretilmiştir. Farklı bakır içeriklerine sahip (ağırlıkça %0, %10, %20 ve %40 bakır içeren) katalizörler, $MgAlO_4$, $Cu_{10}MgAlO_4$, $Cu_{20}MgAlO_4$ ve $Cu_{40}MgAlO_4$ olarak isimlendirilirken farklı (Cu+Mg)/Al oranlarına sahip (iki, üç, dört ve altı oranlarına sahip) katalizörler $Cu_{20}MgAlO_2$, $Cu_{20}MgAlO_3$, $Cu_{20}MgAlO_4$ ve $Cu_{20}MgAlO_6$ olarak isimlendirilmiştir.

CuMgAl karma metal oksitler ve bunların öncüleri olan Çift Tabakalı Hidroksitler, öncelikle N_2 Fiziksel Adsorpsiyonu, X-Işını Kırınım Yöntemi (XRD) ve CO_2 Sıcaklık Programlı Desorpsiyon (CO_2-TPD) teknikleri gibi farklı tekniklerle karakterize edilmiştir. Karakterizasyonun ardından bu katalizörler, Protobind 1000 ligninin süperkritik etanolde katalitik depolimerizasyonunda test edilmiştir. Gerek karakterizasyonu sonuçları gerekse katalizörlerin katalitik depolimeriasyon üzerindeki etkileri incelendiğinde çalışılan katalizörler içerisinde en iyisinin $Cu_{20}MgAlO_4$ olduğu belirlenmiştir. Sarıçamın süperkritik etanolde katalitik depolimerizasyonu ise, $Cu_{20}MgAlO_4$ kullanılarak gerçekleştirilmiştir. Sarıçamın katalitik depolimerizasyonu iki farklı sıcaklıkta yürütülerek sıcaklığın etkisi incelenmiştir. Ayrıca, lignoselülozik biyokütlenin bir model bileşeni olarak selüloz ve selülozun model bileşeni olarak glukoz da Sarıçam katalitik depolimerizasyon koşullarında $Cu_{20}MgAlO_4$ kullanılarak depolimerize edilmiştir.

Son olarak tüm katalitik depolimerizasyon reaksiyonlarına ait ürünler gaz faz, sıvı faz ve katı fazda elde edilmelerine göre farklı analiz yöntemleri ile analiz edilmiştir. Gaz faz ürünler, Gaz-Katı Kromatografisi (GSC) kullanılarak niteliksel ve niceliksel olarak tanımlanırken sıvı faz ürünleri Gaz Kromatografisi Kütle Spektroskopisi (GC-MS) yöntemi ile belirlenmiştir. Gaz fazda elde edilen ürünler; CH_4, C_2H_6, C_2H_4, C_3H_8, C_3H_6, CO, CO_2 ve H_2'dir. GS-MS ile sıvı faz ürünlerin analizi sonuçları, katalitik depolimerizasyon sonucu başlıca alkol, aldehit, alkan, alken, ester, eter ve ketonlar olmak üzere yedi farklı ürünün ortaya çıktığını göstermiştir. Bu ürünlerden alkoller ve esterler, en çok tespit edilen ürünlerdir. Çalışmada, Sarıçamdan elde edilen sıvı faz ürünleri ile selüloz ve glukozdan elde edilen ürünler karşılaştırılmıştır. Ayrıca, ürün

seçiciliğine göre sıvı fazda elde edilen ürünler oksijen içeriklerine göre dört farklı gruba ayrılmıştır. Bu ürünler, oksijen içeren (+O) ve oksijen içermeyen (-O) hidrojenlenmiş halkalı bileşikler ile oksijen içeren ve oksijen içermeyen aromatiklerdir. Bu ürünlere bakılarak katalitik lignin depolimerizasyonunda kullanılan katalizörlerin dehidrojenleme ve deoksijenleme yetenekleri kıyaslanmıştır. Sarıçamın ve Protobind 1000 ligninin katalitik depolimerizasyonu sonucu sıvı fazda tatmin edici monomer verimleri elde edilmiştir. Sıvı fazda elde edilen çok sayıda monomer, pek çok biyoyakıtın ve/veya biyokimyasalın öncüsü olarak ya da yakıt katkısı olarak kullanabilecek ürünlerdir. Süperkritik etanolde katalitik depolimerizasyon yöntemi ile lignoselülozik biyokütle ya da sadece lignin kullanılarak kimya endüstrisi için oldukça değerli ürünler elde edilebilmektedir. Bu çalışma; lignoselülozik biyokütle ve ligninden, fosil kökenli yakıt ve kimyasalların biyo-kökenli alternatiflerinin üretilebileceğini ortaya koymaktadır.

1. INTRODUCTION

Energy is an indispensible need for humanity to continue its life. As the energy demand on earth has an increasing trend with the contributions of the growing population and changing life style of people, the energy sources become one of the most important issues worldwide. In the 21st century, the main energy sources are fossil, nuclear and renewable energy sources. Fossil energy sources comprises coal, crude oil, and natural gas, while renewable energy sources (RES) are solar, wind, biomass and water (hydro, geothermal and ocean (tidal, currents, wave, the temperature gradients and salinity gradients)) [1, 2].

Global primary energy production was 552 Exajoules (EJ) in 2011, shown in Figure 1.1 and dominated by fossil energy sources. Crude oil is accounted for 32% of the total energy production worldwide and coal, natural gas, and renewables are accounted for 29%, 21%, and 13% respectively [3].

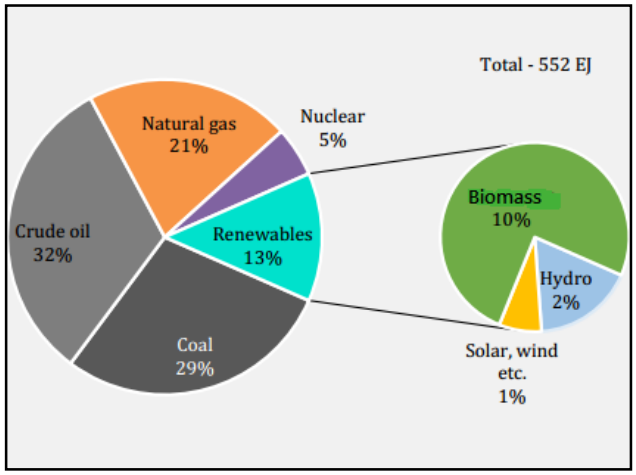

Figure 1.1: Global primary energy production of energy sources in 2011[3]**.**

Since the beginning of the Industrial Era, crucial amount of the world's energy is obtained from fossil fuels, however this brings about environmental problems. Fossil fuels are primarily responsible for the greenhouse gas emissions that triggers the climate change as it is indicated in the Fifth Assessment Report of Intergovernmental Panel on Climate Change (IPCC). According to the mentioned report, the atmospheric

concentration of CO_2 which is known as the primary greenhouse gas emitted on earth is anticipated to rise due to the dependence on fossil fuels for energy production [4].

Although the main drivers for the energy production are fossil energy sources, they will face with the problem of depletion in the future due to their finite reserves. In addition, the unevenly distributed fossil energy sources and concerns about their environmental effects lead the world to new and renewable ways to produce energy [5]. Also, world is looking for sustainable and available sources to supply its growing energy demand as well as to undertake the production of the industrial fuels, chemicals and materials.

At this point, renewable energy sources are suggested as good substitutes of fossil energy sources. Renewable energy sources have potential to reduce the world's dependence on fossil fuels in an environmentally friendly way [6]. Because renewable energy sources can introduce a good solution to the problems arising from fossil fuels [7]. Particularly they are highlighted as one of the most efficient and effective solutions for environmental problems [8]. They reduce the health and environmental impacts associated with fossil and nuclear energy, mitigate greenhouse gas emissions, improve energy security [7, 9]. Renewable energy sources can enhance diversity, energy access and affordability [10]. Also they can be associated with further acquirements by creating new jobs and reducing poverty. Renewable energy sources can act as a bridge provide a transition to the sustainable economy considering their potential to produce energy [7, 9].

According to Renewable Energy Policy Network for the 21 Century (REN21) Global Status Report declared in 2014, renewable energy provided an estimated 19% of global final energy consumption in 2012 and continued to grow in 2013. Modern renewables accounted for approximately 10% of the total share in 2012 and the remainder was belonged to traditional biomass which refers to fuelwood, charcoal, and agricultural residues used for household cooking, lighting and space-heating in developing countries. By early 2014, at least 144 countries had renewable energy targets and 138 countries had renewable energy support policies in place [9, 11].

Biomass is the prominent renewable and sustainable source among other renewable sources. Biomass can be utilized for energy generation, energy generated from biomass is defined as 'biomass energy'. Total share of biomass energy in the global primary energy production in 2011 can be seen as 10% in Figure 1.1. Biomass has the

technical potential to produce electricity, heat, cold, and bio-based products including biofuels (transportation fuels), biochemicals and biomaterials [12].

Biomass is considered the only sustainable source of organic carbon available on earth compared to fossil fuels so that while electricity can be generated by all renewable energy sources, the production of biofuels and bio-based products as alternatives to the their fossil-based counterparts mainly depends on biomass [13]. It is stated that the development of a sustainable industrial society, the effective management of greenhouse gas emissions and energy independence can be maintained by the transition from petroleum to biomass [14]. As the world's focus is mostly on the low carbon economy comprising all sectors and cleaner production, biomass is a significant candidate to meet the global targets. Especially, biomass valorization meaning the conversion of biomass into biofuels and value-added bio-based products is anticipated to contribute to a sustainable chemical industry in the future. A wide spectrum of biomass sources can be valorized to produce biofuels, biochemicals and biomaterials.

Biomass is mainly divided into two broad categories: woody and non-woody biomass. Woody biomass is the most important source both for the production of energy and bio-based products especially for biofuels. Woody biomass is an abundant and readily available source worldwide. Also it is an inedible source and thus it does not compete with the food industry. Woody biomass is a carbon-neutral source, in case of being utilized in a sustainable and steady manner. Because it can capture the carbon dioxide in the atmosphere while it grows and this process is considered to offset the amount of carbon dioxide released due to the conversion of biomass into energy [15]. Lately this vast potential of woody biomass as a source gains attention and the new researches have focused on woody biomass valorization. Woody biomass can be utilized to produce heat, steam and electricity as well as can be converted to solid, liquid and gaseous biofuels, to biochemicals and biomaterials [16].

The largest component of woody biomass is lignocellulose. Lignocellulose is composed of three main biopolymers which are cellulose, hemicellulose, and lignin. All biomass components are valuable for the production of biofuels and/or bio-based products, however lignin has a remarkable potential besides cellulose and hemicellulose. This potential has been lately gained attraction of both researchers and industry.

Traditionally, lignin is considered as a waste material arised from existing processes and as a low value by-product, which is converted directly into energy by combustion [17]. Still, the majority of lignins are utilized to produce heat and electricity by combustion [18]. Nevertheless, a lignin produced as a by-product in the biorefineries, paper and pulp mills, is the most promising feedstock for the production of many value-added products [19, 20]. Lignin can be valorized into biochemicals, biofuels, and biomaterials via different technologies likewise biomass. Lignin valorization is significant to improve the long-term, economic viability of biomass, to provide efficient and cost effective biorefineries and to construct a sustainable bio-based economy [18, 21]. Importantly, lignin is the only available and renewable source of aromatic compounds [20, 22, 23], so it is anticipated to be "a future green source of aromatic compounds (e.g. phenols)" [18]. Lignin valorization is still an immature technology for industrial application and should be developed. Although many studies focus on the lignin valorization, further studies are required to better understand both the complex lignin structure and the possible conversion technologies.

Biomass conversion technologies basically composed of biochemical and thermochemical conversion technologies can convert cellulose, hemicellulose and lignin. However, the pursuit of effective and efficient technologies engender new studies regarding biomass valorization. Novel technologies are being discovered every day. Among these technologies, catalysis is an attractive technology recently makes headway thanks to heterogeneous and homogeneous catalysts. Catalytic depolymerization is one of the catalysis techniques, found quite promising due to its ability to convert biomass or lignin in one-pot (one-step) fashion.

All in all, catalytic depolymerization of woody biomass and lignin is aimed in this study. With this regard, Turkish-origin Scotch Pine (*Pinus sylvestris* L.) as a woody biomass source and pure Protobind 1000 lignin catalytically depolymerized in supercritical ethanol. CuMgAl mixed oxide catalysts, one of the prominent heterogeneous catalysts, are used to ensure a successful depolymerization. In addition, a group of $CuMgAlO_x$ mixed oxide catalysts are tested in order for the evaluation of their effect on catalytic depolymerization.

2. THEORETICAL STUDY

In theoretical study, main topics will be presented are biomass energy and statistics, biomass sources, biorefineries, and Scotch Pine and literature review prior to experimental study section.

2.1. Biomass Energy and Statistics

Biomass is an abundant, competitive and environmentally strategic energy source among other sources. It exists in the biosphere which is a thin surface layer of earth. Although it constitute a small fraction of the total mass of the earth, its energy storage capacity is known to be huge. The energy storage replenishes by the flow of energy from the sun through the photosynthesis and this solar energy stored is equivalent to almost seven times the world's total primary energy consumption [24].

Biomass term contains both plant biomass and animal biomass. Plants use solar energy through photosynthesis and convert carbon dioxide into biomass in the presence of chlorophyll and water. In this mechanism, the solar energy is converted to chemical energy and stored in plant biomass. Animals grow by taking food from plant biomass. Plant biomass is eaten by animals and converted into animal biomass. Since this process bring in reproducibility to the biomass, biomass is identified as renewable [25, 26].

Recently, utilization of woody biomass has gain much attention. Besides being an abundant and cheap source, woody biomass does not compete with the food industry and does not fall under the argument regarding the usage of food as feedstock. Biomass feedstock can recycle in a short time whereas it takes millions of years for fossil fuels to be formed [25]. Taking into account the long rotation period of fossil fuels, biomass is seen as an important source for sustainable and stable supply of energy [15].

Energy derived from biomass is defined "biomass energy" , while biomass energy is captured by "biomass energy technologies", which make biomass energy available in useful forms. Biomass, can be produced by minimal requirements, are suitable to produce power, fuels as well as heat and cold. Traditionally, biomass has been utilized

through direct combustion and this process is still widely used in many parts of the world, however modern biomass utilization depends on the conversion technologies [27].

Heat and cold, biopower (bioelectricity) and transportation sectors are the main sectors that utilize biomass energy [28]. In 2013, biomass supplied almost 57 EJ, which means biomass represents 10% of global annual primary energy consumption. Traditional biomass had 60% of the total while the remainder was belonged to biomass energy including solid, liquid, and gaseous biofuels [9]. Global biomass energy supply regarding the different regions of the world is shown in Figure 2.1. Global biomass energy supply has steadily increased in the period of 2000-2010, as the share of biomass energy in the total energy supply has remained stable [29].

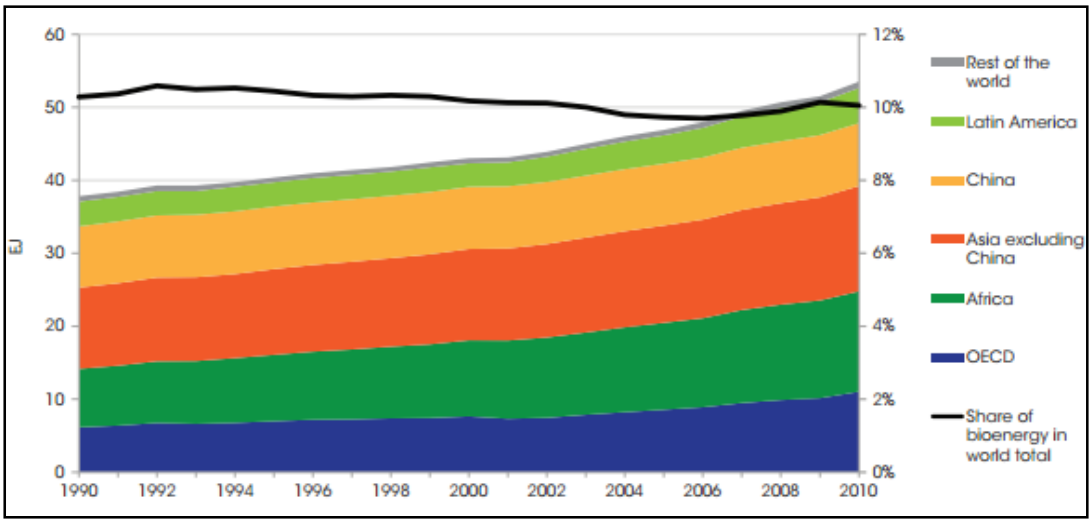

Figure 2.1: Global biomass energy supply (EJ) and its share in total energy supply (%) [29].

Heat and cold sector has a greater share compared to biopower and transportation. In 2011, biomass energy contributed to gross final energy consumption with 48.5 EJ and heat and cold sector is accounted for 92% of this consumption, shown in Figure 2.2 [3]. In 2013, the dominant region for the heat and cold generation from biomass was Europe. The leading countries are Germany, Sweden and Finland.

Biopower sector is also promising for the utilization of biomass energy. 405 TWh of the world's electricity is generated from biomass in 2013. The top bioelectricity producers are the United States and Germany [8]. While power generation from biomass is important for OECD countries, China and Brazil are stated to become powerful producers recently [28]. The U.S. generated 60 TWh as a leader producer

and the EU generated 79 TWh of electricity with an increase of 7.9% compared to 2012.

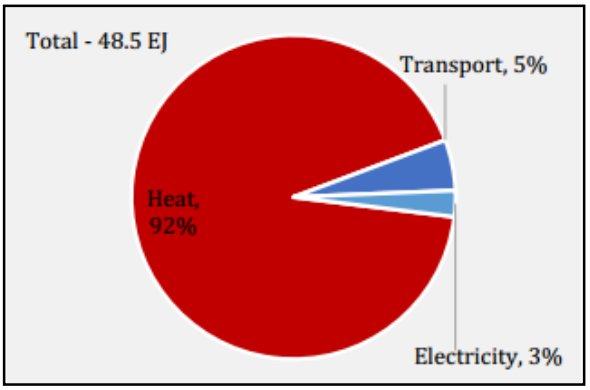

Figure 2.2 : Gross final energy consumption of biomass energy in 2011 [3].

As for transportation sector, biofuels production reached to 116.6 billion litres in 2013. Bioethanol and biodiesel are the primary biofuels produced worldwide. The U.S. was the leading country for bioethanol production with a production of approximately 50 billion litres in 2013. This country is followed by Brazil (25.5 billion litres), China (2 billion litres), and Canada (1.8 billion litres). In addition, the top regional biodiesel producer was the EU in 2013. EU's share for biodiesel production has not changed significantly for years and remained approximately 42%. The U.S., Germany and Brazil are the primary countries for biodiesel production [9].

In Turkey, biomass energy accounted for two-thirds of the renewable energy supplied is mostly used for the household purposes in rural areas. Heating, cleaning and cooking are indicated as the main needs to use biomass energy [30]. Turkey has a significant potential of biomass energy. Total biomass energy potential of Turkey is stated as 32 million tonnes of oil equivalent (Mtoe), but the recoverable amount of the total biomass energy potential is about 17 Mtoe [31]. It is indicated that the amount of production of biomass will be 52.5 Mtoe in 2030 [32].

Considering the biomass energy potential, biomass energy is anticipated to play an important role in the primary energy supply in the future. The total primary energy supply (TPES) of Turkey, shown in Figure 2.3 was 114.5 Mtoe in 2011 and biomass energy supplied was 4.52 Mtoe, which compensate almost 4% of the total primary energy supply [2]. Regarding the statistical data in 2009, biomass utilized for household purposes is accounted for approximately 5.9% of TPES of the same year [33].

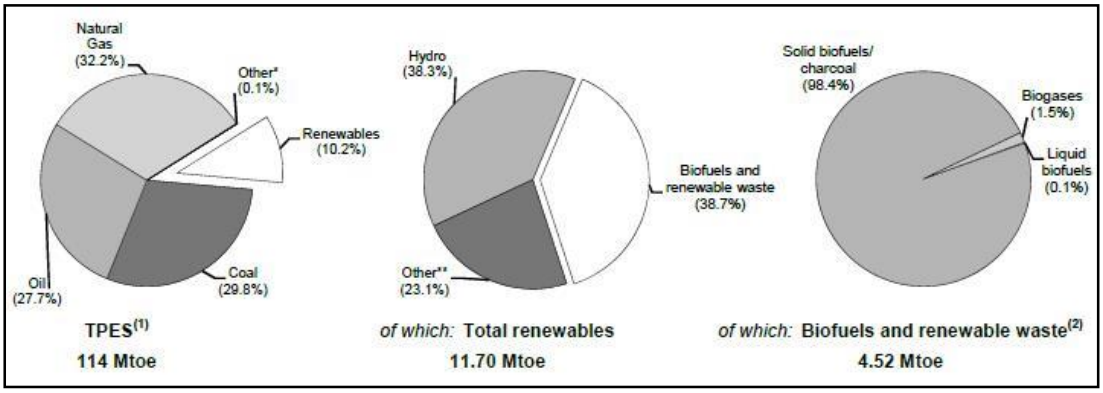

Figure 2.3: Total primary energy supply of Turkey and share of biomass energy in 2011 [2].

According to UNDP (United Nations Development Programme), in Turkey biomass has 16,000 MW of technical potential for installed renewable electricity capacity [34]. For instance, 469.2 Gigawatt Hour (GWh) of electricity is produced from animal and vegetal waste in 2011 with an increase of 2.45% compared to previous year [35].

To sum up all these statistical information of biomass energy, a significant amount of biomass are utilized for the production of heat/cold, electricity and biofuels worldwide. Each country or region prefers to supply energy from different combinations of a wide range of biomass sources. In the following section, biomass sources are explained.

2.2. Biomass Sources

Biomass source types can be divided into two broad categories: woody biomass and non-woody biomass. However, there is no clear-cut division between these sources [36]. Woody biomass include forest residues, energy forests, wood processing industry residues, however non-woody biomass is composed of agricultural crops, herbaceous crops or animal wastes and so on. Woody biomass mostly comprises lignocellulose in its structure, but the non-woody biomass comprises not only lignocellulose but also oil, sugar, starch. Biomass types and components are shown in Figure 2.4.

The main components of the structure of the woody biomass are classified as cell wall components, extractives, and ash [25]. Lignocellulose is the main component of cell wall and the largest component of the biomass [25, 36]. Extractives include proteins, lipids, free sugars and starch. Ash contains the inorganic molecules of the biomass [25].

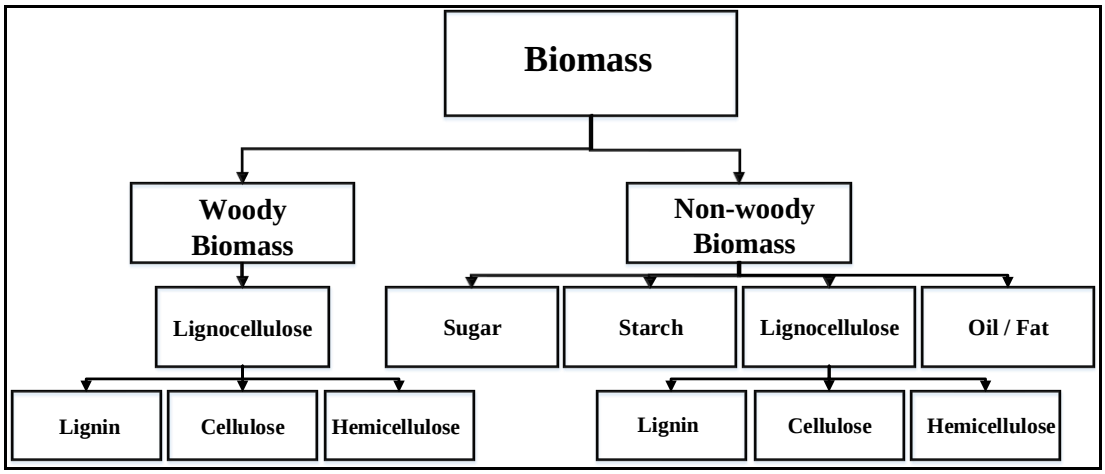

Figure 2.4: Biomass types and components (Adopted from [37]).

Lignocellulose is typicaly composed of three important biopolymers: cellulose, hemicellulose, and lignin. While carbohydrates (mainly cellulose and hemicellulose fibers) are liable for the strength of plant structure, lignin is the component that holds together the fibers. Cellulose is a carbohydrate polymer composed of glucoses linked by covalent bonds [38]. It comprises about 45% of woody biomass [39]. Glucoses constitute long chains and these long chains come together through hydrogen bonding and form fibers, and this well ordered structure gives the cellulose its crystallinity. Hemicellulose is composed of different pentose and hexose sugars (arabinose, galactose, glucose, mannose, and xylose) and pectin. Compared to cellulose, hemicellulose is a branched material due to incorporated compounds, such as acetyl and it is not crystalline [38]. Hemicellulose comprises about 25-35% of the dry weight of wood and agricultural residues [24]. Average distribution of these biopolymers in several representative feedstocks (wt%) is given in Figure 2.5 [16].

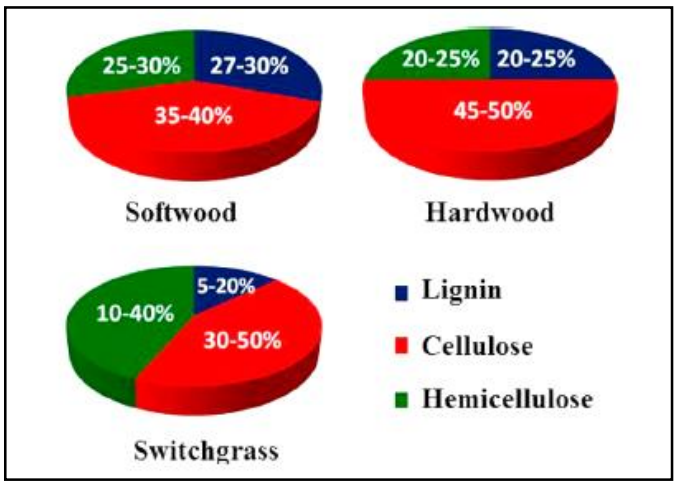

Figure 2.5: Average distribution of biopolymers in lignocellulosic biomass [16].

The second abundant component on earth is lignin following cellulose [40]. About 15-30% of the biomass is lignin that has a function of holding the cellulose and hemicellulose together [38]. Lignin, which is the most important component of biomass is explained in detail in the following section of this thesis.

2.2.1. Lignin

Lignin is a complex, amorphous and three-dimensional polymer composed of three basic types of monomer; namely p-coumaryl alcohol, coniferyl alcohol, and sinapyl alcohol, shown in Figure 2.6 [16, 41].

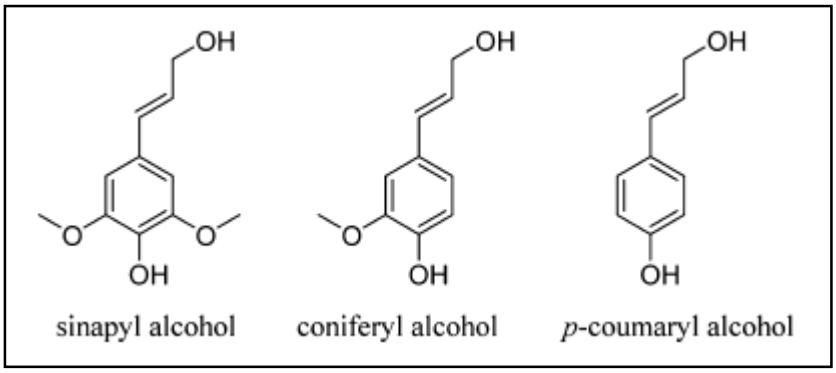

Figure 2.6: Lignin monomers [12].

These units are linked by C-C and C-O bonds including β-O-4, α-O-4, β-5, β-β, 4-O-5, 5-5, and β-1 The most common linkage between monomers is the β-O-4 ether bond, forms almost 50% of all bonds within lignin structure. [16, 42].

These three p-hydroxycinnamyl alcohol precursors are thought to constitute lignin by the dehydrogenative polymerization and each of the alcohols are responsible for different units of lignin. Lignin units are called H (p-hydroxyphenyl), G (guaiacyl) and S (syringyl) units [43].

While coniferyl alcohol is the principal monomer for softwood lignins, coniferyl and sinapyl alcohols are two main monomers of hardwood lignins containing methoxyl groups on both the C-3 and C-5 positions. The third monomer, p-coumaryl alcohol, is more prominent in grasses and compression wood. Lignin contents of the softwoods and hardwoods are about 28% and 20%, respectively [40].

Lignin is explained to provide the plant secondary cell wall its robust, rigid and hydrophobic properties. Lignin, exists in the tissues of woody biomass, is responsible both of the recalcitrant structure of the biomass and the water and food transport inside

the vascular system [44]. Lignin is indicated to prevent the evaporation of water and to canalize water into critical areas [40].

Techniques such as acidolysis, thioacetolysis, and hydrogenolysis based on chemical degradation reactions played an important role to understand the structure of lignin before the invention of Nuclear Magnetic Resonance (NMR) methods. These chemical degradations reactions can be categorized according to the mechanism underlying the depolymerization of lignin network as oxidative, solvolytic, and hydrogenolytic reactions [40].

The monomer structures in lignin differ in the degree of oxygen substitution on the phenyl ring. The H, G, and S units have a single, two, and three hydroxy or methoxy groups per aromatic ring, respectively. To mention, hardwood lignin contain S and G units with S in majority and H units are dominant in softwood lignin [20]. Hardwood lignin has a more linear structure than softwood thanks to its additional methoxy groups that hamper the formation of some spesific linkages [16].

These monomer structures can be bonded by different types of links that form various distributions in the source of lignin. Both the properties of lignin and the product distributions formed on deploymerization are determined by these cross-linked functionalities.

Lignin is basically classified into six categories with regard to the isolation or extraction method from biomass [18] and they are named as technical lignins. These lignins are:

- Kraft lignin
- Lignosulfates
- Organosolv lignin
- Hydrolysis lignin
- Ionic liquid lignin
- Soda lignin

Kraft lignin is produced by kraft process arised out of the developments on soda process and industrially advantageous in terms of chemical recovery and pulp strength [45]. The Kraft or Sulfate Process divide the ether bonds in lignin for pulp extraction using sulfate and hydrogen sulfate under alkaline conditions [18]. Kraft pulping process produces the black liquor that contains a mixture of sulfonated and

unsulfonated degraded lignin with many decomposition products. Kraft lignin is recovered by the filtration and acidic precipitation of the black liquor. This type of lignin is water insoluble due to its highly condensed and modified structure [46]. Lignosulfates are produced when biomass is pulped with a sulfite and sulfur dioxide under acidic conditions, while organosolv lignins are formed through pulping process with organic solvents such as ethanol, methanol, acetic acid and formic acid. It is indicated that organosolv lignin has the highest purity among others and it is sulfur free and highly hydrophobic [20]. Hydrolysis Lignin is produced by enzymatic hydrolysis or (dilute) acid hydrolysis. Another type of lignins is Ionic Liquid Lignins. Ionic liquids, also defined as "Green Solvents", can also be used in biorefineries because they are promising for the fractionation of lignocellulosic biomass. It is reported in a research that they are able to solve 93% of lignin in bagasse. Lignin seperation by ionic liquids are not commercially applied yet but the process is known as successful [18]. Here below soda lignin, which is subject to the following experimental study, will be described in detail.

2.2.1.1. Soda lignin

Soda lignin refers to lignin extracted from biomass by soda process in which lignin is in which lignin is solubilized from biomass by an alkaline solution of NaOH at medium temperature (150-170 °C) [19, 47]. Soda process is the first chemical pulping process developed in 1851 by Hugh Burgess and Charles Watt in England [48]. At the present time, soda process is one of the most common pulping processes [47] and it is applicable to both woody and non-woody biomass. However, soda lignin is stated to difficult to utilize because of its modified and unstable structure [46]. Main structure of soda lignin can be seen in Figure 2.7. Protobind lignins are a series of industrial soda lignins obtained by soda pulping process of annual plants. Several commercial Protobind lignins can be counted as Protobind 1000, Protobind 2400, Protobind 4000 and Protobind 6000 with high lignin content (<90 wt%) [49, 50].

2.3. Biorefineries

Biorefinery is defined as "the key for the access to an integrated production of food, feed, chemicals, materials, goods, and fuels of the future" by National Research Council of the US [39]. In literature, it is one of the most preferred definition of biorefinery [13, 49].

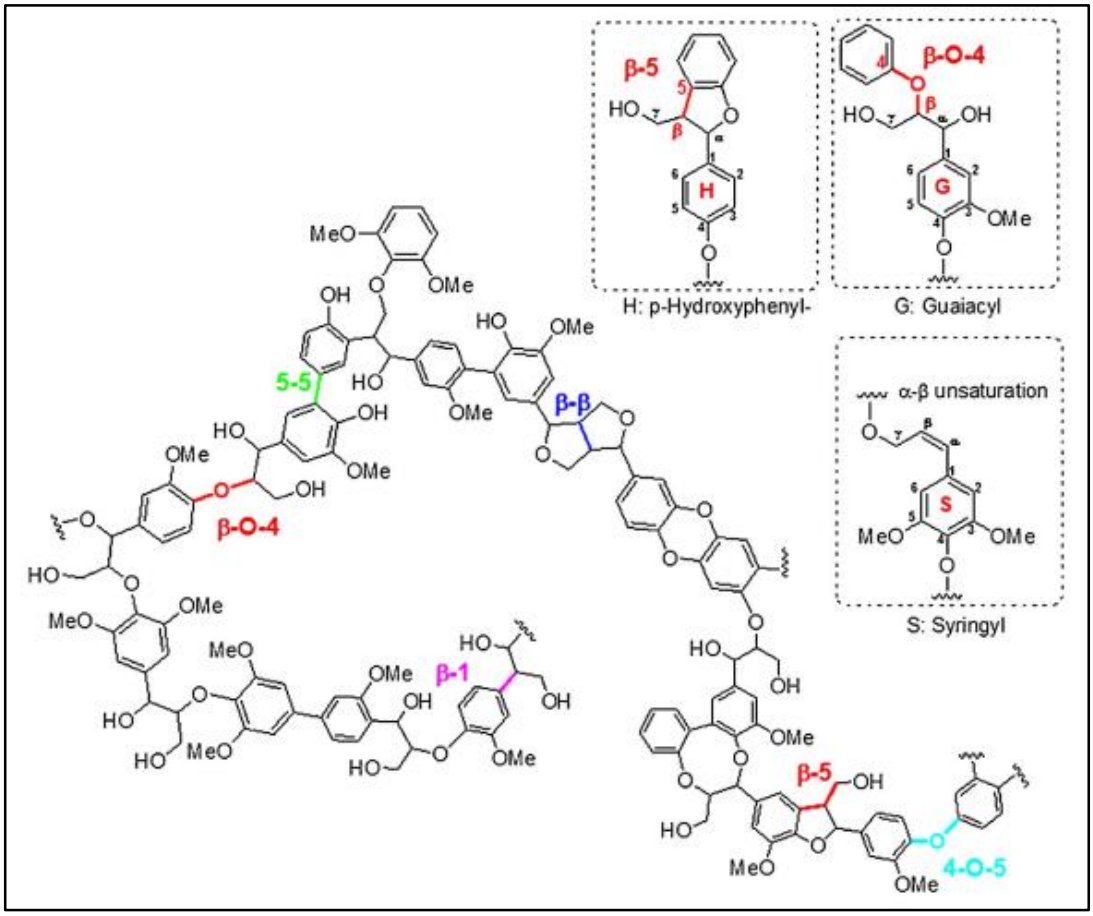

Figure 2.7: Soda lignin structure [50].

With a more comprehensive definition used, "biorefinery is an integrated and multifunctional concept that uses biomass as a source for the sustainable and simultaneous generation of a spectrum of different intermediates and products" [51]. Biorefineries provide a lot of advantages over conventional refineries. Conventional refineries use fossil fuels to produce energy and a wide range of chemicals, and are defined as fossil-based refineries. Biorefineries are analogues to the fossil-based refineries however they utilize biomass as a unique source [27]. All biomass components can be utilized in biorefineries and converted into not only biofuels and bio-based products which are biochemicals and biomaterials but also heat, cold, and bioelectricity [27, 51]. Biorefineries can produce many other products that fossil-based refineries could not, such as foods and feeds. The other dissimilarities between fossil-based refineries and biorefineries are the type of raw materials, the composition and complexity of raw materials, the nature and process of primary refining, principles and core processes of secondary refining [51].

Biorefinery concept provides high economic and environmental benefits compared to both the fossil-based biorefineries and other concepts for biomass utilization. Bio-

based products are considered more environmentally friendly because they are produced by less polluting analogous processes than in the petrochemical industry [24]. The combination of conversion processes benefits the waste and water management and the utilization of energy and heat during the production. This technology can reduce the costs, so that bio-based products can compete with fossil-based products. Also substituting with fossil fuels, agricultural and forest raw materials could provide moderate price and less disruption of supply in international petroleum markets [51]. All these benefits, provided by biorefineries, are important factors to make a shift from the existing industry to a bio-based industry. Biorefinery is the keystone of the bio-based industry, which depends on the production of biofuels and bio-based products. In the 21st century, the bio-based economy is widening and it is expected that bio-based products and biofuels will be introduced into our daily life at an increasing rate [27]. Bio-based products and biofuels could have the potential to improve the sustainability of natural resources, environmental quality, and national economical security [12]. Production of biofuels, biochemicals and biomaterials are significant to improve the overall profitability and productivity of all products in biorefineries and they are indicated to make a notable contribution to the bio-based economy [52]. In addition, biorefineries could offer economic opportunities for agriculture or chemical industry and apply hybrid technologies from different fields including polymer chemistry, bioengineering and agriculture [12].

The most important criteria emphasized about biorefineries are the environmental, economic and social sustainability. According to International Energy Agency (IEA), biorefineries address issues of sustainability from all aspects. Since biomass, processed in biorefineries, is a domestic and renewable source, the production of significant amounts of value added products from biomass yield great benefits to the public at large scale. They have the potential to reduce the national dependence on fossil fuels providing affordable and secure supply. Biorefineries provide rural development and employment with new job opportunities and importantly they reduce both the production costs and carbon costs. Being a cheap source, lignocellulosic feedstock is the most important candidate to transform existing processes into inexpensive and effective ones [21, 53].

In biorefineries, existent production technologies are adapted to provide new and feasible solutions for the provision, conditioning and conversion of biomass. These

technologies alter depending on biomass characteristics. The process from raw materials to products contains primary and secondary refining steps. Primary refining involves the separation of biomass components into intermediates such as cellulose, starch, sugar, lignin etc. The pretreatment and conditioning of biomass is as well carried out in primary refining. Secondary refining refers to conversion and processing of these intermediates to many (semi-) finished products [51].

An abundant supply of biomass is valorized in biorefineries. Thanks to biomass valorization, raw materials such as starch, cellulose, oil and lignin derived from biomass are converted into many value-added products through biorefinery technology, shown in Figure 2.8. Currently a flexible product mixture that involves biochemicals, biomaterials, and biofuels, as well as the production of biopower (heat, cold, and electricity) can be obtained by both thermochemical conversion technologies (combustion, co-firing, gasification, pyrolysis, carbonization, liquefaction) and biochemical conversion technologies (fermantation, anaerobic or aerobic digestion, enzymatic hydrolysis) in biorefineries [25, 27].

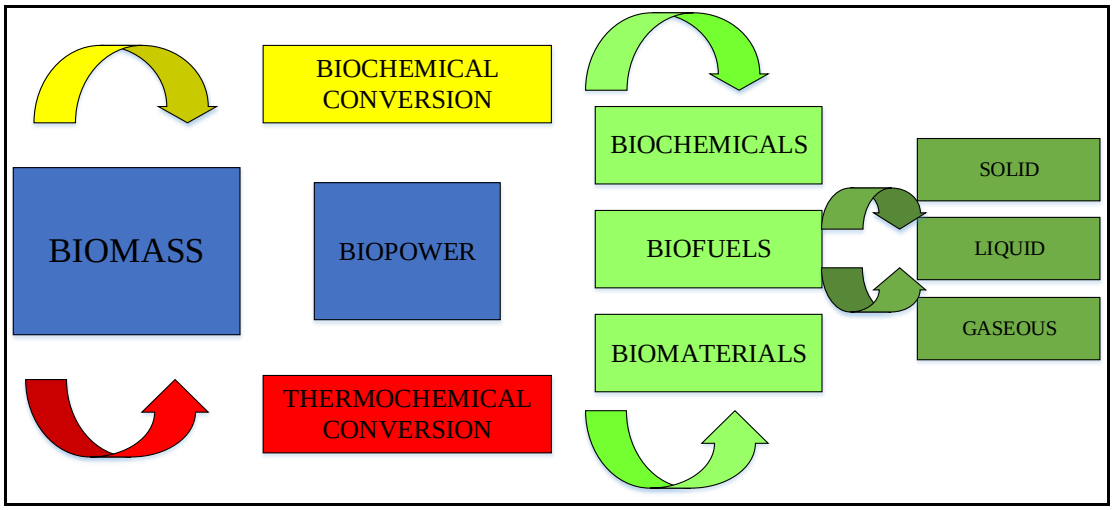

Figure 2.8: Biorefinery technology (Adopted from [27]).

There are various types of biorefinery classifications in literature. One of them is based on biorefinery platforms which are classified regarding the intermediate product that is obtained by primary refining in advance of secondary refining. Examples are sugar-based biorefinery, starch-based biorefinery, lignocellulose-based biorefinery and green biorefinery, vegetable oil and algal lipid biorefinery, synthesis gas biorefinery and biogas biorefinery. Also biorefineries could be entitled to their end-products such as bioethanol biorefinery, biodiesel refinery, and biogas refinery [51]. Of them, bioethanol biorefinery is the early example of the biorefineries. Bioethanol (ethanol

derived from biomass) production by fermentation is a well-known process carried out in existing bioethanol biorefineries [54]. This process is a good model for biomass valorization. Because the first generation bioethanol are produced from sugar- and starch-based feedstocks and second generation bioethanol is produced from lignocellulose-based feedstocks. Bioethanol biorefineries has formed a base for the modern biorefineries. Modern biorefineries are divided into four concepts regarding the feedstock used:

- Whole-crop biorefinery
- Green biorefinery
- Two platform concept
- Lignocellulosic feedstock (LCF) biorefinery [13, 55].

According to Kamm et al (2010) Green biorefinery uses natural wet feedstocks such as grass obtained from grass lands, closure fields, nature preserves or green crops such as immature cereal or clover. This concept is a multi-product concept that isolates the substances from their natural form by wet fractination technology. Whole crop biorefinery utilizes cereals such as rye, wheat, triticale or maize and is divided into two category as whole crop biorefinery based on dry mill and wet mill. Both categories of whole crop biorefinery separate the feedstock into straw and grain however they follows different processes. Fourth biorefinery is Two platform biorefinery, which is stated to contain the sugar platform and syngas platform. Two platform biorefinery uses biomass that contains 75% carbohydrates on average. Biochemical conversion technology is applied to sugar platform, whereas thermochemical conversion technology applied to syngas platform. Lignocellulosic feedstock biorefinery uses nature and dry lignocellulosic biomass as a feedstock [55]. In this context, lignocellulosic feedstock biorefinery is the most promising biorefinery for the large scale commercial implementation and it is explained in the following section.

2.3.1. Lignocellulosic Feedstock Biorefineries

Lignocellulosic feedstock (LCF) biorefineries are anticipated to be more successful than the other biorefinery concepts [13, 55]. For example, LCF biorefineries are more advantageous than other biorefineries in terms of costs, because lignocellulosic feedstock is an abundant and cheap feedstock [38]. Still, valorization of all components of the lignocellulosic feedstock is indispensable and emphasized to be the ideal

strategy to compensate the costs of the biorefinery process [56]. Beside many other advantages, LCF biorefineries have ability to convert a wide range of available lignocellulosic feedstock into the products that are substitutes of the fossil-based products [38]. As lignocellulosic feedstock can be converted as a whole, in LCF biorefineries it can be utilized via the separation of lignocellulosic feedstock into its constituents; namely cellulose, hemicellulose and lignin. Seperation of lignocellulosic feedstock aims to improve the overall biomass utilization and to increase efficiency of conversion. To ensure a successful biorefinery concept, the inherit complexity and heterogenity of these components should be taken into consideration and a comprehensive understanding of their structure and composition is needed [56]. These constituents are further converted into the desired products through various conversion pathways, which differs according to the feedstock used [57].

Valorization of cellulose and hemicellulose is conventionally carried out by biomass conversion technologies. Combustion, co-firing, gasification, pyrolysis, carbonization and liquefaction are the thermochemical conversion technologies applied to biomass, whereas biochemical conversion technologies contain fermentation, anaerobic and aerobic digestion, as it is shown in Figure 2.9 [25, 27]. Valorization of cellulose and hemicellulose is today a well-known and effective strategy, finds a wide application area in the industry. Many products such as ethanol, sorbitol, furfural, lactic acid, levulinic acid, succinic acid, xylytol are produced from cellulose and hemicellulose, are placed on the industry for further use [58]. Compared to cellulose and hemicellulose the third important contituent of the biomass, lignin has not gained much attention so far because of its complex structure to break down and the absence of sufficient technologies to prosess lignin. Lignin come out of the industry and the existing biorefineries was an undervalued component of the biomass. Despite the fact that, lignin had been previously treated as a by-product in the industry or biorefineries, its huge potential has been realized [57, 59].

Today, in LCF biorefineries lignin comes into prominence beside cellulose and hemicellulose in the matter of valorization of woody and non-woody biomass. Lignin is an important potential feedstock for many value-added products and lignin valorization is favourable instead of using lignin only as a fuel source [46]. In conclusion, future biorefineries will be capable to utilize lignin as successfully as they utilize cellulose and hemicellulose.

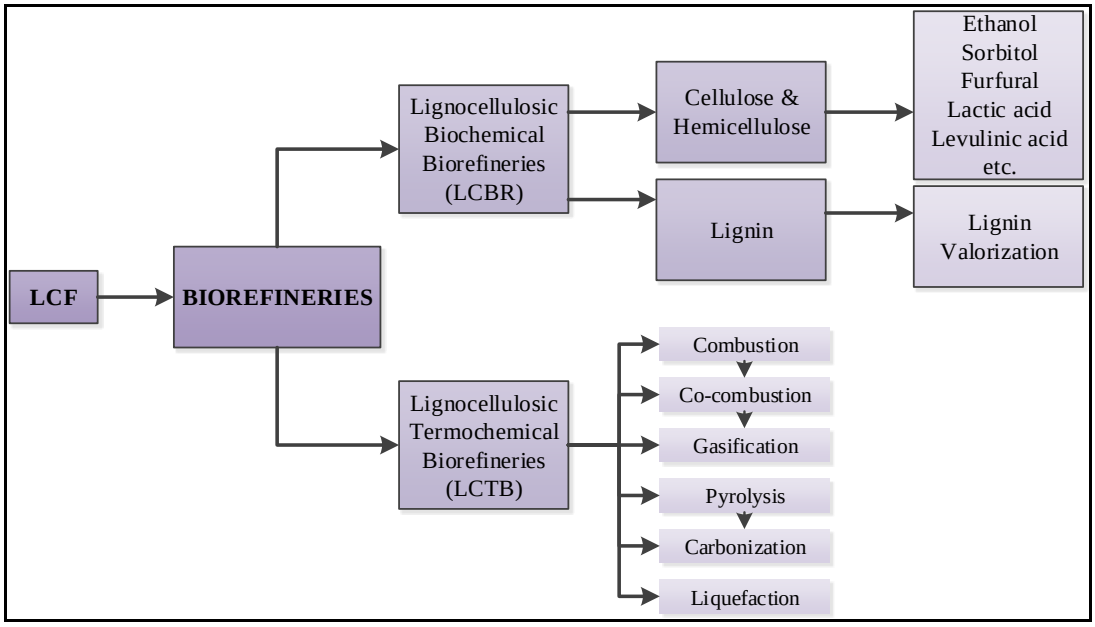

Figure 2.9: LCF conversion technologies (Adopted from [60, 61]).

2.3.2. Lignin Valorization

Lignin can be valorized into many valuable biofuels, biochemicals and biomaterials [62-64]. For example, lots of aromatic products as subtitutes to the petroleum-based products can be produced from lignin [46]. Potential products of lignin valorization are phenols, oxidized products, syngas products (e.g. ethanol, methanol), macromolecules (e.g. adhesives, binders, resins) etc. [21]. Taken into account the huge amount of lignin generated as a by-product by the biorefineries along with the paper and pulp mills, lignin takes on a new significance [57]. Only in the pulping processes, about 70 millions tons of lignin is generated annually [16]. It is indicated that lignin is important to be economically benefited by developing suitable cost-effective and sustainable conversion technologies [21].

Lignin valorization technology comprise various processes such as gasification, pyrolysis, hydrolysis, hydrogenolysis, carbonization, oxidation and combustion [65]. These processes and their potential products are shown in Figure 2.10.

Processes such as gasification, pyrolysis, hydrolysis and hydrogenolysis can produce a mixture of gases and a stream containing bio-oil, phenols, aldehydes, aliphatics etc. Oxidation can produce same products with these processes, but the main difference is biochar production. Also carbonization forms biochar at relatively high temperatures [65].

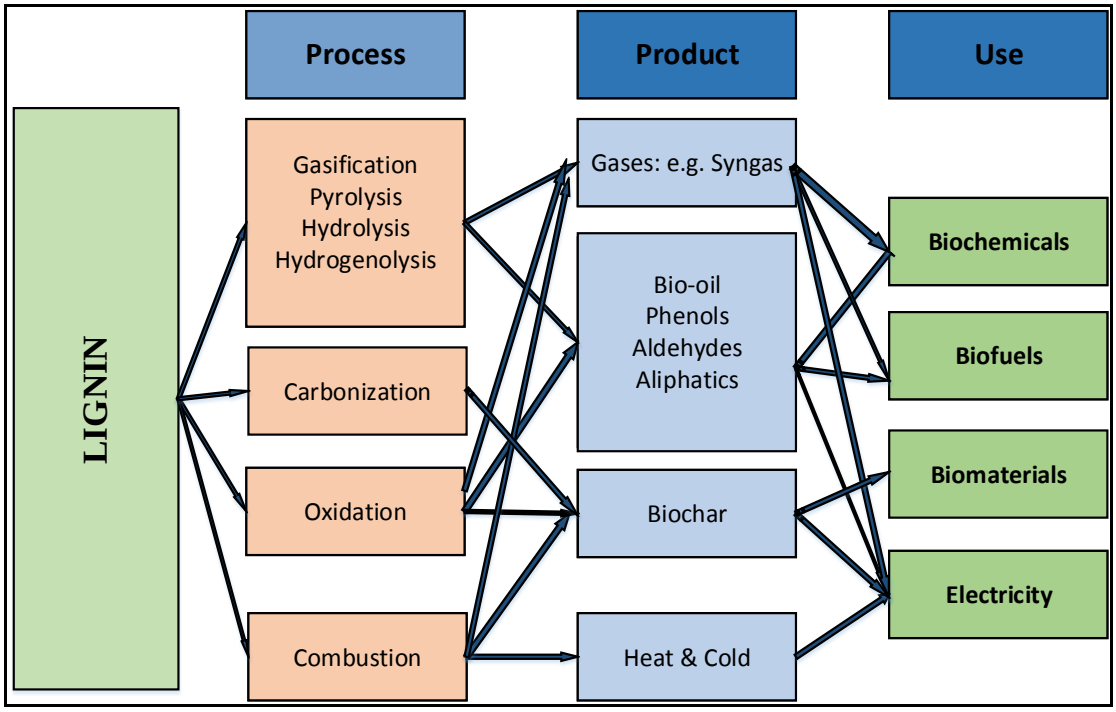

Figure 2.10: Lignin valorization technology (Adopted from [65]).

Combustion is one of the oldest conversion processes and utilizes lignin as a low value compound. Lignin is directly utilized by combustion in order to produce energy (biopower), which has two principal forms: heat/cold and electricity [25]. All these streams are responsible for the production of biochemicals, biofuels, biomaterials and biopower [65]. Following section focuses on lignin valorization and presents a detailed information to the production of biochemicals, biofuels and biomaterials.

Lignin valorization is an ideal strategy for the transition from fossil-based chemical industry to bio-based one in the future. Lignin valorization provides long-term opportunities like the enhancement of economic viability of biomass and the contribution to the economics of the biorefinery. Lignin is an obvious candidate to produce the substitutes of fossil-based products, as lignin can be converted into a wide range of biofuels and value-added bio-based products in biorefineries [63, 66].

Valorization of lignin can derive new aspects to the production of biofuels. For instance; Phenolic oils derived from lignin can be upgraded to gasoline, kerosene, and diesel at high selectivity controlling the hydrogenation, dehydration and alkylation reactions on the suitable metal and acid sites. Moreover industrially valuable phenols, known to be generated as a result of the hydrogenolysis of C-O bonds in high molecular weight components, can be produced by means of lignin depolymerization.

The success of the fully integrated lignin valorization processes in biorefineries depends on the development of suitable catalytic technologies to achieve the desired depolymerization of lignin [67]. Lignin can be valorized by three pathways with the aim of biofuels and bio-based products production, shown in Figure 2.11. The first pathway include syngas conversion which is composed of gasification and syngas processing steps [68]. In gasification, lignin is heated in the presence of a gasifiying agent such as oxygen, steam and air. Heating is followed by pyrolysis and the further reactions between pyrolysis products and gasifiying agents [69]. Although lignin can be converted into a mixture of gases such as H_2, CO, CO_2 and CH_4 by gasification, syngas composed of H_2 and CO is the most important product of lignin gasification [65, 70]. Syngas can be further processed to produce many desired products [70].

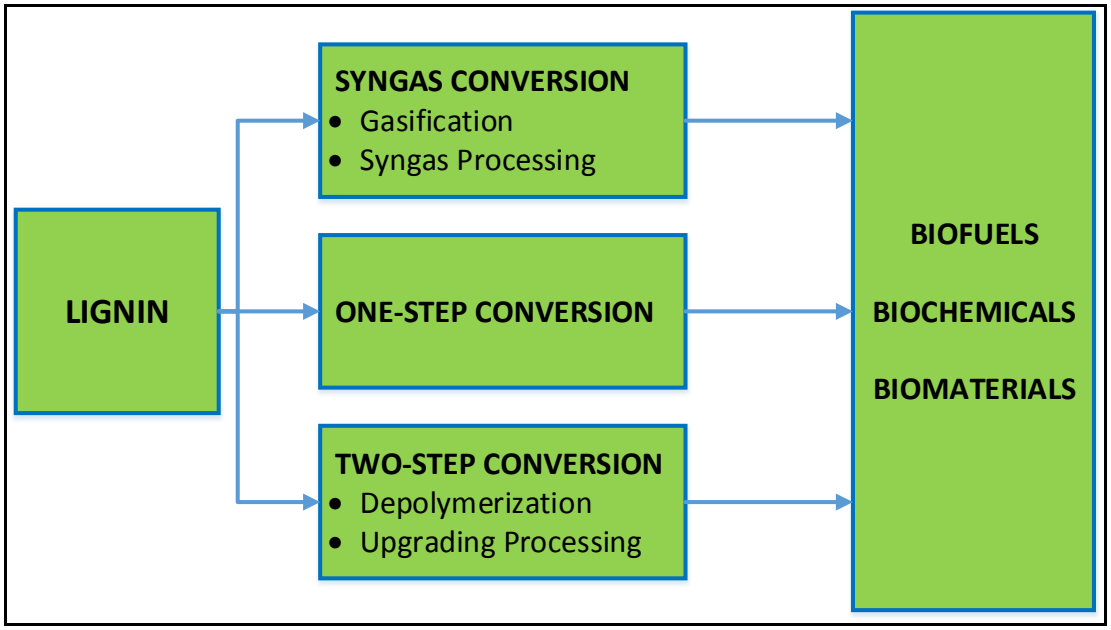

Figure 2.11: Pathways of lignin valorization (Adopted from [70]).

The second pathway is one-step conversion which is the newest pathway contain one step catalysis of lignin directly to produce biofuels and bio-based products including bulk and fine chemicals. This pathway is needed highly selective catalysts to break specific functionalities and linkages. One-step conversion is especially favorable for the production of fine chemicals with a high degree of functionality. Also the catalytic technology can be improved to produce more complicated target molecules such as aromatics [70]. Direct and effective conversion of lignin is determined as an urgent and attractive goal to achieve high-volume, low-molecular weight aromatic molecules [16], thanks to the unique potential of lignin valorization for such aromatic compounds [20, 22].

Finally, the third pathway is so-called two-step conversion. In this pathway, first the complex lignin structure is degraded into a depolymerized lignin and upgrading is applied according to the end product desired [67]. Lignin is first catalyzed to simple aromatic compounds such as phenols, benzenes etc. by the removal of the functional groups via new conversion technology. This step is followed by the conversion of platform chemicals into the product via a second catalysis based on current conversion technology [70]. Two-step conversion is stated to be more flexible than one-step conversion due to the availability to independently select the second conversion step following the depolymerization step [67].

Depolymerization of lignin can be carried out by thermochemical, hydrolytic, reductive and oxidative approaches [70]. Thermochemical approach comprises a process such as pyrolysis and carbonization to thermally depolymerize lignin [71, 72]. Pyrolysis is carried out at temperatures above 200^{o}C, at which thermal decomposition begins, up to 1000^{o}C [67]. Lignin decomposes over a wide range of temperature but slowly than cellulose and hemicellulose, considering its aromatic content. Also, lignin is indicated to produce more biochar than lignocellulosic biomass [59, 73]. Pyrolysis products of lignin are liquids (40-60 wt%), gases (8-20 wt%) and biochar (30-40 wt%) [74]. Liquid product of pyrolysis generally named as bio-oil, tar or biocrude. Bio-oil derived from lignin includes small molecules and macromolecules from lignin decomposition [75]. These pyrolytic liquid products include aqueous components (water, methanol, acetic acid, acetone etc.), unsaturated compounds and aromatic monomers such as phenols or high-boiling complex phenols [74-76]. Phenols are one of the significant products formed as a result of the break of ether and carbon-carbon (C-C) linkages of lignin. Pyrolysis is convenient for the production of low molecular weight products from lignin and it is one of the most preferred method to produce biofuels and value-added chemicals [76].

Carbonization produces biochar, which is promising for the production of biomaterials. While the main goal for pyrolysis to increase the production of liquid product and decrease biochar formation, carbonization aims to produce a solid product with a maximum fixed carbon content [25]. Lignin is a remarkable source in terms of bulk synthesis of biomaterials, especially for the production of carbon materials thanks to its high carbon content and phenolic structure [77]. Carbon materials such as activated carbon [72, 78], and carbon fibers (CFs) [77] can be formed from lignin by

carbonization. Compatible CFs can be produced from lignin, for instance; lignin based CFs have similar mechanical properties with polyacrylonitrile-based CFs. The production of activated carbon include carbonization of lignin followed by activation of biochar. In this process, lignin is pyrolitically carbonized to biochar in the temperature range of 600-850^{o}C and biochar can be physically activated using an oxidant gas such as steam or CO_2 or treated chemically by heating under nitrogen flow and using a base catalyst such as H_3PO_4, KOH or NaOH [72].

In hydrolysis, lignin is degraded by aqueous solvents at moderate temperatures using an acid or base resulting mainly low molecular weight products and biochar [74]. Alkaline hydrolysis is the most used hydrolysis type and generate a wide range of products such as syringol, guaiacol and vanillin [67]. If lignin is converted to the desired product using an organic solvent such as water, alcohol, ammonia and glycol) in sub/supercritical condition, this method is called solvolysis, defined as a type of solvent molecule substitution or elimination reaction [79]. In addition, some current studies discussed solvolysis in the presence of formic acid or isopropyl alcohol as a hydrogen donor and a co-solvent such as ethanol [80, 81].

Supercritical water depolymerization has some advantages over hydrolysis, because of its ability to enable oxidation and hydrolysis reactions without a need of catalyst besides its properties such as thermal stability and miscibility with gases, hydrocarbons and aromatics. In addition, supercritical water depolymerization do not require catalyst usage for oxidation and hydrolysis reactions [67]. However many studies center on supercritical solvent depolymerization utilizing the solvents such as ethanol and methanol [59, 78, 79, 82]. Supercritical solvents have distinctive physicochemical properties such as more compressibility than dilute gases and more powerful than liquids [78].

Reactions involved in both oxidative and reductive approaches are carried out by the catalysis, in which various catalyts selected regarding the desired products is used [83]. Catalysis can be divided into three methods: heterogeneous catalysis, homogeneous catalysis and electrocatalysis. Reductive reactions utilizes different catalysts than oxidative reactions. Although there are lots of catalyst for heterogeneous catalysis, they can mainly classified as Co-Mo- and Ni-Mo-based catalysts and non-conventional catalysts. Homogeneous catalysts reported are not as much as heterogeneous catalysts. Electrocatalysis is a more selective method than the classical

catalysis in terms of hydrogenation. The aim of the electrolysis is the hydrogenation of ether bonds faster than the hydrogenation of aromatic rings. Researchs on electrolytic hydrogenation is said to focus on lignin model compounts instead of lignin [70].

Reductive approach involves hydrogenolysis (hydrogenation) followed by hydrodeoxygenation (HDO) and hydrocracking. Hydrogenolysis can be stated as pyrolysis carried out in the presence of hydrogen [65]. It occurs as a result of a reductive condition. In hydrogenolysis, the C-O-C linkages of lignin are broken down under H_2 attack and the alkanes are formed via hydrogenation or hydrodeoxygenation reactions. This method is usually carried out at high temperatures and pressures using catalysts like Pt, Pd, Rh, Ru [79]. The other catalysts used for lignin depolymerization are $NiCl_2$, $ZnCl_2$, $FeCl_3$ and $AlCl_3$ [72]. A hydrogen atmosphere or hydrogen-donating solvents makes possible the formation of monomeric compounds such as BTX (the mixture of benzene, toluene and xylene), phenol and cresol [57].

Alcohols have been shown to act as a source of hydrogen in the reaction medium and a nucleophilic reagent to break C-O-C bonds [78]. Particularly, these bonds can be selectively cleaved into phenols by hydrogenolysis or hydrogenation, of which hydrogenolysis is a favourable way for the production of phenols [65], despite the fact that hydrogenolysis is mentioned not to be used in industry due to the low selectivities of phenolic compounds [67]. Base catalyzed depolymerization (BCD) also receive attention producing phenolic monomer compounds among other thermochemical methods [84]. In this method, lignin is converted using sodium hydroxide aqueous solution at high temperature [85].

Alcohols are commonly used as the source of hydrogen in the reaction medium [77]. Also the dissolution of lignin in alcohols such as ethanol, methanol or ethylene glycol prior to the lignin fragmentation is a frequently encountered method, because alcohols are suitable solvents due to their act as nucleophilic reagent for cleavage of C-O-C linkages [86].

Catalysts such as CuCr oxide, Co-Mo-S/Al_2O_3, activated carbon- alumina- or silica-supported Ru or Pt are the major catalysts in the literature used for hydrogenation of lignin or model compounds to monomeric phenols [86]. Particularly, hydrogenolysis is a favorable way for the production of phenols [65]. Hydrogenolysis is emphasized not to be used in industry due to the low selectivity of phenolic compounds [67]. Base

catalyzed depolymerization (BCD) also receive attention producing phenolic monomer compounds among other thermochemical methods [87]. In this method, lignin is converted using sodium hydroxide aqueous solution at high temperature [85].

Hydrodeoxygenation and hydrocracking are mostly employed for lignin depolymerization thanks to the weak linkages in lignin structure, which are α-aryl-ether, β-aryl-ether and aryl-aryl bonds. Especially HDO is subject to various researches. A recent study on HDO of mono- and dimeric lignin showed that noble metal catalysts such as Pd, Pt, Ru or Rh on SiO_2 are advantageous than the sulfide-base catalysts. Nobel metal catalysts provide complete hydrogenation of aromatic rings and forms cyclic alcohols and cycloalkanes, while sulfide-base catalysts has low efficiency on lignin conversion [84].

Oxidative reactions aim to valorize lignin to produce complex aromatic compounds with additional functionality. Heterogeneous catalysts are mostly utilized for oxidation reactions in paper and pulp industry. The most employed heterogeneous catalyst is stated as TiO_2. Homogeneous catalysts for oxidative reactions constitute a large group that is subdivided into various categories. To mention, these can be accounted as biomimetic catalysts, metallosalen catalysts, metallo–TAML, –DTNE and –TACN catalysts, polyoxometalate-based catalysts, and simple metal-based catalysts. Oxidation is used to obtain fine chemicals and functionalised aromatics, however reduction is indicated to convenient for the production of biofuels or aromatic and phenolic compounds [70].

Also depolymerization of lignin is indicated to carry out through enzyme catalyzed oxidative reactions along with non-enzymatic rearrangements [88]. In fact, biological conversion of lignin is not easy as cellulose or hemicellulose because lignin is emphasized as "highly resistant to break down by the vast majority of microorganisms" [89]. Lignin can be biochemically broken down using the oxidative enzymes of fungi or bacteria [62, 90]. Most employed types of fungi are white-rot and brown-rot fungi [91].

Lignin valorization will open a new route to produce not only low-carbon biofuels and low-molecular-weight aromatics but also high-molecular-weight materials for high value applications [63, 64, 70]. Not only for biomass but also for lignin, efficient and sustainable valorization pathways are essential to be investigated and followed through in order to ensure a green future for the production of the foregoing biofuels,

chemicals, and materials. One of these possible pathways of biomass and lignin valorization is catalytic depolymerization in supercritical ethanol which is the main concern of this study. The aim of the study is to have a remarkable insight on the lignin and biomass depolymerization over heterogeneous catalysts in supercritical ethanol.

2.4. Scotch Pine

Being one of the most widely distributed softwood in the world, Scotch Pine (*Pinus sylvestris* L.) is found across Europe and Asia, grows naturally from Scotland to Pasific Oceanand from bove the Arctic Circle in Scandinavia to the Mediterranean [92]. Scotch Pine, also known as Scots Pine, is the most widespread kind of pine in the world and is an evergreen tree growing up up to 36 m [93, 94]. Among many characteristics, its susceptibility to cold, heat and drought and resistance to insects and disease can be counted [95]. Figure 2.12 shows Scotch pine tree and its cones and needles.

Figure 2.12: Scotch Pine tree, cones and needles [96].

In Turkey, Scotch Pine is a widespread kind of tree. The Republic of Turkey General Directorate of Forestry (OGM) indicates that Scotch Pine is widespread around the Blacksea coasts and is distributed over an area of 1479647 Hectares (Ha) in Turkey

[97]. Distribution of Scotch Pine in Turkey is shown in Figure 2.13. Scotch Pine becomes dominant on North Anatolian Mountains as the elevation increases. It has a wide vertical distribution in the form of pure and mixed stands in Eastern Blacksea forests. In addition, Scotch Pine is resistant to draught and cold and takes place in the region of Central, East and South east Anatolia. It takes the advantage of being the highest forest line in Turkey spreading at altitudes around 2800 m in Sarıkamış, Turkey. Especially in the East Anatolia, pure Scotch Pine forests are the most significant forests [98].

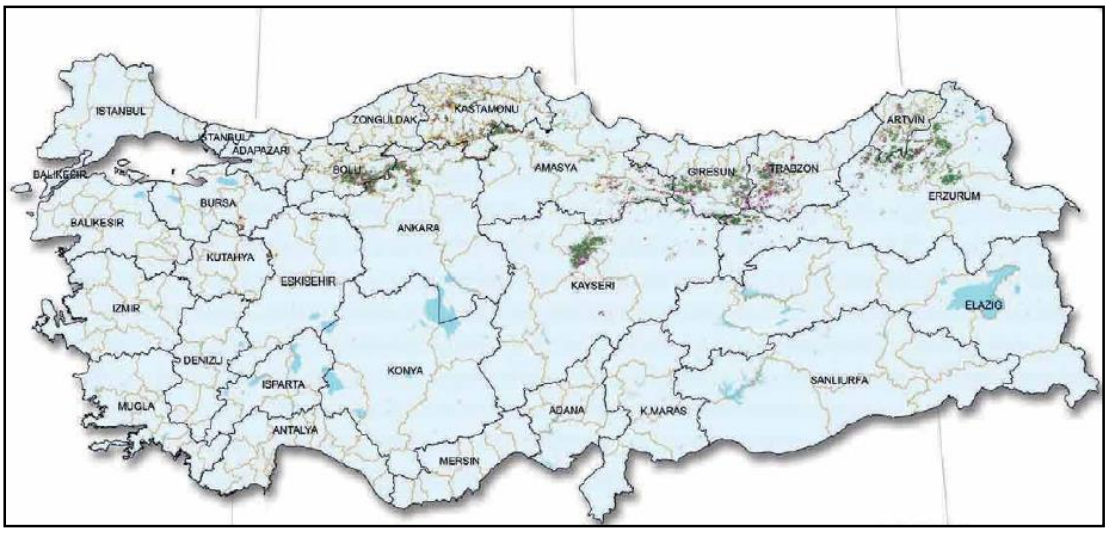

Figure 2.13: Geographic distribution of Scotch Pine in Turkey [79].

2.5 Literature Review

Literature review focuses on the recent researches regarding the valorization of lignocellulosic feedstock and lignin. Herein, selected papers on catalytic and non-catalytic depolymerization technology applied to LCF and lignin are summarized.

Rewardingly, many studies focus on LCF valorization through a wide range of different techniques. Of them, catalytic conversion distinguishes to obtain a variety of renewable products ready to be in use either as bulk chemicals or fuel additives. Nowadays great strides are being made in one-step (one-pot) catalytic conversion using well-designed multifunctional catalysts [99]. In this context, one-step (one-pot) conversion can be successfully integrated into biorefinery technology, in which well-managed direct conversion of lignocellulosic biomass is essential. Especially, heterogeneous catalysis received strong attention and many microporous and mesoporous materials are used as catalyts for lignocellulosic biomass conversion [100, 101].

In literature, many one-step conversion studies carried out by solid catalysts such layered transition metal oxides, to ensure an efficient and selective conversion of lignocellulosic biomass into the desired products, can be attained. Cu-doped metal mixed oxide catalysts are one of the attractive catalysts used. For instance; Yin et al (2015) depolymerized woody biomass and cellulose over Cu-doped porous metal oxide in supercritical methanol and satisfactory conversion was gained at 320 °C and 160-220 bar pressure [102].

Not only the catalyst, but also the reaction environment is important for successful break down. Sub- or supercritical solvents such as methanol [22, 103] and ethanol [77, 104] and water [105] have been commonly studied for woody biomass depolymerization. The presence of hydrogen in the reaction medium stated to have no effect on lignin conversion, because alcohols used as solvents are capable to provide the active hydrogen species [86]. In some studies, both supercritical ethanol and methanol were used [106]. As a result of literature research, catalytic Scotch Pine depolymerization study can not be found, however pine is used for other catalytic conversion techniques such as pyrolysis. Torri et al (2010) catalytically pyrolized pine sawdust over lots of different catalyts including Fe/Zn/Cu mixed oxides and Fe/Cu/Al/Zn mixed oxides. More than thirty metal oxide catalysts such as Al^{3+}/SiO_2, Cu^{2+}/SiO_2, CuO were tested for catalytic pyrolysis of pine sawdust at 500 ºC to observe the effect of these catalysts on the carbon yield of bio-oil, gas products and solid residue. The yields of bio-oils were between 14% and 58%. CuO showed the highest yield of semi-volatile compounds, whereas mixed metal oxides declined the propertion of heavy fraction in bio-oil. [107].

Moreover, cellulose was depolymerized as one of the main components of lignocellulosic biomass and the conversion of glucose as a model compound of sugar in supercritical ethanol was observed. Zhou et al (2011) published a comprehensive study on the catalytic conversion techniques for cellulose along with various catalysts used for this aim [99]. Matson et al (2011) converted raw woody biomass, cellulose and glucose over Cu-doped mixed oxide catalyst in supercritical methanol [108]. Supercritical alcohol is stated not only to prevent the repolymerization reactions which are not desired during depolymerization but also to stabilize sugar fractions. The biofunctional role of CuO-based catalysts ensuring the H_2 production by methanol reforming and subsequently H_2 consumption by hydrogenolysis of cellulose to C_4-C_7

alcohols was indicated by Wu et al (2013), in the scope of cellulose conversion. In the study, the metals such as Mg, Mn, Ni, Zn were used coupled with CuO and CuO-ZnO/Al_2O_3 and this was said to provide the highest activity with 88% conversion of cellulose [109].

Similarly, catalytic lignin depolymerization is one of the prominent ways of lignin valorization and broadly being studied in the literature. Many researches have been approaching to the lignin depolymerization from different aspects. Reaction conditions such as hydrogen-donating solvent, reaction temperature and catalyst are often the main parameters being optimized in the studies.

Huang et al (2014) published a recent study focuses on one-step depolymerization of lignin in supercritical ethanol over a Cu-doped MgAl mixed oxide ($CuMgAlO_x$) catalyst [110]. This catalyst was revealed to provide both high deoxygenation and low ring-hydrogenation activity, obtaining high monomer yield. In this study, Ni-, Pt-doped, and Cu-free $MgAlO_x$ catalysts led to lower yields of monomer, leaving Cu the best option in terms of lignin depolymerization. Monomer yield was 23% after the reaction over $CuMgAlO_x$ catalyst at 300°C for 8h in supercritical ethanol without char formation. Aromatics were the main cyclic products together with some linear products [110]. These linear products were derived from the ethanol conversion by Guerbet-type reactions [111]. Ethanol is a suitable solvent, because it can be produced from renewable biomass, and its critical point is relatively low (243 C, 6.39 MPa) [79]. Moreover, ethanol was found to exhibit several advantages according to by Huang et al (2014). First of all, ethanol acts as hydrogen-donating solvent and another advantage of ethanol is its role as capping agent which can stabilise the highly reactive phenolic intermediates by O-alkylation of hydroxyl groups and by C-alkylation of the aromatic rings [110]. In order to achieve higher monomer yield, repolymerization in the reaction medium should be suppressed whereas depolymerization is promoted. Highly reactive phenolic intermediates exist during the lignin condensation reactions, are tend to form new C-C bonds therefore they are the main actors of repolymerization [110].

The use of ethanol as a solvent for lignin depolymerization have also been reported by other researchers [79, 84]. For example, Ma et al (2014) studied catalytic lignin conversion over an activated-carbon-supported α-molybdenum carbide catalyst in supercritical ethanol and inert environment. Lignin was depolymerized into high-value small molecules of C_6-C_{10} liquid products. Ethanol was found to be the most effective

solvent for the degradation of lignin concerning liquid product yield compared to water, methanol and isopropanol. Both catalyst and solvent are important contributors on monomer yield and product composition. They also highlighted that the absence of hydrogen in the initial gas phase of the reaction medium was more efficient than that in the presence of hydrogen [112]. In another work, Dutta et al (2014) mentioned that lignin fragments can be immediately stabilized on the surface of the catalyst under supercritical conditions of ethanol [113].

$CuMgAlO_x$ catalysts are recently become one of the prominent catalyst for dehydrogenation reactions [114], C-C coupling reactions [115] and alcohol conversion reactions [116]. Porous metal oxides (PMOs) are capable to perform hydrogenolysis and hydrogenation reactions without char or with minimal formation of char, therefore these catalysts are highlighted to improve the efficiency of lignin conversion and help to prevent catalyst deactivation. Cu-doped PMOs are reported to form reducing equivalents by reforming methanol under supercritical conditions. In these conditions, lignin or lignocellulosic biomass samples can be converted into highly deoxygenated liquid products such as cyclic or aliphatic alcohols [78]. CuPMO catalysts are used to convert lignin and lignocellulosic biomass in supercritical methanol at short reaction times (40 and 60 mins). Cu_{20}PMO is pointed out to be the best catalyst to achieve an effective conversion of biomass, although it was not possible to completely convert lignin with any of CuPMOs in this timescale. CuPMOs are proved to promote the yield of methanol-soluble products and to suppress recondensation reactions compared to the PMOs, not based on Cu [78].

Layered double hydroxides (LDH) or hydrotalcite-like compounds (HLC), illustrated in Figure 2.14, are the precursors of the CuMgAl mixed oxides. Their general formula is $[M_{1-x}^{2+}M_x^{3+}]^{x+}(A_{x/n}^{n-}).mH_2O$. M^{2+} and M^{3+} stand for divalent cation like Mg^{2+}, Cu^{2+} and trivalent cation like Al^{3+}, respectively and $A_{x/n}^{n-}$ represents anion [117]. In the LDHs, the isomorphic substitution of M^{2+} cations by M^{3+} cations in a brucite-like ($Mg(OH)_2$) layer builds up a layered structure, in which metals are well-dispersed. Thanks to this substitution, positively charged layers stack together are defined to form where anions occupy the interlamellar region to balance the charge. Mg and Al oxides, providing easy preparation and good activity in C-C coupling reactions of alcohols, are commonly chosen for the synthesis of LDHs. Also Cu is presented as the favorable metal addition to the Mg and Al containing catalyst in order to perform the

dehydrogenation of lower alcohols, hydrogenation of C-C coupled unsaturated intermediates and to promote C-C coupling reactions of alcohols [115].

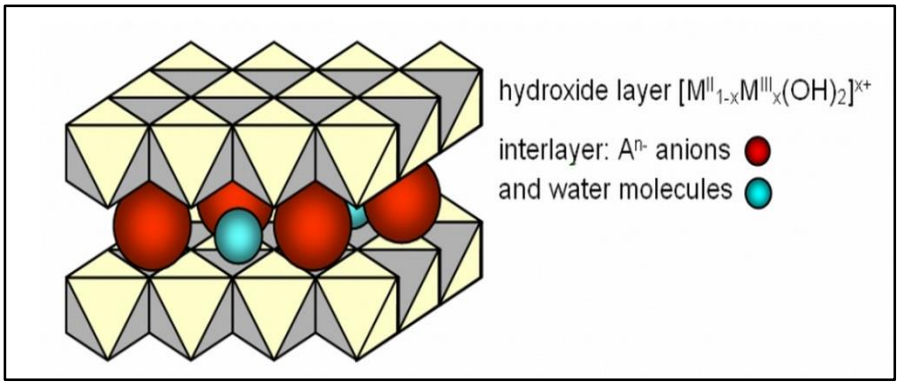

Figure 2.14: Structure of Layered Double Hydroxide [118].

Marcu et al (2012) catalytically converted ethanol into butanol over M_5MgAl mixed oxide catalysts where M indicates the metals used (e.g. Pd, Ag, Cu, Fe). Considering the strong relationship between the catalytic activity and the acidic-basic properties of the catalysts related to the nature of the support metal, $CuMgAlO_x$ is pointed out to be active on the activity and the conversion. Cu_5MgAlO catalyst had a higher total acidity and more strong acid sites compared to others. This confirms the important role of the acidic properties of the catalyst for the ethanol conversion to butanol [119].

Haider et al (2007) investigated the catalytic activity of gold nanoparticles supported on $CuMgAlO_x$ for the alcohol oxidation. It was reported that Cu- and Mg- containing mixed oxides are important to promote the activity of gold nanoparticles [120]. Effectiveness of Cu-doped catalysts on the selective C-O hydrogenolysis by minimizing hydrogenation of the furan ring was also mentioned in the literature [119]. Cu-doped porous metal oxides were subject to another study which aims the catalytic upgrading of pyrolysis oils and sugars derived from pyrolysis oil in supercritical methanol and ethanol. Yin et al (2015) observed aliphatic monoalcohols, diols and esters as three main product groups for the conversion of 15 wt% sugar fractions obtained by aqueous extraction of pyrolysis oils using supercritical ethanol at 300 C for 8h. Besides, no solvent reforming was reported to be occurred due to the addition of 50 bar H_2 to the reaction medium [121].

Although there is a couple of catalytic lignin depolymerization over mixed metal oxides in supercritical ethanol, the direct depolymerization of lignocellulosic biomass over metal mixed oxides in supercritical ethanol and the detailed analysis of the conversion products are not available in the literature.

Here, a better understanding of the depolymerization mechanism of lignocellulosic biomass and lignin was aimed. This study contributes to have a new insight to the depolymerization of Scotch Pine and Protobind 1000 Lignin over Cu-doped mixed oxide catalyst in supercritical ethanol.

3. EXPERIMENTAL STUDY

Experimental study covers both the catalytic depolymerization of Scotch Pine and Protobind 1000 Lignin over mixed metal oxides.

3.1. Materials

Protobind 1000 alkali lignin, which was obtained by the soda pulping of wheat straw (sulfur-free lignin with less than 4 wt% carbohydrates and less than 2 wt% ash), was purchased from GreenValue. Elemental composition of one of the soda lignins, namely Protobind 1000 lignin, is presented in Table 2.1.

Table 3.1 : Elemental analysis of Protobind 1000 Lignin [50].

Characteristics	Protobind 1000 lignin
Ultimate Analysis (wt%)	
Carbon	59.4
Hydrogen	5.6
Oxygen	25.7
Nitrogen	1.1
Sulfur	0.1
Ash	4.9
Moisture	3.0
H/C molar ratio	1.1
O/C molar ratio	0.3

Turkish-origin Scotch Pine (*Pinus sylvestris* L.), also known as Scots Pine (SP), was harvested from the field in the vicinity of Bursa, Turkey in 2014 and chopped into small pieces on site. SP in the form of sawdust was used for the experiments. First, Suitable amount of the SP was ground and sieved to a particle size below 125 μm and then dried at 105°C for 12 h before use (Figure 3.1).

Cellulose and D-(+)-Glucose were purchased from Sigma Aldrich. Extra-dry absolute ethanol and methanol were purchased from Biosolve. $Cu(NO_3)_2.2.5H_2O$, $Mg(NO_3)_2.6H_2O$ and $Al(NO_3)_3.9H_2O$ were purchased from Alfa Aeser. 50% NaOH solution was purchased from Merck. Dimethylsulfoxide-d_6 (DMSO-d_6) was purchased from Sigma-Aldrich. All other chemicals were purchased from Sigma-Aldrich. All commercial chemicals were analytical reagents and were used without further purification. All samples were stored in a desiccator when they were not in use.

Figure 3.1: SP seived and dried at 105°C for 12 h.

3.1.1. Catalyst Preparation

Two series of Cu-based MgAl hydroxide (hydrotalcite) catalysts were prepared by calcination of Layered Double Hydroxides (LDH) precursors. The catalyst samples were donated by Cu_yMgAlO_x, where y corresponds to the Copper loading as weight percent (wt%) with respect to cations and x indicates the M^{2+}/M^{3+} ratio meaning $(Cu^{2+}+ Mg^{2+})/Al^{3+}$ ratio of the catalyst.

For the first series of the catalysts, Cu_yMgAlO_x mixed oxides with different Cu loadings (0 wt%, 10 wt%, 20 wt% and 40 wt%) and a fixed M^{2+}/M^{3+} ratio of 4 were prepared. Table 2.2 indicates the amount of substances used to prepare the catalysts with different Cu loadings, namely $MgAlO_4$, $Cu_{10}MgAlO_4$, $Cu_{20}MgAlO_4$ and $Cu_{40}MgAlO_4$.

Table 3.2 : The amount of chemicals used to prepare catalysts with different Cu loadings

Catalysts / Chemicals	**$Mg_8Al_2O_{11}$**		**$Cu_{0.7}Mg_{7.3}Al_2O_{11}$**		**$Cu_{1.5}Mg_{6.5}Al_2O_{11}$**		**$Cu_{3.6}Mg_{4.4}Al_2O_{11}$**	
	PMO_4		$Cu_{10}PMO_4$		$Cu_{20}PMO_4$		$Cu_{40}PMO_4$	
	mol	*g*	*mol*	*g*	*mol*	*g*	*mol*	*g*
CuMgAlO	0,015	6,37	0,015	6,78	0,015	7,26	0,015	8,45
$Mg(NO_3)_2x6H_2O$	0,120	30,77	0,109	28,04	0,097	24,92	0,067	17,13
$Al(NO_3)_3x9H_2O$	0,030	11,25	0,030	11,25	0,030	11,25	0,030	11,25
$Cu(NO_3)_2x2.5H_2O$	0,000	0,00	0,011	2,48	0,023	5,30	0,053	12,37
Na_2CO_3	0,036	3,82	0,036	3,82	0,036	3,82	0,036	3,82
NaOH	0,300	12,00	0,300	12,00	0,300	12,00	0,300	12,00

That means Mg^{2+} content of the catalyst had been decreased, while Cu content increased. For the second series, the M^{2+}/M^{3+} ratio of the catalyst was changed as 2, 3, 4, and 6 with a fixed 20 wt% Cu on the catalyst. $Cu_yMgAlOx$ catalysts prepared in this

series are named as $Cu_{20}MgAlO_2$, $Cu_{20}MgAlO_3$, $Cu_{20}MgAlO_4$, and $Cu_{20}MgAlO_6$. The molar weights of chemicals used to prepare the catalysts with the different M^{+2}/M^{+3} ratios can be seen in Table 2.3.

Table 3.3: The amount of chemicals used to prepare catalysts with different M^{+2}/M^{+3} ratios

Catalysts / **Chemicals**	**$CuMg_3Al_2O_7$**		**$Cu_{1.2}Mg_{4.8}Al_2O_{19}$**		**$Cu_{1.5}Mg_{6.5}Al_2O_{11}$**		**$Cu_{2.1}Mg_{9.9}Al_2O_{15}$**	
	$Cu_{20}PMO_2$		$Cu_{20}PMO_3$		$Cu_{20}PMO_4$		$Cu_{20}PMO_6$	
	mol	*g*	*mol*	*g*	*mol*	*g*	*mol*	*g*
CuMgAlO	0.020	6.01	0.02	7.85	0.015	7.26	0.010	6.68
$Mg(NO_3)_2x6H_2O$	0.061	15.67	0.095	24.44	0.097	24.92	0.099	25.39
$Al(NO_3)_3x9H_2O$	0.040	15.01	0.040	15.01	0.030	11.25	0.020	7.50
$Cu(NO_3)_2x2.5H_2O$	0.019	4.40	0.025	5.75	0.023	5.30	0.021	4.88
Na_2CO_3	0.048	5.09	0.048	5.09	0.036	3.82	0.024	2.54
NaOH	0.24	9.60	0.320	12.80	0.300	12.00	0.280	11.20

Catalyst preparation initiated with the preparation of LDH precursors, because catalysts are formed by the calcination of LDH precursors. Cu-based LDH precursors were prepared by co-precipitation method as follows: Suitable amounts of $Cu(NO_3)_2.2.5H_2O$, $Mg(NO_3)_2.6H_2O$ and $Al(NO_3)_3.9H_2O$ were dissolved in 100 ml de-ionized water and a solution was formed. simultaneously with 100 ml of a Sodium Hydroxide (NaOH) solution, this solution was slowly added through 100 ml dropping funnels into a well-stirred 500 ml beaker containing 150 ml of Na_2CO_3 solution at 60°C. NaOH was used as the precipitant. During the addition, the pH is kept at 10 by adjusting the flow rate of these two solutions and monitored by pHenomenal pH 1000 H model pH-meter. The addition was complete after ca. 45 min and the slurry formed was aged overnight (24h) at 60°C under stirring. The milk-like light-blue slurry formed for all of the LDH precursors with different M^{+2}/M^{+3} ratios. As the Cu content of the catalyst had been increased, the color of the slurry obtained after co-precipitation turned dark blue and finally the color became black for the catalyst including 40 wt% Cu content. The precipitate was filtrated and washed with deionized water until a pH of 7 was reached. The solid gained was dried at 110°C overnight, ground and sieved to a particle size below 125 μm.

To produce Cu-based mixed metal oxides, LDH precursors were calcined with a heating rate of 2°C/min from 40°C to 460°C and kept at this temperature for 6 h in static air. By means of calcination, the layered structure was destroyed and the

corresponding mixed metal oxides were obtained. According to the early studies, LDH undergoes some changes with increasing temperature. First, the removal of interlayer and interparticle water up to 250 °C and then the dehydroxylation of the layers from around 150 °C to 500°C are observed. The layered structure is destroyed by calcination at or above the dehydroxylation temperature and forms mixed metal oxides [122]. All catalysts with different M^{+2}/M^{+3} ratios prepared by calcination were green. However, the resulting colors of the catalysts with different Cu loadings were scaled from the green to dark green and finally to black for $Cu_{40}MgAlO_4$.

Also Cu_{20}/MgO was prepared by the same method that previously described and this notation corresponds to that 20% of the catalyst is composed of Cu and the rest was comprised of MgO. Exceptionally Cu_{20}/γ-Al_2O_3 was prepared by incipient wetness impregnation method, for which 5.86 g of $Cu(NO_3)_2.2.5H_2O$ was contacted with the solution of slightly excess Al_2O_3 (6.40 g). Then the wet powder was prepared by mixing and dried.

3.2. Catalytic Depolymerization Setup

Catalytic depolymerization experiments were carried out in the Lignin Laboratory of Molecular Catalysis Group in Chemistry and Chemical Engineering Department at Eindhoven University of Technology in the Netherlands. The catalytic depolymerization experiments were performed in two 100 ml stainless steel Parr batch autoclaves, equipped with thermocouple, pressure gauge and back-pressure regulator and heated by oven, shown in Figure 3.2.

3.3. Methods

In this part,

- Scotch pine characterization
- Catalyst characterization
- Catalytic depolymerization reactions
- Catalytic depolymerization products characterization are given.

Figure 3.2: Catalytic depolymerization setup

3.3.1. Scotch Pine Characterization

Proximate and ultimate analyses of the Scotch Pine were performed in Energy Institute Solid Fuel Analysis Laboratory at The Scientific and Technological Research Council of Turkey (TÜBİTAK) Marmara Research Center. Lignocellulosic properties of the SP was characterized in the laboratory of Forest Industry Engineering in Forest Products Chemistry and Technology Department at Istanbul University.

Proximate and ultimate analyses of the SP are determined in accordance with American Society for Testing and Materials (ASTM) and International Organization for Standardization (ISO). Methods used for each analysis and characterization results can be seen at Table 3.1. Ultimate analysis was made by LECO Truspec CHN-S Elemental Analysis Equipment in this laboratory. Termogravimetric analysis and calorimetric analysis are carried out by LECO TGA 701 Proximate Analysis Equipment and LECO AC 600 Calorimetry Equipment, respectively.

3.3.2. Catalyst characterization

The characterization of both LDH precursors and the catalysts was carried out by several physico-chemical techniques such as the N_2 Physisorption, X-Ray Diffraction (XRD), Temperature Programmed Desorption (CO_2-TPD) and Scanning Electron

Microscopy (SEM). Following sections explain the characterization methods sequentially.

Textural characteristics of the mixed metal oxides were investigated by N_2 Physisorption technique. Micromeritics TriStar II Gas Sorption Analyzer was run for the analysis since the parameters such as the specific surface area and the pore size distribution are the essential parameters to characterize the catalysts. Nitrogen physisorption isotherms were automatically interpreted by the Analyzer using Brunauer, Emmett and Teller theory (BET). As a result, the specific surface area (S_{BET}), pore volume (V^a) and pore diameter (D^b) were calculated.

Powder X-Ray Diffraction (XRD) patterns were analyzed using Bruker D2 Phaser Diffractometer and monochromatic Cu-Kα radiation. They were recorded with 0.02° (2) steps over the 5-80° angular range.

Temperature programmed desorption of CO_2 (CO_2-TPD) experiments were carried out to determine the strength and basic sites distribution of the catalysts. After the catalyst (50 mg) was pre-treated at 460°C for 1 h under He stream (50 mL/min), it was cooled down to 100°C and CO_2 (25 vol%) was introduced for adsorption at this temperature for 0.5 h. After the catalyst was swept with He for 60 min to remove the physisorbed CO_2 from catalyst surface, the temperature was increased linearly with rate of 10°C/min in He and the signal of CO_2 (M/e = 44) was recorded by online mass spectrometry (Quadrupole Mass Spectrometer, Balzers TPG-300). The amount of CO_2 was quantified by a calibration curve, which was established by thermal decomposition of certain amounts of $NaHCO_3$.

SEM analysis was made by FEI Quanta 3D FEG Dual Beam Instrument enables 3D material characterization and analysis. The instrument was operated at 1.5 kV pass energy for all the samples (except 3 kV for catalyst).

3.3.3. Catalytic depolymerization reactions

In a typical run, the autoclave was loaded with a suspension of 500 mg catalyst and 1000 mg Protobind 1000 lignin or SP in 40 mL ethanol. All reactions were performed in an inert environment. The reactor was sealed and purged/flushed with nitrogen several times to expel air and provide an inert atmosphere before the reaction was started. The autoclave was tested in case of a possible leak and then pressurized with N_2 to 10 bar. The reaction mixture inside the autoclave was heated up to the desired

reaction temperature under continuous stirring at 500 rpm within 1 h. The reaction was carried out for 4 h and the autoclave was cooled down to room temperature by a water bath.

Protobind 1000 lignin depolymerization reactions were carried out at 340 °C using all the catalysts previously prepared, although SP depolymerization reactions were carried out at two different temperatures (300°C and 340°C) over $Cu_{20}MgAlO_2$. According to Huang et al (2014), reaction temperatures were chosen between 300°C-350°C, because the rate of depolymerization becomes important in the range of these temperatures. Also supercritical ethanol was found more advantageous than other solvents. Reaction time was determined 4h based on the results indicating the disappearance of highly active phenolic hydroxyl groups after 4h which is desired for less repolymerization reaction [110].

Moreover, another series of depolymerization reactions were performed by SP. The amount of SP fed into the autoclave increased to 3000 mg keeping all the parameters the same. Cellulose and glucose were also depolymerized over $Cu_{20}MgAlO_2$ at 300 °C, similar to SP depolymerization. All other operating conditions were indentical to those set for Protobind 1000 lignin and SP for cellulose and glucose depolymerization.

3.3.4. Catalytic depolymerization products characterization

Catalytic depolymerization products gained at the end of reaction are gas phase products, liquid phase products and char. Also solid catalysts particles are found in the reaction medium. Catalytic products characterization starts with the characterization of gas phase products.

Gas phase products collected from the reaction medium, before the autoclave was opened (1) and analyzed by Gas-Solid Chromatography (GSC). Collected gas products sent to an Interscience Compact Gas Chromatography (GC) system, equipped with a Molsieve 5 Å and Porabond Q column each with a Thermal Conductivity Detector (TCD), and a Al_2O_3/KCl column with a Flame Ionization Detector (FID). The identification and quantification of gas products were done by using a gas cylinder containing known quantities of permanent gases.

The autoclave was checked for possible remaining gas product inside by adjusting the pressure to 0 bar. Then, the autoclave was opened to the ambient air. The product mixture remained inside the autoclave is composed of liquid phase products, solid

catalyst particles and char. A workup procedure developed by Huang et al (2014) was applied to the product mixture inside the autoclave [110]. The work-up procedure is schematized in Figure 3.3 where the numbers between brackets refer to the steps applied. Right after opening the autoclave, 10 µl n-dodecane was added as internal standard (ISTD) and approximately 1 ml of sample was taken from the reaction mixture, filtrated using 0.45 µm syringe filter and sent to GC-MS in order to identify the monomers yielded via depolymerization (2). The liquid phase products were analyzed by a Shimadzu 2010 GC-MS system equipped with a RTX - 1701 column (60 m × 0.25 mm × 0.25 µm) and a flame ionization detector (FID) with a mass spectrometer detector. Identification of products was achieved based on a search of the MS spectra with the NIST11 and NIST11s MS libraries. The peaks with the same molecular weight (M_w) were unified and presented by the structure determined by GC-MS. These products were further divided into four groups, namely hydrogenated cyclics (-O (oxygen-free)), hydrogenated cyclics (+O (oxygen-containing)), aromatics (-O) and aromatics (+O), according to the nature of the ring structure and functional groups. All the quantitative analyses of liquid phase product were based on GC-FID. Experimentally determined weight response factors of cyclohexane (1.221), cyclohexanone (0.992), ethyl benzene (1.103) and ethyl guaiacol (0.803) were used for these four groups related to *n*-dodecane as the ISTD.

Then all of the remaining product mixture is carefully collected from the autoclave and the residual inside the autoclave was gained by washing with ethanol (3) and added to the product mixture. Subsequently, the mixture was filtrated and the filter cake was washed with ethanol several times (4). The volume of the filtrate was leveled to 40 ml by adding ethanol, followed by acidification by adding 15 ml of a 0.1 mol/l HCl solution (final pH=1) (5), and 50 ml de-ionized water to precipitate unconverted Protobind 1000 lignin or SP and their high molecular-weight fragments (6). After aging for 30 min, the resulting mixture was filtered over a 0.45 µm filter membrane (7). The filter cake was retrieved by washing with Tetrahydrofuran (THF) (7). The solid residue from step (4) was then washed with excess THF in order to retrieve the unconverted Protobind 1000 lignin or SP adsorbed on catalyst (9). The residue was obtained by combining the two THF solutions and removing THF by rotary evaporation at 60 ºC. This fraction is donated as THF-soluble lignin residue (LR) or THF-soluble SP residue (SPR), which contains smaller fragments.

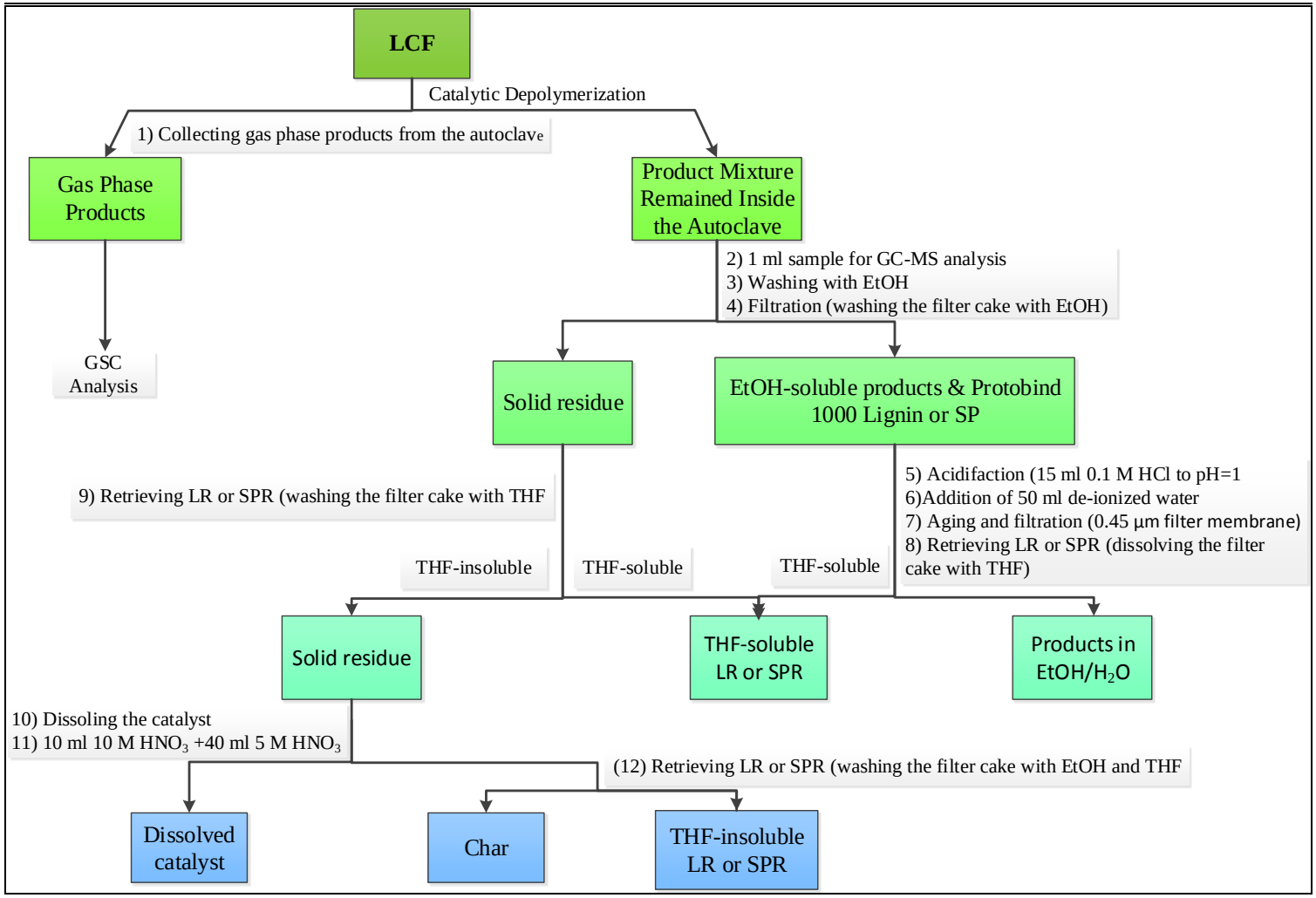

Figure 3.3: Work-up procedure of product mixture of catalytic Protobind 1000 Lignin and SP depolymerization [110].

After the separation of THF-soluble LR or SPR from the filter cake, the filter cake contains the solid catalyst particles, repolymerized products resulted from the undesired repolymerization reactions and char. In order to separate repolymerized products, first catalyst was dissolved respect to the procedure, explained in the literature [108]. 200 mg solid residue obtained from step (10) was subjected to a 50 ml flask. 10 ml 10 mol/L HNO3 was initially added to dissolve Cu. The slurry was further treated with addition of 40 ml 5 mol/L HNO_3 (11). The resulting mixture was filtered over a filter crucible (porosity 4).

The filter cake was retrieved by washing with excess ethanol and THF (12). After removing THF solvent by rotary evaporation, another fraction of LR or SPR was obtained and denoted as THF-insoluble LR or SPR residue. The remaining filter cake was regarded as char. Overall, the monomer and THF-soluble residue reflect the extent of depolymerization, while the THF-insoluble residue and char reflect the extent of repolymerization. The yields belong to the foregoing monomers, THF-soluble LR, THF-insoluble LR and char were calculated by Equations (3.1)-(3.4) given below:

$$\text{Yield of monomers (wt\%)} = \frac{\text{weight of monomers (calculated from GC-FID)}}{\text{weight of feedstock fed into the autoclave}} \times 100 \quad \textbf{(3.1)}$$

$$\text{Yield of THF-soluble residue (wt\%)} = \frac{\text{weight of THF-soluble residue}}{\text{weight of feedstock fed into the autoclave}} \times 100 \quad \textbf{(3.2)}$$

$$\text{Yield of THF-insoluble residue (wt\%)} = \frac{\text{weight of THF-insoluble residue}}{\text{weight of feedstock fed into the autoclave}} \times 100 \quad \textbf{(3.3)}$$

$$\text{Yield of char (wt\%)} = \frac{\text{weight of char\&undissolved catalyst}}{\text{weight of feedstock fed into the autoclave}} \times 100 \quad \textbf{(3.4)}$$

Fourier Transform-Infrared Spectroscopy (FT-IR) spectra of untreated SP, untreated Protobind 1000 lignin and THF-soluble SPRs were recorded on a Bruker D2 Phaser FT-IR spectrometer with a resolution of 4 cm^{-1} and 32 scans in the region of 4000-400 cm^{-1}. SEM was carried out by FEI Quanta 3D FEG Scanning Electron Microscope and the instrument was operated at 1.5 kV pass energy for all the samples (exceptionally operated at 3 kV for $Cu_{20}MgAlO_2$ catalyst).

4. RESULTS AND DISCUSSION

In this part, the results of

- Catalyst characterization
- Catalytic lignin depolymerization
- Scotch Pine characterization
- Catalytic Scotch Pine depolymerization will be presented.

4.1. Catalyst characterization

The effects of Cu content and M^{+2}/M^{+3} ratio of the catalyst on the catalyst properties were observed.

4.1.1. Effect of Cu content on the properties of catalysts

Various characterization techniques were applied to investigate the effect of Cu content on the physico-chemical properties of the catalysts. First of all, textural properties and elemental compositions of catalysts were obtained, seen in Table 4.1. The $MgAlO_4$ catalyst shows relative high surface area (245 m^2/g) and pore volume (0.82 cm^3/g). Surface area and pore volume are tend to decrease while the Cu content of the catalyst is increasing. Replacing the Mg by 10 wt% or 20 wt% of Cu results in a slightly decrease of the surface area and pore volume. Especially the presence of 40 wt% Cu on the catalyst decreases the surface area by half compared to Cu-free metal oxide. Therefore an excessive Cu content is anticipated to be undesired.

Table 4.1: Textural properties of the catalysts with different Cu loadings.

Catalysts	**S_{BET} (m^2/g)**	**V^a (cm^3/g)**	**D^b (nm)**	**Cu (wt%)**	**Mg (wt%)**	**Al (wt%)**	**(Cu+Mg)/Al atomic ratio**
$MgAlO_4$	245	0.82	13.0	-	36.50	9.77	4.20
$Cu_{10}MgAlO_4$	240	0.73	12.1	8.08	33.64	9.66	4.27
$Cu_{20}MgAlO_4$	206	0.72	13.8	16.33	28.30	9.13	4.24
$Cu_{40}MgAlO_4$	125	0.56	24.5	31.43	16.67	7.54	4.25

In all cases, the catalysts are found to be mesoporous materials (2nm <pore diameter <50nm). Similarly, the hysteresis loop in the isotherm of $Cu_{10}MgAlO_4$, $Cu_{20}MgAlO_4$ and $Cu_{40}MgAlO_4$ indicate the formation of mesoporosity, shown in Figure 4.1. Elemental analysis results show that the actual amount of Cu loading is slightly lower than the theoretical ones, which could be due to the adsorption of atmospheric CO_2 and H_2O that increasing the weight of catalysts. The actual (Cu+Mg)/Al ratios are between 4.20 and 4.27.

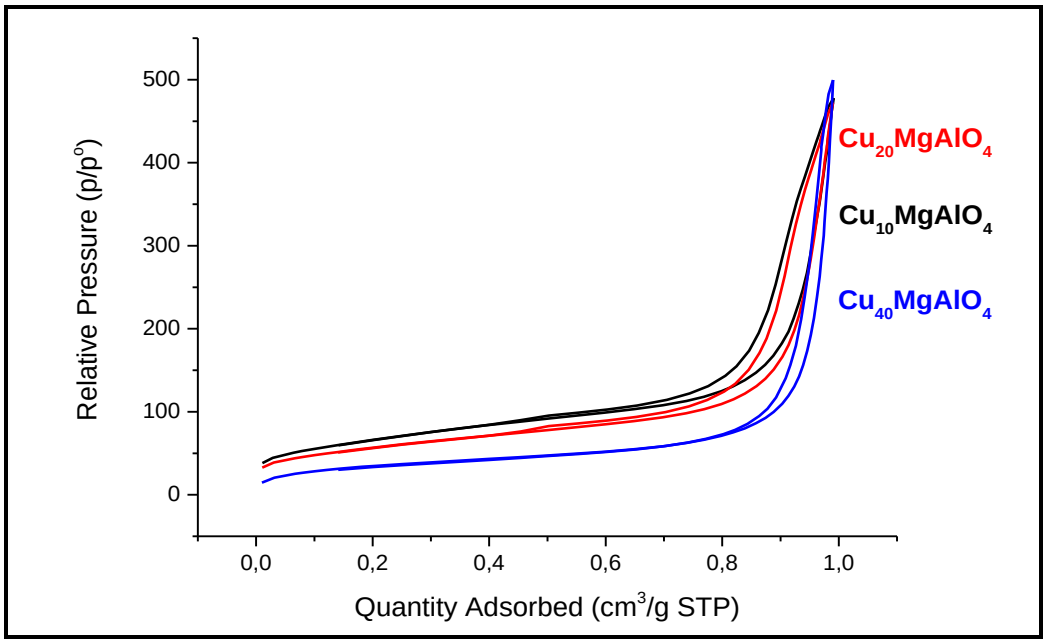

Figure 4.1: N_2 adsorption isotherms of the catalysts with different Cu loadings.

XRD patterns of LDH precursors is introduced in Figure 4.2. The patterns of Cu-free precursor contains the characteristic peaks corresponding to a well-defined hydrotalcite structure [123]. The trend observed for LDH precursor is consistent with a previous study, which investigated the characterization and catalytic activity of Cu-doped mixed metal oxides with the different Cu/Mg/Al ratios in dehydrogenation of 2-octanol and carried out by Crivello et al (2005) [114]. Partially replacing the Mg by 10 wt% or 20 wt% of Cu doesn't notably change the double-layered structure. However, further increasing the Cu loading to 40 wt% results in the formation of CuO. New characteristic diffraction peaks associated with CuO were observed. This observation points out the CuO species in the forms of highly dispersed/clustered state on the surface of $MgAlO_4$. The intensities of the characteristic peaks corresponding to the hydrotalcite structure were also seen to decrease. This indicates that excess amount of Cu loading results in collapsing the hydrotalcite structure.

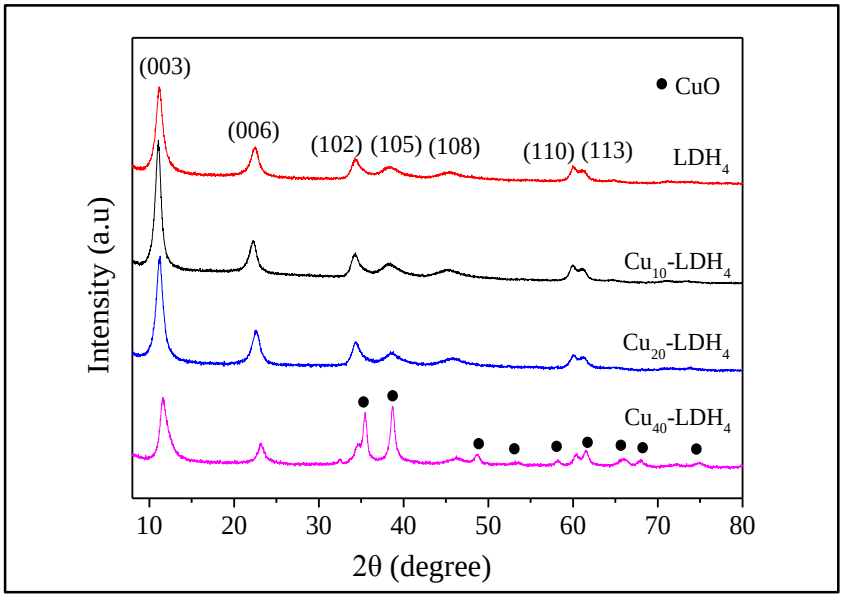

Figure 4.2: XRD patterns of LDHs with different Cu loadings.

After calcination of the LDHs at 460 °C for 6 h, XRD patterns of the samples changed, seen in Figure 4.3. The $MgAlO_4$, $Cu_{10}MgAlO_4$ and $Cu_{20}MgAlO_4$ samples have MgO-like structure where Cu^{2+} and Al^{3+} cations are dissolved in the lattice to form a solid solutions [124]. For the $Cu_{40}MgAlO_4$ samples, both of the MgO-like structure and CuO phases were detected.

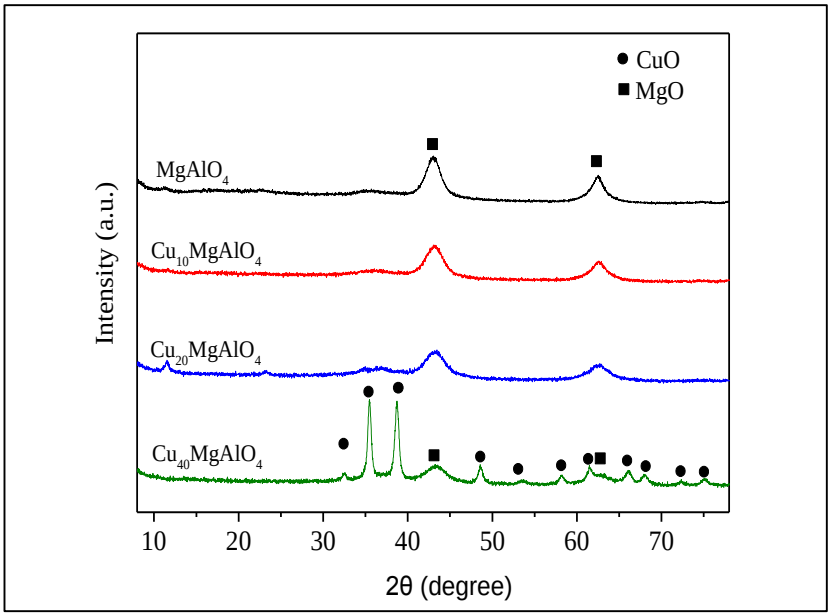

Figure 4.3: XRD patterns of the catalysts with different Cu loadings.

CO_2-TPD is applied to the mixed metal oxides derived from calcination of LDH precursors in order to determine the density and strength of basic sites over mixed metal oxides. In all cases, a broad desorption band, shown in Figure 4.4, is observed between 100°C and 460°C. However peaks indicating weak, medium and strong

strengths were changed for all catalysts. Peaks obtained for CO_2-TPD of $Cu_{20}MgAlO_4$ can be deconvoluted into three peaks at about 165°C (weak strength), 200°C (medium strength) and 255°C (strong strength). Weak, medium and strong strength peaks for CO_2-TPD of $Cu_{10}MgAlO_4$ were observed at about 170°C, 210°C and 270°C, respectively. As the Cu content of the catalyst was increasing, a shift was observed to the lower temperatures for all peaks.

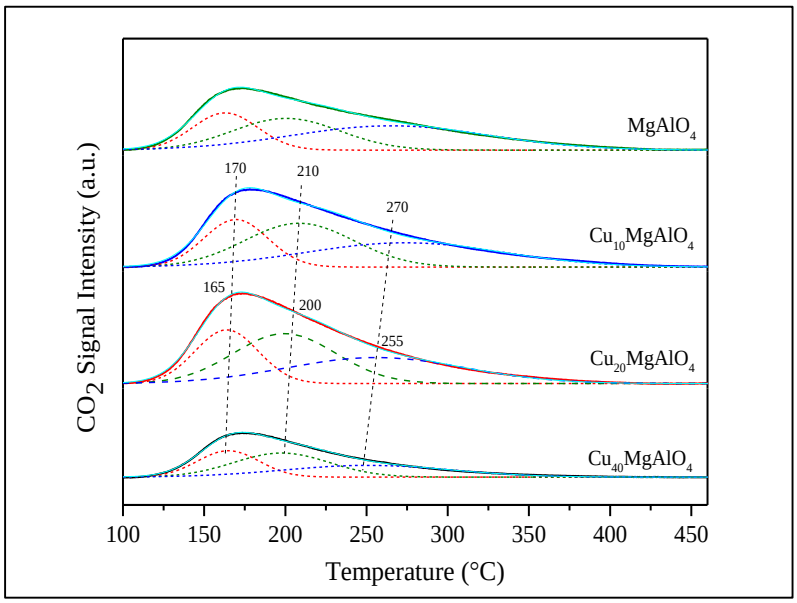

Figure 4.4: Basic site strengths of the catalysts with different Cu loadings.

The low-temperature desorption peak corresponds to OH^- groups. The medium-temperature peak can be ascribed to the Mg^{2+}-O^{2-}, Al^{3+}-O^{2-} and Cu^{2+}-O^{2-} acid-base pairs. The high-temperature peak is attributed to the strong basic sites associate with low coordinated O^{2-} anions. The amount of CO_2 desorbed in these peaks allowed to calculate the number of basic sites and basic sites density as shown in Table 4.2. The Cu-free catalyst ($MgAlO_4$) mainly contains medium (28%) and strong strength basic sites (52%).

Table 4.2: CO_2-TPD results of the catalysts with different Cu loadings.

Catalysts	CO_2 Desorption Peak (Area %)			Total CO_2 Adsorption (mmol CO_2/g)	Basic Sites Density (µmol/m^2)
	Weak (~165°C)	Medium (~200°C)	Strong (~255°C)		
$MgAlO_4$	20	28	52	0.27	1.09
$Cu_{10}MgAlO_4$	24	38	38	0.32	1.32
$Cu_{20}MgAlO_4$	29	38	33	0.35	1.72
$Cu_{40}MgAlO_4$	30	39	31	0.15	1.19

With increasing the amount of Cu loading, the ratio of strong-strength basic sites tends to decrease, while the weak- and medium-strength basic sites were seen to increase. Consistently, the desorption peaks of these three basic sites were all shift to lower temperature side (Figure 4.4). The overall basic sites and basic sites density were seen to increase with the increase of Cu loading up to 20 wt%. However, further increasing the Cu loading to 40 wt% results in significantly decreasing the amount of basic sites and density. This could be explained by the formation of CuO during the synthesis of its hydrotalcite precursor. This indicates that the doping of proper amount of Cu (<40 wt%) decreasing the strength of basic sites, but increasing the number and density of basic sites.

The $Cu_{20}MgAlO_4$ shows the maximum basic sites (0.35 mm/g) and basic sites density (1.72 μmol/m^2), as it is seen in Figure 4.5 and Table 4.2. The weak, medium and strong basic sites are 29%, 38% and 33% respectively.

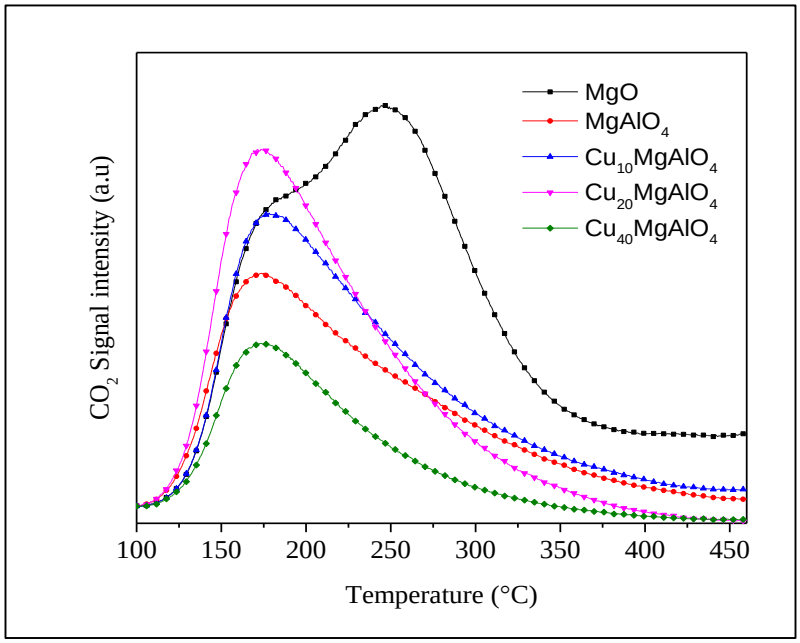

Figure 4.5: CO_2-TPD profiles of the catalysts with different Cu loadings.

4.1.2. Effect of M^{2+}/M^{3+} ratio on the properties of catalysts

First, N_2 Adsorption isotherms of $CuMgAlO_x$ mixed metal oxides and Cu_{20}/γ-Al_2O_3 were recorded. Hysteresis clearly seen in Figure 4.6 is the indicative of the presence of mesopores for all catalysts.

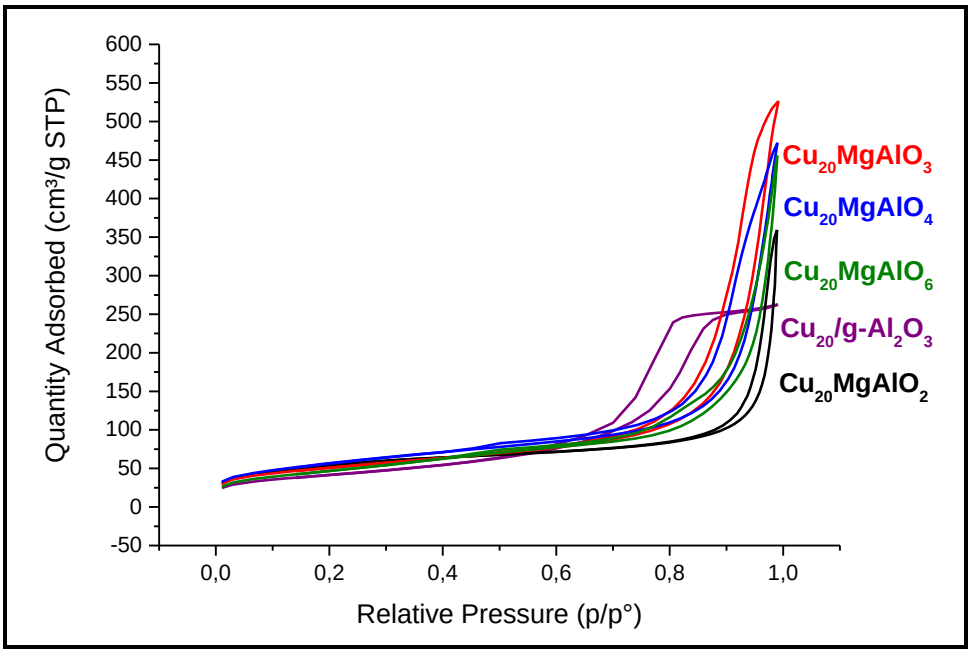

Figure 4.6: N_2 Adsorption Isotherms of the catalysts with different M^{2+}/M^{3+} ratios.

Textural properties of the mixed metal oxides were obtained by N_2 Adsorption and they can be seen at Table 4.3. Although all Cu-doped mixed oxides have similar surface areas, the highest surface area belongs to $Cu_{20}MgAlO_4$ catalyst. Notably, this catalyst has relatively low pore diameter. Despite the fact that pore volume increased when the M^{+2}/M^{+3} ratio had increased from 2 to 3, considerable change could not observe for further increment in M^{+2}/M^{+3} ratio. Similar to the mixed metal oxides with different Cu loadings, the catalysts are found to be mesopores materials.

Table 4.3: Textural properties of the catalysts with different M^{2+}/M^{3+} ratios.

Catalysts	S_{BET} (m^2/g)	V^a (cm^3/g)	D^b (nm)
Cu_{20}/γ-Al_2O_3	150	0.41	7.6
$Cu_{20}MgAlO_2$	189	0.53	15.6
$Cu_{20}MgAlO_3$	183	0.80	17.0
$Cu_{20}MgAlO_4$	206	0.72	13.8
$Cu_{20}MgAlO_6$	170	0.71	14.9
CuO/MgO	173	0.49	10.9

Surface functionalities of LDH precursors and catalysts were investigated by XRD method. It is known that the surface basicity of the catalyst is highly affected by the (Cu+Mg)/Al ratio or the Cu content [120]. In all cases, LDH or hydrotalcite structure were seen to be destroyed after calcination of the LDH precursors. As it is clearly seen

in Figure 4.7, similar trend was observed for all LDH precursors, but higher Mg content of the samples led broader peaks than those contain less Mg. Before calcination, higher (Cu+Mg)/Al ratio tends to form amorphous phase.

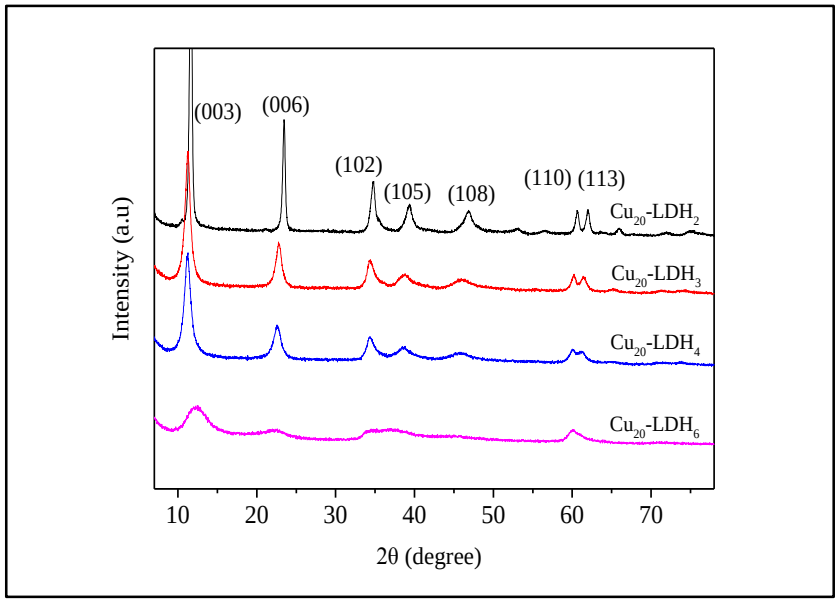

Figure 4.7: XRD patterns of LDHs with different M^{2+}/M^{3+} ratios.

XRD patterns of the catalysts prepared by the calcination of LDH precursors are shown in Figure 4.8. Mainly Cu ions, such as Cu^{+2} and Cu^{+} were mainly observed on the surface of the catalysts. Although the similar diffraction peaks were observed in the case of $CuMgAlO_x$ catalysts, $Cu_{20}/\gamma\text{-}Al_2O_3$ catalyst gave different peaks indicating the presence of CuO and $\gamma\text{-}Al_2O_3$.

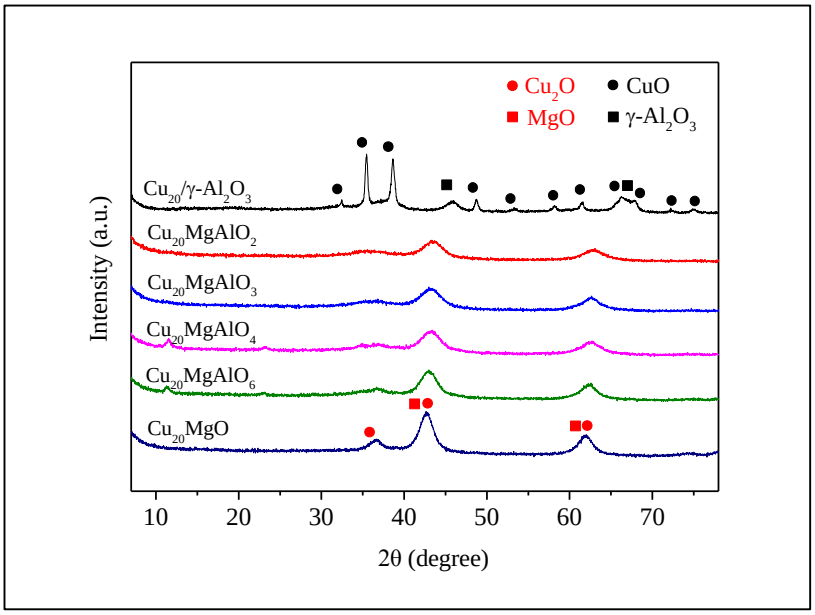

Figure 4.8: XRD patterns of the catalysts with different M^{2+}/M^{3+} ratios.

In addition, Cu_2O and MgO were recognized on Cu_{20}/MgO catalyst after calcination. CO_2-TPD profiles in which desorption peaks are shown between 100°C and 500°C in all cases.

Base strength of the catalysts were aimed to be associated with their different M^{2+}/M^{3+} ratios. Distinctively, three main peaks with maxima at about 165°C (weak basic strength), 200°C (medium basic strength) and 255°C (strong basic strength) were observed only with $Cu_{20}MgAlO_4$. The distribution of weak, medium and strong sites can be clearly seen in Figure 4.9.

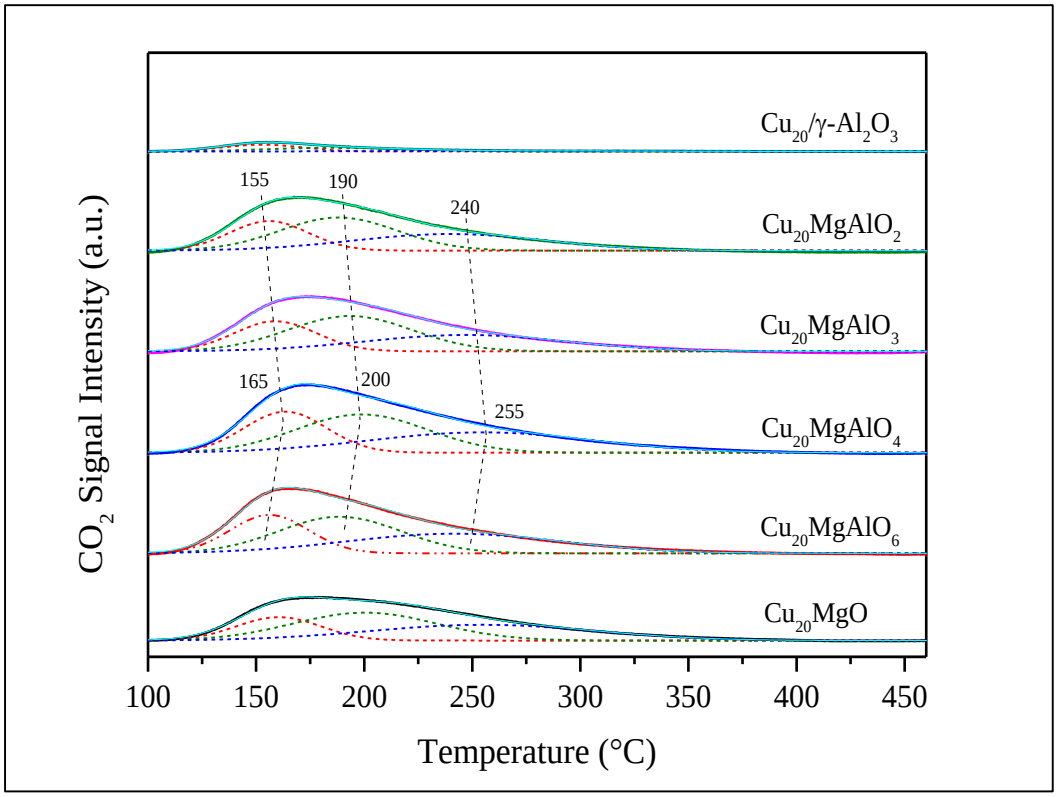

Figure 4.9: Basic site strengths of the catalysts with different M^{2+}/M^{3+} ratios.

$Cu_{20}MgAlO_2$ and $Cu_{20}MgAlO_3$ have similar medium temperature peaks, related to Mg^{2+}- O^{2-} and CuO pairs [125]. Nonetheless, one high temperature peak was observed in the presence of $Cu_{20}MgAlO_6$ and this peak was associated with strong Lewis basic sites of O^{2-} anions [125]. Also Table 4.4 shows the CO_2 desorption peaks areas of basic sites.

Table 4.4: CO_2-TPD Results of the catalysts with different M^{2+}/M^{3+} ratios.

Catalysts	CO_2 Desorption Peak (Area %)			Total CO_2 Adsorption (mmol /g)	Basic Sites Density ($\mu mol/m^2$)
	Weak (165°C)	Medium (200°C)	Strong (255°C)		
$Cu_{20}MgO$	20	47	33	0.18	1.05
$Cu_{20}MgAlO_6$	0	44	56	0.37	2.16
$Cu_{20}MgAlO_4$	29	38	33	0.35	1.72
$Cu_{20}MgAlO_3$	28	38	34	0.27	1.46
$Cu_{20}MgAlO_2$	24	39	38	0.26	1.36
Cu_{20}/γ-AlO_3	81	6	13	0.02	0.13

Catalytic depolymerization reactions carried out at 340 ºC for 4h by the catalyst with different Cu loadings resulted in different product yields, shown in Table 4.5.

Table 4.5: Product yield of the reactions carried out with catalysts with different Cu loadings.

Entry	Reaction Conditions		Product Yield (wt%)				Mass Balance (wt%)
	Catalysts	T (ºC)	Monomers	THF-soluble LR	THF-insoluble LR	Char	
1	$MgAlO_4$	340	9	32	14	<1	56
2	$Cu_{10}MgAlO_4$	340	21	61	13	<1	96
3	$Cu_{20}MgAlO_4$	340	36	69	6	<1	111
4	$Cu_{40}MgAlO_4$	340	26	79	8	<1	114

Liquid phase products' identification of all reactions was obtained by GC-MS analysis. Products originated from lignin, cellulose, hemicellulose were distinguished the products originated from ethanol via reference reactions of ethanol at relevant temperatures. After product identification, all products were contrasted with the products which are obtained by ethanol conversion reactions and identified by GC-MS. Thus, ethanol products distinguished from other products.

Considering monomer yields, Cu-free $MgAlO_x$ catalyst found to generate very low monomer yield (9%) compared to Cu-based catalysts. The presence of Cu in catalysts resulted in two- to four-fold increase in monomer yield (21, 36 and 26%, respectively). The highest monomer yield was observed with $Cu_{20}MgAlO_4$ catalyst, however further increase in Cu content caused a negative effect on the monomer yield. In addition, the amount of THF soluble and THF insoluble lignin residues (LRs), extracted from the product mixture in reaction medium, differs according to the catalysts.

Interestingly, the THF-soluble LR almost doubled by 10% Cu addition to $MgAlO_4$ and had an uptrend while Cu content was increasing up to 40%. Overall, the yield of THF-soluble residue and mass balance increased with increasing Cu loading. This indicates that reactions (alkylation and esterification) between ethanol and lignin were enhanced due to the Cu content. On the contrary, THF-insoluble LR declined with increasing Cu loading with an exception of $Cu_{40}MgAlO_4$. Catalysts without Cu and excess amount of Cu resulted in more THF-insoluble LR and more repolymerization. These catalysts are previously indicated to show less basic sites and basic sites density in Table 4.2. Based on this, more basic sites and higher basic sites density favor of hindering repolymerization. The amount of char obtained by the reactions slightly changed for all catalysts and remained below 1 wt%.

To sum up, product yields deduced that 20% of Cu loading had the desired catalytic activity for lignin depolymerization in supercritical ethanol at 340°C for 4h. $Cu_{20}MgAlO_4$ provided the highest monomer yield, relatively acceptible THF-soluble LR and lowest THF-insoluble LR. Highest monomer yield indicates higher depolymerization, whereas lowest THF-insoluble LR is the indicator of less repolymerization. Consequently, this indicates that $C_{20}MgAlO_4$ shows highest depolymerization and lowest repolymerization activity. Another important criteria was selectivity in terms of catalytic activity in this study. Figure 4.10. shows the monomeric product distribution and the selectivities after 4h reaction with aforementioned catalysts.

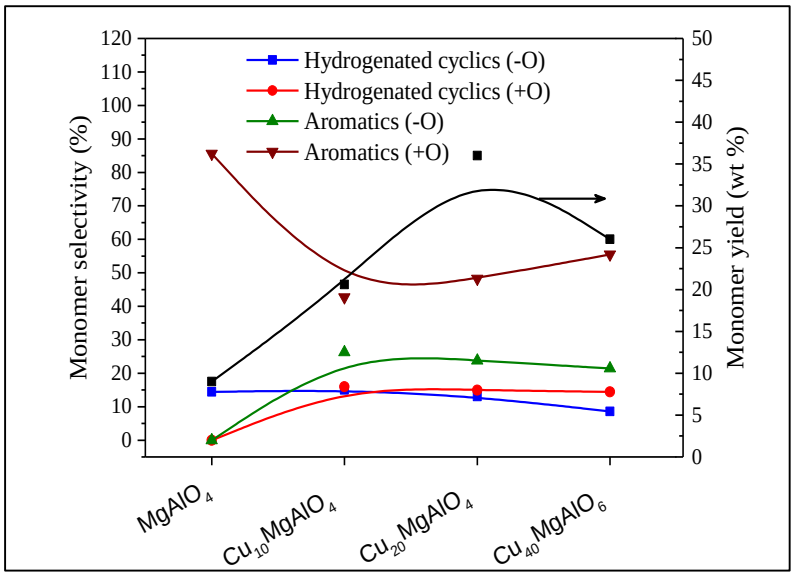

Figure 4.10: Monomeric product distribution and selectivity following the reactions carried out with the catalyst with different Cu loadings.

Oxygenated aromatics decreased and similarly deoxygenated aromatics enhanced by Cu loading to the catalyst compared to Cu-free $MgAlO_4$. Therefore, Cu inferred to be essential for the deoxygenation of aromatics. Although the selectivities of hydrogenated cyclics did not changed considerably regarding $Cu_{10}MgAlO_4$, $Cu_{20}MgAlO_4$ and $Cu_{40}MgAlO_4$, the selectivities of aromatics were sensible to varying Cu loadings. $Cu_{10}MgAlO_4$ shows highest deoxygenation activity and $Cu_{20}MgAlO_4$ presents good deoxygenation activity.

Also, gas products' distribution analyzed by GC gives information about catalytic activities of the catalysts. Seven gas products (CH_4, C_2H_6, C_2H_4, C_3H_8, CO_2, H_2 and CO) quantitatively analyzed by GC, shown in Table 4.6.

The amounts of gas products except H_2 did not dramatically changed with increasing Cu content of the catalysts. However, H_2 formation revealed the dehydrogenation ability of the catalysts. It is known that lignin conversion at high temperatures forms H_2 proves the cracking of aromatic rings [65]. Importantly, dehydrogenation ability was figured out to be in line with the monomer yields previously presented. H_2 formation was very low as a result of the reaction catalyzed by $MgAlO_4$. Cu loading up to 20% was seen to increase H_2 formation and further Cu loading had a negative effect.

Cu is found to be essential as a supporting material in the catalyst. Both the presence of Cu on the catalysts and an optimum distribution of basic and acidic sites on the catalysts were found essential for catalytic depolymerization of lignin. Results show that there is an optimum distribution of acidic and basic sites over the catalyst in order to achieve an optimum dehydrogenation.

Neither CuO/MgO nor Cu_{20}/γ-Al_2O_3 achieved high monomer yields. Similarly, a recent study focusing on alcohol coupling reactions over mixed metal oxides reported that Mg and Al oxide phases together maximize C-C coupling reactions rates, was not the case in the presence of monometallic oxides (MgO or Al_2O_3). Because the contact between these phases is said to bring along the optimum distribution (specific combination) of weak Lewis acid and strong Brønsted base pair sites [115].

Table 4.6: Gas products in case of the catalysts with different Cu loadings.

Entry	Reaction Conditions			mmol								Sum (mmol)
	Catalysts	T (°C)	t (h)	CH_4	C_2H_6	C_2H_4	C_3H_8	C_3H_6	CO_2	H_2	CO	
1	$MgAlO_4$	340	4	1.00	1.16	0.83	0.09	0.22	1.56	6.81	1.19	12.85
2	$Cu_{10}MgAlO_4$	340	4	2.63	2.48	2.14	0.17	1.38	1.41	24.06	2.59	36.86
3	$Cu_{20}MgAlO_4$	340	4	2.57	2.45	1.61	0.16	0.95	1.88	29.97	2.73	46.24
4	$Cu_{40}MgAlO_4$	340	4	2.63	2.45	1.61	0.16	0.95	1.88	29.97	2.73	42.38

Table 4.7: Gas products in case of the catalysts with different M^{2+}/M^{3+} ratio.

Entry	Reaction Conditions			mmol								Sum (mmol)
	Catalysts	T (°C)	t (h)	CH_4	C_2H_6	C_2H_4	C_3H_8	C_3H_6	CO_2	H_2	CO	
1	$Cu_{20}/\gamma\text{-}Al_2O_3$	340	4	1.70	3.29	5.08	0.17	0.28	2.23	7.59	1.96	22.29
2	$Cu_{20}MgAlO_2$	340	4	2.77	2.07	1.68	0.12	1.05	1.51	33.46	2.70	45.36
3	$Cu_{20}MgAlO_3$	340	4	2.34	1.79	1,54	0.12	0.87	1.86	30.76	2.50	41.79
4	$Cu_{20}MgAlO_4$	340	4	2.57	1.95	1.75	0.14	0.90	1.80	34.76	2.38	46.24
5	$Cu_{20}MgAlO_6$	340	4	2.33	1.74	1.46	0.11	0.98	1.49	27.39	2.06	37.56
6	CuO/MgO	340	4	2.03	1.92	2.40	0.14	2.00	1.49	22.33	1.69	34.01

4.2.2. Effect of M^{2+}/M^{3+} ratio of catalysts on catalytic lignin depolymerization

Table 4.7. shows the gas products' distribution of lignin depolymerization reaction in the presence of catalysts with different M^{2+}/M^{3+}. Excluding H_2, the amounts of gas products obtained from reaction medium did not considerably change. However, H_2 production was found to be very low in case of $Cu_{20}/\gamma\text{-}Al_2O_3$ catalyst and increased as a result of the presence of basic sites in the catalyst. The variation in the amount of hydrogen produced during lignin depolymerization was associated with the catalytic activity. Basic sites were revealed to be more active for dehydrogenation and Guerbet reaction. The highest H_2 production was yielded in the presence of $Cu_{20}MgAlO_4$ catalyst, which makes this catalyst preferable among other Cu-doped mixed metal oxide catalysts.

Catalytic depolymerization reactions carried out at 340 ºC for 4h by the catalyst with different M^{2+}/M^{3+} ratio resulted in different product yields, shown in Table 4.8. According to the yields, the highest monomer yield (36%) and relatively low yield of THF-soluble fraction were reached with $Cu_{20}MgAlO_4$ [Entry 4]. Surprisingly, Lewis acid sites are found out to cause 26 wt% char formation, which was quite high compared to all other samples [Entry 1].

Table 4.8: Product yield of the reactions with catalysts with different M^{2+}/M^{3+} ratio.

Entry	Reaction Conditions		Product Yield (wt%)				Mass Balance (wt%)
	Catalysts	T (ºC)	Monomers	THF-soluble LR	THF-insoluble LR	Char	
1	$Cu_{20}/\gamma\text{-}Al_2O_3$	340	26	40	4	23	93
2	$Cu_{20}MgAlO_2$	340	30	72	8	<1	111
3	$Cu_{20}MgAlO_3$	340	31	75	8	<1	115
4	$Cu_{20}MgAlO_4$	340	36	69	6	<1	111
5	$Cu_{20}MgAlO_6$	340	31	70	7	<1	109
6	CuO/MgO	340	20	47	15	0	82

This observation of undesired char formation in the case of $Cu_{20}/\gamma\text{-}Al_2O_3$ necessitated the presence of basic sites for minimal char formation during lignin depolymerization. In contrast, basic sites converted lignin without char formation [Entry 6]. However, they led to a higher yield of THF-insoluble fraction obtained at the end of reaction.

Moreover, selectivity of the monomers were identified respect to the ratio and they can be seen along with monomer yields in Figure 4.11. $Cu_{20}MgAlO_4$ catalyst showed the

highest monomer yield and deoxygenation activity. Basic sites accomplished the cleavage of $–OCH_3$ groups and facilitated deoxygenation regarding the less oxygenated products obtained, whereas more oxygenated products were observed in the presence of acidic sites, which were interpreted to be less effective for deoxygenation. Reactions carried out by $Cu_{20}/\gamma\text{-}Al_2O_3$ and CuO/MgO revealed that both acidic and basic sites were crucial to be together in the consideration of the desired monomer yield.

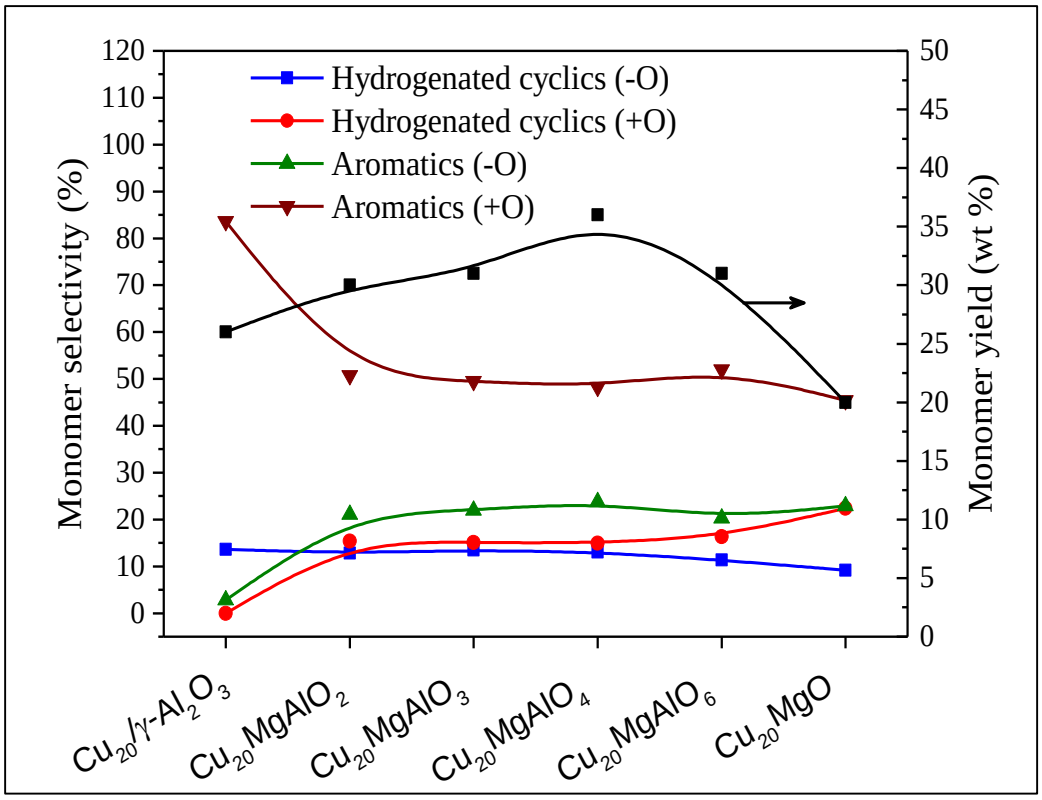

Figure 4.11: Monomeric product distribution and selectivity following the reactions carried out with the catalyst with changing M^{2+}/M^{3+} ratio.

4.2.3. Monomeric products of catalytic lignin depolymerization

Detailed identification of monomers by GS-MS revealed that hydrogenated cyclics (-O and +O) and aromatics (-O and +O) are the main products obtained by lignin depolymerization over $CuMgAlO_x$ catalysts. Although monomeric products of each catalytic lignin depolymerization reaction were not identified, the monomeric product distribution of catalytic lignin depolymerization at 340°C for 4h using $Cu_{20}MgAlO_4$ catalyst is illustrated in Figure 4.12. Interpreting the monomeric products given below, Oxygen-containing aromatics were found dominant followed by Oxygen-free aromatics. Yields of oxygen-containing and oxygen-free hydrogenated cyclics were almost similar.

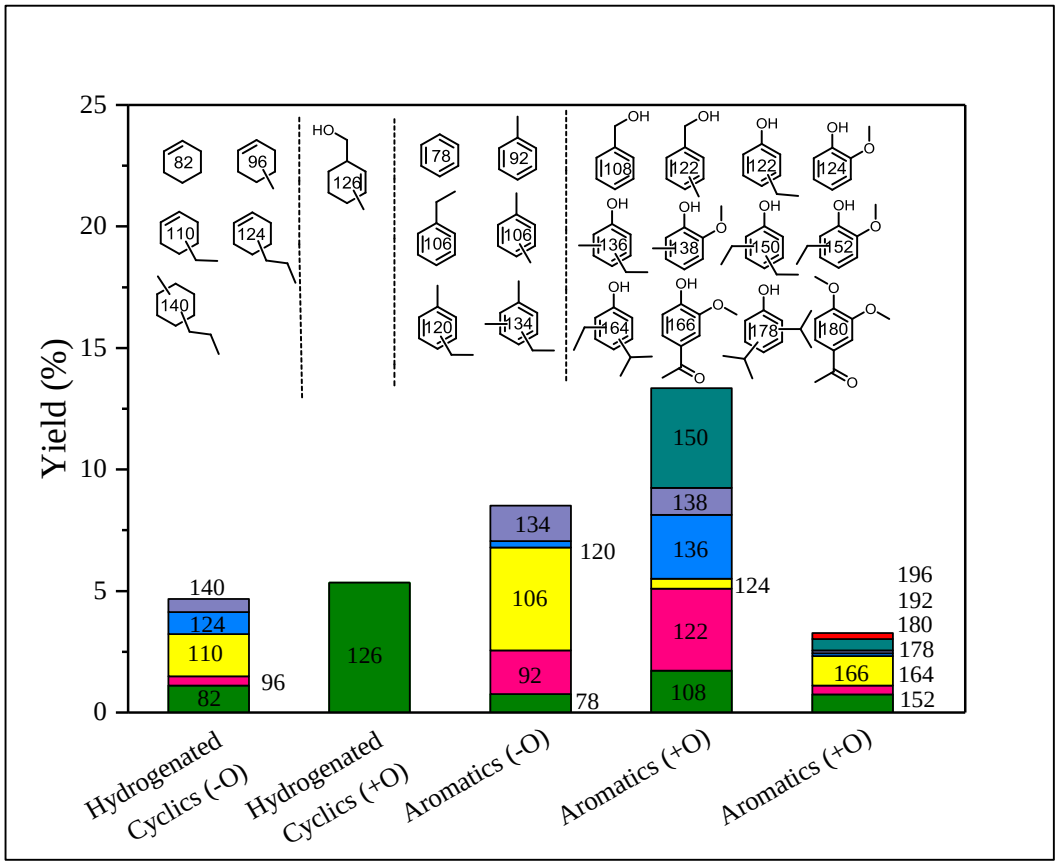

Figure 4.12: Monomeric product distribution following lignin reaction at 340°C for 4h using $Cu_{20}MgAlO_4$ catalyst.

As it varies according to the monomeric product, molecular weights were found to be between 82 and 196 g/mol. Consistent with a study carried out by Ma and co-workers, some high molecular weight alcohols, known to occur by Guerbet reaction between ethanol and the aliphatic fragments in lignin, were observed [112].

4.3. Scotch Pine Characterization

Proximate and ultimate analysis results and lignocellulosic composition of SP is given in Table 4.9. SP used in the experimental study contains about 52% C, 6% H, 39% O and a small amount of N and S on dry basis, however the original sample has almost 9% moisture on wet basis (as-received). Volatile matter comprises 82.42% of the SP on dry basis. Also lignocellulosic composition of the SP including holocellulose (cellulose and hemicellulose), lignin etc. was determined. The empirical formula of SP is $CH_{1.41}O_{0.56}N_{0.005}$ found by further calculations.

Table 4.9: Characterization results of SP.

Characteristics	Scotch Pine		Methods
	Wet Basis	Dry Basis	
Proximate Analysis (wt%)			
Fixed Carbon	15.29	16.82	ASTM D 3172-13
Volatile Matter	74.9	82.42	ASTM D 7582-12
Moisture	9.13	-	ASTM D 7582-12
Ash	0.69	0.76	ASTM E 1755-01
Ultimate Analysis (wt%)			
Carbon	47.62	52.40	ASTM D 5373-14
Hydrogen	6.66	6.21	ASTM D 5373-14
Oxygen	35.49	39.41	ASTM D 3176-09
Sulfur	0.82	0.91	ASTM D 4239-14
Nitrogen	0.28	0.31	ASTM D 5373-14
Ash	0.69	0.76	ASTM E 1755-01
Empirical formula	$CH_{1.67}O_{0.69}N_{0.005}$	$CH_{1.41}O_{0.56}N_{0.005}$	Calculation
H/C molar ratio	1.67	1.41	Calculation
O/C molar ratio	0.69	0.56	Calculation
Upper Heating Value (MJ/kg)	18.27	20.10	ASTM D 5865-13
Lower Heating Value (MJ/kg)	16.88	18.81	ASTM D 5865-13 ISO 1928-09
Lignocellulosic Composition (wt%)			
Holocellulose		72.97	Wise method [126]
Lignin		27.2	Runkel method [127]
Ash		0.38	TAPPI T 211 om-85

4.4. Catalytic Scotch Pine Depolymerization

Catalytic SP depolymerization over $Cu_{20}MgAlO_4$ in supercritical EtOH resulted in liquid monomers sourced from lignin, cellulose and hemicellulose, THF-soluble SPR, THF-insoluble SPR and char at 300 °C and 340 °C. Also pure cellulose as a model compound of SP and glucose as a model compound of cellulose were catalytically depolymerized in the same operating conditions to compare product yields and product distribution. Product yields of the catalytic depolymerization reactions according to the reaction conditions can be seen in Table 4.10. Liquid phase products' identification of all reactions was obtained by GC-MS. Products originated from lignin, cellulose, hemicellulose were distinguished the products originated from ethanol via reference reactions of ethanol at relevant temperatures. After product identification, all products were contrasted with the products which are obtained by ethanol conversion reactions and identified by GC-MS. Thus, ethanol products distinguished from other products. Figure 4.13 shows the related screen of GC-MS Data Comparison belongs to catalytic SP depolymerization at 300 °C and ethanol conversion at 300 °C. In this figure, pink peaks refer to the products of catalytic SP depolymerization and blue peaks refer to the products of ethanol conversion.

Table 4.10: Product yields of SP depolymerization reactions in supercritical ethanol.

Entry	Reaction conditions			Product yield (wt %)				
	Feedstocks		T (°C)	Monomers		THF-soluble SPR	THF-insoluble SPR	Char
				L[a]	H&C[b]			
1	SP	1g	300	5	20	11	7	12
2	SP	3g	300	6	8	10	2	2
3	SP	1g	340	19	31	14	0	1
4	SP	3g	340	12	14	11	0	4
5	Cellulose	1g	300	NaN	52*	1	0	1
6	Glucose	1g	300	NaN	57**	N/A	N/A	N/A

[a] Lignin
[b] Hemicellulose & Cellulose
* This data only shows the weight percent of the monomers arised from cellulose.
** This data only shows the weight percent of the monomers arised from glucose.

The second step was the determination of the products originated from lignin and products originated from cellulose and hemicellulose. This time, the product identification of catalytic lignin depolymerization at relevant temperatures over $Cu_{20}MgAlO_4$ were taken as a reference. Lignin products distinguished from cellulose and hemicellulose products. Finally, the individual monomer yields of carbohydrates (cellulose and hemicellulose) and lignin were calculated separately.

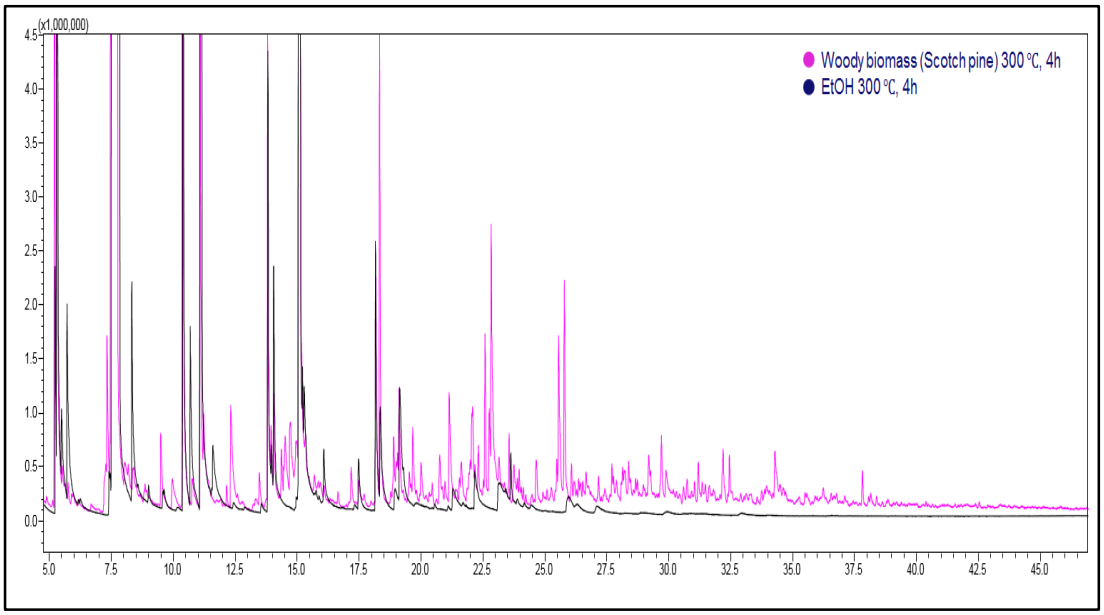

Figure 4.13 : GC-MS data comparison of catalytic SP depolymerization at 300 °C and ethanol conversion at 300 °C for 4h.

Entries 1-4 in Table 4.10 show the catalytic depolymerization products of SP in supercritical ethanol over $Cu_{20}MgAlO_4$ for 4 h. Of them, Entry 2 and Entry 4 belong to the catalytic SP depolymerization carried out by 3000 mg of SP. Because the effect

of the increased amount of SP fed into the autoclave with the same amount of the catalyst was questioned. The total monomer yield of catalytic SP depolymerization at 300 °C for 1000 mg of SP and 3000 mg of SP are 25 wt% and 14 wt%, respectively [Entry 1 and 2]. In addition, The total monomer yield of catalytic SP depolymerization at 340 °C for 1000 mg of SP and 3000 mg of SP are 50 wt% and 26 wt%, respectively [Entry 3 and 4]. It is clearly seen that, increased amount of SP fed into the autoclave resulted in an almost one-half decrease in total monomer yield, mostly affected by carbohydrates' monomer yield. However, monomer yield almost doubled in reactions at 340 °C, compared to those at 300 °C [Entry 1 and 3]. Monomer yield of catalytic cellulose depolymerization was 52 wt% as high as expected compared to the monomer yield of SP.

Neither the amount of the SP feed nor the reaction temperature drastically changed the yield of THF-soluble residue. Remarkably, high temperature eliminated the production of THF-insoluble residue. Although a trend could not observe, char production were keen to decrease with increasing temperature promotes the depolymerization. Increased amount of SP came up with relatively higher char formation.

Table 4.11 displays the products of hemicellulose and cellulose as a result of catalytic SP depolymerization. The compound names are given with their weight amounts, can be compared with the specific amount of internal standard, n-dodecane added to the table. Overall results put forward seven main product group obtained from cellulose and hemicellulose, namely alcohols, aldehydes, alkanes, alkenes, esters, ethers, and ketones. Aliphatic and aromatic hydrocarbons were detected ranging from C_5 to C_{17}, where alcohols and esters constitute the majority of the monomers identified.

SP depolymerized at 340 °C resulted in much more hemicellulose and cellulose products than the reaction carried out at 300 °C, shown in Table 4.12. Based on this observation, the depolymerization at 340 °C can be interpreted to facilitate the depolymerization. In this case ethers were not detected among the monomers, differently from the reaction at 340 °C.

Table 4.11: Cellulose and hemicellulose products of SP depolymerization at 340°C for 4h over $Cu_{20}MgAlO_4$ catalyst.

Name of Compound	C Number	Molecular Weight (g/molg)	The Amount (mg)
Alcohols			
1-Butanol, 2-methyl-	C5	88	60.36
3-Hexen-1-ol	C6	100	19.10
1-Hexen-3-ol	C6	100	8.40
5-Methyl-1-heptanol	C8	130	13.91
1-Heptanol, 2-propyl-	C9	158	28.84
1-Heptanol, 2-propyl-	C10	158	5.15
2-Decanol	C10	158	2.39
1-Octanol, 2-butyl-	C12	186	5.34
1-Octanol, 2-butyl-	C12	186	5.56
1-Dodecanol	C12	186	4.83
2-Octenal, 2-butyl-	C12	182	2.38
2-Octenal, 2-butyl-	C12	182	7.44
2-Octenal, 2-butyl-	C12	182	2.82
Aldehydes			
2-Butenal, 2-ethyl-	C6	98	18.34
Octanal	C8	128	12.79
Hexanal, 2-ethyl-	C8	128	4.03
Alkanes			
Cyclopropane, 1-heptyl-2-methyl-	C11	154	4.72
Cyclopropane, nonyl-	C12	168	6.59
Alkenes			
2-Heptene, 3-methyl-	C8	112	10.36
2-Octene	C8	112	4.45
3-Ethyl-3-hexene	C8	112	5.54
1-Heptene, 6-methyl-	C8	118	6.88
3-Undecene, 3-methyl-	C12	168	0.42
4-Dodecene	C12	168	5.72
Esters			
Propanoic acid, 2-hydroxy-, ethyl ester	C5	118	10.28
Pentanoic acid, ethyl ester	C7	130	8.80
Pentanoic acid, ethyl ester	C7	130	8.62
Butanoic acid, 2-methyl-, ethyl ester	C7	130	17.89
Hexanoic acid, ethyl ester	C8	144	4.26
Butanoic acid, 3-methyl-, butyl ester	C9	158	13.92
Propanoic acid, 2-methyl-, 2-methylbutyl ester	C9	158	4.76
Heptanoic acid, ethyl ester	C9	158	12.37
Acetic acid, octyl ester	C10	172	5.80
Hexanoic acid, 2-ethyl-, ethyl ester	C10	172	5.66
Octanoic acid, 4-methyl-, ethyl ester	C11	186	12.43
Butyl 2-ethylhexanoate	C12	200	5.27
2-Ethylbutyl hexanoate	C12	200	12.42
Butyl 4-ethyloctanoate	C14	228	8.02
Octanoic acid, 4-methylpentyl ester	C14	228	6.51
n-Butyl laurate	C16	256	3.84
n-Capric acid n-heptyl ester	C17	270	5.43
Ethers			
Ethane, 1,1-diethoxy-	C6	118	18.57
Butane, 1,1-diethoxy-	C8	146	8.90
Ketones			
3-Nonen-2-one	C9	140	3.27
3-Nonen-2-one	C9	140	5.34
3-Decanone	C10	156	1.93
Cycloheptanone, 2-(3-buten-1-yl)-	C11	168	20.85
6-Undecanone	C11	170	14.27
2-Dodecanone	C12	184	6.30
Internal Standard (ISTD)			
n-dodecane	C12	170	7.5

Cellulose depolymerization was carried out following woody biomass depolymerization. Pure cellulose was converted over the same catalyst in supercritical ethanol at 300 °C for 4h and products can be seen in Table 4.13.

Table 4.12: Cellulose and hemicellulose products of SP depolymerization at 300°C for 4h over $Cu_{20}MgAlO_4$ catalyst.

Name of Compound	C Number	Molecular Weight (g/molg)	The Amount (mg)
Alcohols			
2-Penten-1-ol, 2-methyl-	C6	100	47.45
3-Hexen-1-ol	C6	100	21.49
2-Hexen-1-ol, 2-ethyl-	C8	128	28.19
2-Hexen-1-ol, 2-ethyl-	C8	128	13.86
5-Methyl-1-heptanol	C8	130	6.51
1-Octanol	C8	130	56.96
1-Decanol	C10	158	3.38
Aldehydes			
2-Ethyl-2-hexen-1-al	C8	126	23.43
2-Hexenal, 2-ethyl-	C8	126	11.84
2-Ethylhexylaldehyde	C8	128	5.50
Alkenes			
Cyclopentene, 1-methyl-	C6	82	1.09
2-Hexene	C6	84	2.74
2-Hexene	C6	84	1.02
2-Hexene	C6	84	3.42
Esters			
Pentanoic acid, ethyl ester	C7	130	12.13
Pentanoic acid, 3-methyl-, ethyl ester	C8	144	3.63
3-Octenoic acid, ethyl ester	C10	170	4.41
Hexanoic acid, butyl ester	C10	172	24.70
Hexanoic acid, butyl ester	C10	172	29.57
Caprylic acid n-butyl ester	C12	200	8.90
Decanoic acid, ethyl ester	C12	200	5.61
Ketones			
Cycloheptanone, 2-ethyl-	C9	140	25.84
Cycloheptanone, 2-ethyl-	C9	140	13.69
Cycloheptanone, 2-ethyl-	C9	140	7.67

Compared to the catalytic SP depolymerization at the same temperature, cellulose depolymerization is to produce much more alcohols. Alcohols and esters are the dominant products in the liquid phase formed at the end of depolymerization. Most of the alcohol, ester and ketone products obtained as a result of catalytic cellulose and SP depolymerization were similar, however quite different aldehyde and alkene products are also generated by catalytic cellulose depolymerization.

Depolymerization of glucose as a model compound of cellulose over $Cu_{20}MgAlO_4$ catalyst formed similar products, shown in Table 4.14. In case of catalytic cellulose depolymerization, alcohols and esters are dominated the product distribution.

Table 4.13: Cellulose products of cellulose depolymerization at 300°C for 4h over $Cu_{20}MgAlO_4$.

Name of Compound	C Number	Molecular Weight (g/molg)	The Amount (mg)
Alcohols			
2-Buten-1-ol	C4	72	49.41
4-Penten-1-ol, 3-methyl-	C6	98	27.25
Cyclobutanemethanol	C6	100	2.43
1,5-Hexanediol	C6	118	1.78
2-Hexen-1-ol, 2-ethyl	C8	128	3.36
2-Hexen-1-ol, 2-ethyl	C8	128	10.07
3-Octen-1-ol	C8	128	2.13
1-Heptanol, 6-methyl-	C8	130	2.68
3-Hexanol, 4-ethyl-	C8	130	2.28
1-Hexanol, 2-ethyl-	C8	130	25.51
5-Methyl-1-heptanol	C8	130	5.69
2-Heptanol, 5-ethyl-	C9	144	2.74
1-Nonanol	C9	144	10.63
1-Decanol	C10	158	3.08
1-Decanol	C10	158	10.49
4-Decanol	C10	158	2.38
2,3a-Dimethylhexahydrobenzofuran-7a-ol	C10	170	4.40
1-Undecanol	C11	172	3.07
6-Dodecanol	C12	186	7.76
1-Tetradecanol	C14	214	2.09
2-Ethyl-1-dodecanol	C14	214	6.71
Aldehydes			
2-Butenal	C4	70	13.70
Hexanal	C6	100	41.29
2-Butenal, 2-ethyl	C6	98	42.76
2-Butenal, 2-ethyl	C6	98	4.29
2-Hexenal, 2-ethyl	C8	126	13.22
2-Hexenal, 2-ethyl	C8	126	21.59
Hexenal, 2-ethyl	C8	128	7.37
Octanal	C8	128	8.28
2-Heptenal, 2-propyl-	C10	154	3.65
Alkenes			
4-Decene	C10	140	16.63
4-Dodecene	C12	168	0.38
5-Tetradecene	C14	196	3.05
Esters			
Butanoic acid, ethyl ester	C7	130	6.57
Pentanoic acid, ethyl ester	C7	130	3.36
3-Hexenoic acid, ethyl ester	C8	142	14.19
Acetic acid, octyl ester	C10	172	6.68
Ethyl (E)-2-octenoate	C10	170	4.74
Hexanoic acid, butyl ester	C10	172	7.82
Hexanoic acid, butyl ester	C10	172	28.99
Octanoic acid, ethyl ester	C10	172	29.19
3-Octenoic acid, ethyl ester	C10	170	4.40
3-Octenoic acid ethyl ester	C10	170	5.32
2-Propenoic acid, octyl ester	C11	184	8.79
Decanoic acid, ethyl ester	C12	200	7.03
Butyl caprylate	C12	200	7.35
Ketones			
Cycloheptanone, 2-ethyl-	C9	140	10.51
Cycloheptanone, 2-butyl-	C11	168	4.78
Cycloheptanone, 2-butyl-	C11	168	3.53

Most of the alcohols, aldehydes and esters detected in the liquid phase overlapped with the ones obtained by catalytic cellulose depolymerization at the same temperature.

Table 4.14: Glucose products of glucose depolymerization at 300°C for 4h over $Cu_{20}MgAlO_4$.

Name of Compound	C Number	Molecular Weight (g/molg)	The Amount (mg)
Alcohols			
2-Buten-1-ol	C4	72	62.44
1-Penten-3-ol, 2-methyl-	C6	100	34.72
1-Penten-3-ol, 2-methyl-	C6	100	22.44
3-Hexen-1-ol	C6	100	30.76
2-Heptanol	C7	116	20.80
2-Heptanol	C7	116	4.90
2-Hexen-1-ol, 2-ethyl-	C8	128	6.54
3-Octen-1-ol	C8	128	2.59
1-Heptanol, 6-methyl-	C8	130	1.33
2-Hexanol, 3,4,-dimethyl-	C8	130	2.22
3-Hexanol, 4,4-dimethyl-	C8	130	5.77
1-Hexanol, 2-ethyl-	C8	130	25.57
5-Methyl-1-heptanol	C8	130	5.82
1-Decanol	C10	158	12.47
4-Decanol	C10	158	2.63
3-Octenoic acid, ethyl ester	C10	170	9.37
6-Dodecanol	C12	186	8.41
2-Ethyl-1-dodecanol	C14	214	6.40
Aldehydes			
Hexanal	C6	100	31.13
2-Butenal, 2-ethyl	C6	98	37.51
2-Hexenal, 2-ethyl	C8	126	8.30
2-Hexenal, 2-ethyl	C8	126	12.11
Hexenal, 2-ethyl	C8	128	4.19
Octanal	C8	128	4.00
2-Heptenal, 2-propyl-	C10	154	2.53
2-Octenal, 2-butyl-	C12	182	2.52
Alkenes			
4-Decene	C10	140	9.19
Esters			
Butanoic acid, ethyl ester	C7	130	4.40
Pentanoic acid, ethyl ester	C7	130	4.76
2-Hexenoic acid, ethyl ester	C8	142	31.93
Acetic acid, octyl ester	C10	172	5.58
Ethyl (E)-2-octenoate	C10	170	8.35
Hexanoic acid, butyl ester	C10	172	7.06
Hexanoic acid, butyl ester	C10	172	22.94
Octanoic acid, ethyl ester	C10	172	23.30
Carbonic acid, butyl 2-pentyl ester	C10	188	3.00
Decanoic acid, ethyl ester	C12	200	3.99
Butyl caprylate	C12	200	5.25
Ketones			
4-Undecanone	C11	170	5.13
Ethers			
Ethane, 1,1-diethoxy-	C6	118	49.90
Butane, 1,1-diethoxy-	C8	146	5.88

Moreover, lignin products of woody biomass depolymerization were characterized to obtain monomeric product distribution (Figure 4.14.). These main groups of compounds were in agreement with the products resulted from lignin depolymerization in supercritical ethanol. As it is in the case of lignin, monomers identified by GC-MS can basically be classified as hydrogenated cyclics (-O and +O) and aromatics (-O and +O). Interestingly, oxygenated aromatics constitute the majority of products obtained by catalytic SP depolymerization, indicating considerably low deoxygenation activity. Guaiacol-type molecules were found to be predominant among the monomers.

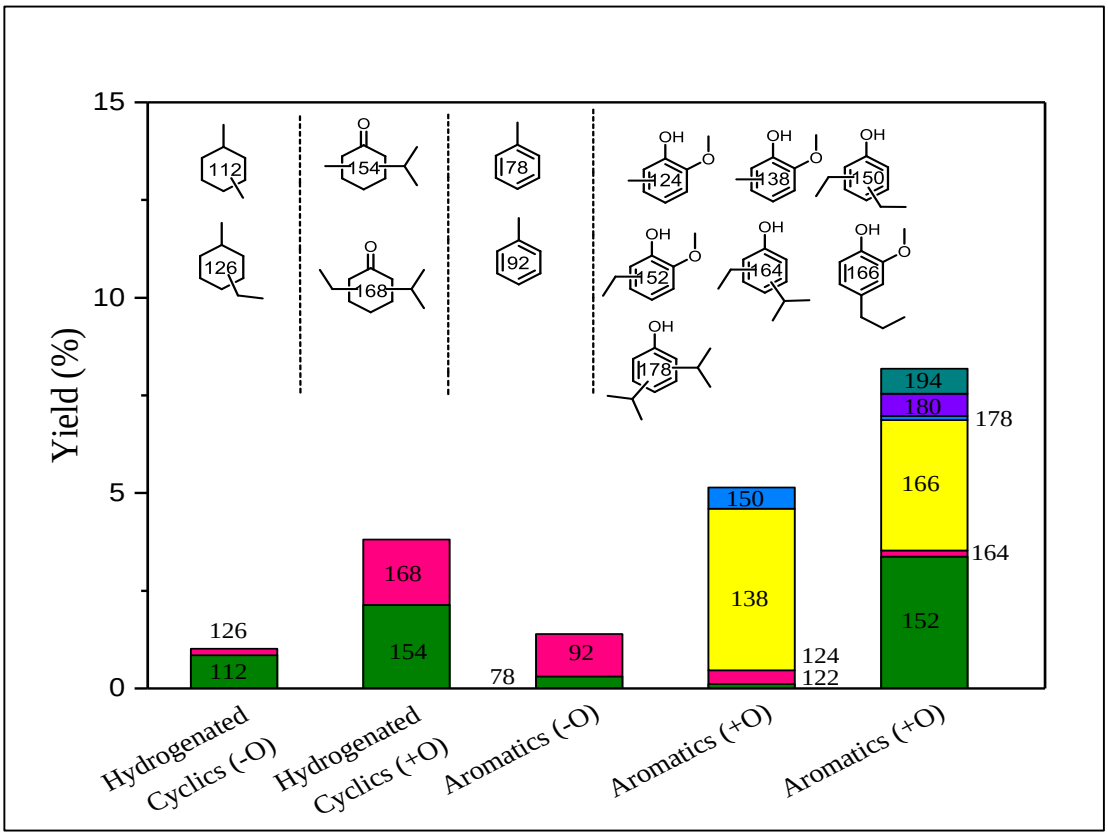

Figure 4.14: Monomeric product distribution following SP reaction at 340 °C for 4h using $Cu_{20}MgAlO_2$ catalyst.

Figure 4.15 shows the FT-IR spectra demonstrates that untreated SP sample, Protobind 1000 lignin sample and THF-soluble SPRs have different characteristics. However, there are some similar bands can be observed. For example; at wave numbers higher than 2500 cm^{-1} SP and Protobind 1000 lignin spectra present similarities.

The strong and broad peak clearly seen around 3300-3400 cm^{-1} for both SP and lignin sample proves the presence of O–H groups in structures [128].

Table 4.15: The samples analyzed by FT-IR.

Entry	Samples	Reaction Conditions	
1	SP	-	-
2	Protobind 1000 Lignin	340	1g
3	THF-Soluble SPR	340	1g
4	THF-Soluble SPR	340	3g

As a woody biomass sample, SP reveals cellulose and hemicellulose characteristics. The appearance of the peaks at 896, 1025, and 1450 cm^{-1} were attributed to the absorbances of cellulose, where the peaks observed at 1423, 1610, and 1725 cm^{-1} were attributed to the stretching of hemicellulose [129]. Also signals detected at about 2800-3000 cm^{-1} can be interpreted as the stretching of $–CH_3$ and $–CH_2$ groups for THF-soluble SPRs [129].

Spectra given as black provides further interpretation of pure lignin structure. One can easily distinguish the peaks below 3000 cm^{-1} in case of lignin, the absorption at 2920 cm^{-1} indicates C–H stretching of alkane groups. The sharp peak at 2162 cm^{-1} is assigned to –C=C– stretching of alkynes. Similarly, the broad peaks belong to THF-soluble lignin residue samples have the same characteristic. C=O stretching is determined interpreting the peak at around 1700 cm^{-1} [130].

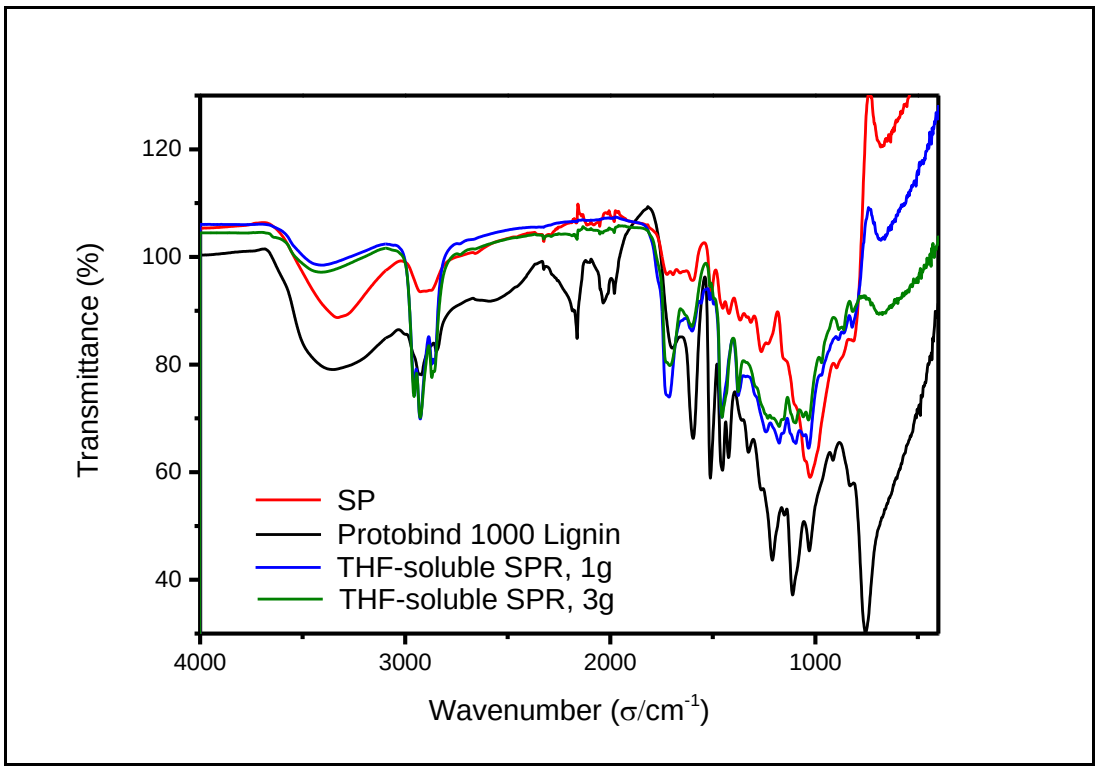

Figure 4.15: FT-IR spectra of the samples given in Table 4.15.

Peak at 1452 cm^{-1} can be attributed to C–H deformations and aromatic ring vibrations whereas peak at 1512 cm^{-1} indicates aromatic skeleton vibrations. Based on the literature, peak at 1030 cm^{-1} represents C–H in-plane deformations in guaiacyl type of lignin and peak around 1111 cm^{-1} indicates the same deformations in syringyl type of lignin [130].

SEM images of untreated SP, char and the mixture of catalyst and char obtained as a result of the SP depolymerization at 340 °C and the image of the untreated Protobind 1000 lignin previously utilized in all reactions mentioned in Catalytic lignin depolymerization Section are shown in Figure 4.16. As it is mentioned before, the mixture of catalyst and char is obtained from catalytic depolymerization medium together. Each sample has distinctive characteristic appearance. In Figure 4.16a irregular spatial structure of SP may be attributed to the various linkages between carbohydrates and lignin [131]. Figure 4.16b shows the char remained at the bottom of the autoclave and seperated from all other products and catalyst. Catalyst particles clustered over the char particles are easily distinguished in Figure 14c. Also Protobind 1000 lignin can be seen in Figure 14d.

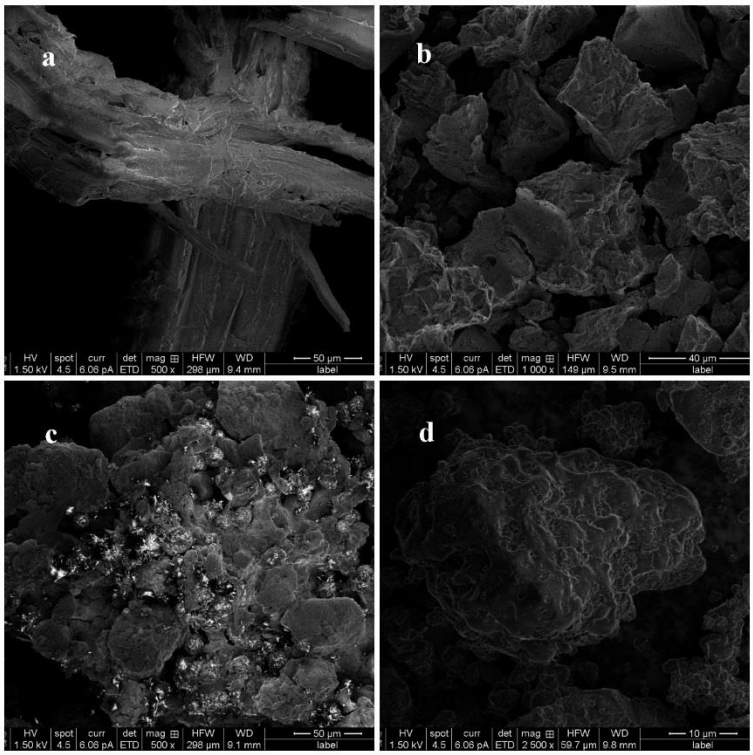

Figure 4.16: SEM images of different samples: [a] Untreated SP, [b] char obtained by the SP depolymerization at 340 °C, [c] catalyst and char obtained by the SP depolymerization at 340 °C and [d] Untreated Protobind 1000 lignin.

5. CONCLUSIONS

In this study, catalytic depolymerization of Protobind 1000 lignin and Scotch Pine in supercritical ethanol have been accomplished. Turkish-origin SP utilized in this study was collected from the vicinity of Bursa. The elemental analysis results showed that SP contains:

- Moisture :9.13 wt%
- Fixed carbon :15.29 wt%
- Volatile matter :74.9 wt%
- Ash :0.69 wt%.

The empirical formula of SP was calculated as $CH_{1.67}O_{0.69}N_{0.005}$ based on ultimate analysis. In addition lignocellulosic composition was mainly comprised of 66.13 wt% holocellulose and 24.67 wt% lignin.

Various $CuMgAlO_x$ catalysts are tested for lignin depolymerization in supercritical ethanol at 340 °C in order to examine the effects of Cu content and (Cu+Mg)/Al ratio of the catalyst on depolymerization. Results revealed that:

- Increasing the Cu loading of the catalyst up to 20 wt% (<20 wt%) ensured less repolymerization during catalytic depolymerization and generated more monomers, more THF-soluble lignin residue (low molecular weight residue) and less THF-insoluble lignin residue (high molecular weight residue).
- Increasing (Cu+Mg)/Al ratio of the catalyst up to four reduced repolymerization and generated more monomers, more THF-soluble lignin residue and less THF-insoluble lignin residue.
- The best catalyst facilitating lignin depolymerization at 340 °C was $Cu_{20}MgAlO_4$ among all other catalysts. $Cu_{20}MgAlO_4$ showed highest monomer yield indicating highest depolymerization and lowest repolymerization and provided more deoxygenation.
- More basic sites and basic sites density were obtained by the Cu loading (<20 wt%), and (Cu+Mg)/Al ratio (<4) while the strength of basic sites dimished.

- Both the presence of Cu on the catalysts and an optimum distribution of basic and acidic sites on the catalysts were found essential for catalytic depolymerization of lignin. Neither CuO/MgO nor $Cu_{20}/\gamma\text{-}Al_2O_3$ achieved high monomer yields.
- Catalytic lignin depolymerization generated a wide range of products such as alcohols, esters, aldehydes etc. Aromatics were the main product.
- Monomer yield found in line with dehydrogenation ability of the catalysts. In addition, basic sites were more active for dehydrogenation and Guerbet reaction.
- The yield of THF-soluble residue and mass balance increased with increasing Cu loading. This indicates that reactions (alkylation and esterification) between ethanol and lignin were enhanced due to the Cu content.
- In all cases except $Cu_{20}/\gamma\text{-}Al_2O_3$ resulted in 23 wt% char, char formation remained below 1 wt% which was desired for a successful lignin conversion into gas and liquid products.

Catalytic depolymerization of Scotch Pine was carried out over $Cu_{20}MgAlO_4$ catalyst at 300 °C and 340 °C. As a result of the study, a wide range of products are obtained from Scotch Pine depolymerization in supercritical ethanol.

- Scotch Pine was depolymerized into seven different product groups, namely alcohols, aldehydes, alkanes, alkenes, esters, ethers and ketones which comprise almost fifty different products. Aliphatic and aromatic hydrocarbons were detected ranging from C_5 to C_{17}, where alcohols and esters constitute the majority of the monomers identified.
- Oxygenated aromatics outnumbered deoxygenated aromatics and hydrogenated cyclics obtained by catalytic SP depolymerization, indicating considerably low deoxygenation activity. Guaiacol-type molecules were found to be predominant among the monomers.
- Highest conversion (50 wt%) was achieved at 340 °C with 1000 mg feed of SP. 50 wt% of monomer yield was mainly obtained by the monomeric products arised from hemicellulose and cellulose in the woody biomass structure. In this case, the share of monomeric products of lignin were relatively low.

- Catalytic depolymerization performed at 300 °C decreased the monomer yield by half compared to the depolymerization at 340 °C and caused 12 wt% char formation, which is not desired for an efficient depolymerization.
- Increasing the amount of SP fed to the autoclave (3000 mg) dramatically decreased the monomer yield, therefore the same amount of catalyst (500 mg) found insufficient to depolymerize the excess amount of SP.

Moreover, catalytic depolymerization of cellulose as a model compound of lignocellulosic biomass and of glucose as a model compound of cellulose were performed at 300 °C. Catalytic cellulose depolymerization led to 52 wt% monomer yield whereas catalytic glucose depolymerization resulted in 57 wt% monomer yield. Most of the alcohol, ester and ketone products obtained as a result of catalytic cellulose, glucose and SP depolymerization were similar. For all feedstocks, alcohols and esters dominated the product distribution. As it is anticipated, catalytic depolymerization of model compounds (cellulose and glucose) ensured more monomer yield in comparison with the catalytic depolymerization of the same amount of SP at the same operating conditions. This result was mainly due to the complex structure of woody biomass embodying different components within itself.

Aforementioned products are significant candidates of biochemicals and/or biofuels. These products are suitable to be further fractionated or converted to variety of bulk chemicals, to be involved in other chemicals processes or to be used as fuel additives. All these routes of valorization are quite inspiring for future technologies taking the advantage of lignocellulosic biomass as a readily available and abundant source. Lignocellulosic biomass is an indispensible feedstock for biorefineries, which are the key pathways for future bio-based economy. Simultaneous, direct and one-step valorization of cellulose, hemicellulose and lignin can be the driving force needed for future biorefineries. Also one-step catalytic depolymerization of lignocellulosic biomass can eliminate the problems regarding pretreatments commonly applied before the conversion and reduce the operational costs, if it is integrated to the existing processes in biorefineries. Also lignin valorization by means of catalytic depolymerization will add value to the existing biorefineries produce lignin as a by-product. Numerous value-added products such as aromatics can be obtained by catalytic lignin depolymerization. Especially, liquid phase products of catalytic depolymerization is very promising for further transformation. Through the

optimization of reaction conditions, the organic liquid fraction obtained from lignin can be tailored in the direction of the production of qualified liquids available as blending components of fuels or fine chemicals [81]. Based on the fact that the biofuels, biochemicals and biomaterials are indispensable in order to preserve the remaining life quality all around the world, this study gives a promising aspect for their production in alternative way. I believe that the results in this study will be helpful for developing effective methods for lignocellulosic biomass and lignin valorization.

REFERENCES

[1] **Cleveland, C.J. and C. Morris,** *Introduction*, in *Handbook of Energy*, C.J.C. Morris, Editor. 2014, Elsevier: Boston. p. 1-2.

[2] **IEA**, *Renewables Information IEA Statistics*. 2012.

[3] **WBA.** *WBA Global Bioenergy Statistics 2014*. 04.07.2014]; Available from: http://www.worldbioenergy.org/userfiles/140526%20-%20WBA%20GBS%202014.pdf.

[4] **IPCC**. *Climate Change 2013*. 21.06.2014]; Available from: http://www.climatechange2013.org/report.

[5] **Luque, R.**, *Catalytic chemical processes for biomass conversion: Prospects for future biorefineries.* Pure and Applied Chemistry, 2014. **86**(5).

[6] **Doherty, W.O.S., P. Mousavioun, and C.M. Fellows**, *Value-adding to cellulosic ethanol: Lignin polymers.* Industrial Crops and Products, 2011. **33**(2): p. 259-276.

[7] **Karytsas, S. and H. Theodoropoulou**, *Socioeconomic and demographic factors that influence publics' awareness on the different forms of renewable energy sources.* Renewable Energy, 2014. **71**(0): p. 480-485.

[8] **Dincer, I.**, *Renewable energy and sustainable development: a crucial review.* Renewable and Sustainable Energy Reviews, 2000. **4**(2): p. 157-175.

[9] **REN21**, *Renewables 2014 Global Status Report*. 2014.

[10] **IEA**, *World Energy Outlook 2013*. 2013.

[11] **WEC**, *World Energy Resources: A Summary*. 2013, World Energy Council.

[12] **Menon, V. and M. Rao**, *Trends in bioconversion of lignocellulose: Biofuels, platform chemicals & biorefinery concept.* Progress in Energy and Combustion Science, 2012. **38**(4): p. 522-550.

[13] **Kamm, B. and M. Kamm**, *Principles of biorefineries.* Applied Microbiology and Biotechnology, 2004. **64**(2): p. 137-145.

[14] **FitzPatrick, M., et al.**, *A biorefinery processing perspective: treatment of lignocellulosic materials for the production of value-added products.* Bioresour Technol, 2010. **101**(23): p. 8915-22.

[**15]** **Liu, S., et al**., *A sustainable woody biomass biorefinery.* Biotechnol Adv, 2012. **30**(4): p. 785-810.

[16] **Chatel, G. and R.D. Rogers**, *Review: Oxidation of Lignin Using Ionic Liquids—An Innovative Strategy To Produce Renewable Chemicals.* ACS Sustainable Chemistry & Engineering, 2014. **2**(3): p. 322-339.

[17] **Cotana, F., et al.**, *Lignin as Co-product of Second Generation Bioethanol Production from Ligno-cellulosic Biomass.* Energy Procedia, 2014. **45**(0): p. 52-60.

[18] **Vishtal, A.G. and A. Kraslawski**, *CHALLENGES IN INDUSTRIAL APPLICATIONS OF TECHNICAL LIGNINS*. 2011. Vol. 6. 2011.

[19] **Kajaste, R.**, *Chemicals from biomass – managing greenhouse gas emissions in biorefinery production chains – a review.* Journal of Cleaner Production, 2014. **75**(0): p. 1-10.

[20] **Fellows, C., T. Brown, and W. Doherty**, *Lignocellulosics as a renewable feedstock for chemical industry: Chemicals from lignin*, in *Green*

Chemistry for Environmental Remediation, R. Sanghi and V. Singh, Editors. 2012, Scrivener Publishing / John Wiley and Sons: United States of America. p. 561-610.

[21] **Bioenergy, I.**, *Bio-Based Chemicals: Value-Added Products from Biorefineries*. 2013.

[22] **Barta, K. and P.C. Ford,** *Catalytic conversion of nonfood woody biomass solids to organic liquids.* Acc Chem Res, 2014. **47**(5): p. 1503-12.

[23] **Huijgen, W.J.J., et al**., *Characteristics of wheat straw lignins from ethanol-based organosolv treatment.* Industrial Crops and Products, 2014. **59**: p. 85-95.

[24] **Boyle, G.**, ed. *Renewable Energy*. 2004, Oxford University Press & The Open University.

[25] **Basu, P.**, *Chapter 1 - Introduction*, in *Biomass Gasification, Pyrolysis and Torrefaction (Second Edition)*, P. Basu, Editor. 2013, Academic Press: Boston. p. 1-27.

[26] *Sources of Biomass*. 2011 25.06.2014]; Available from: http://www.biomassenergycentre.org.uk/portal/page?_pageid=75,15174&_dad=portal&_schema=PORTAL.

[27] **İşler, A. and F. Karaosmanoğlu**, *Biofuels in Turkey*, in *Rethinking Structural Reform in Turkish Agriculture: Beyond the World Bank's Strategy*, B. Karapınar, F. Adaman, and G. Özertan, Editors. 2010, Nova Science Publisher.

[28] **IEA**, *Technology Roadmap: Bioenergy for Heat and Power*. 2012.

[29] **IRENA**, *Statistical issues: bioenergy and distributed renewable energy.* 2013.

[30] **Erdogdu, E.,** *An Expose of Bioenergy and its Potential and Utilization in Turkey*. Vol. 36. 2008: Energy Policy. 2182-2190.

[31] **Saracoglu, N.**, *The Biomass Potential of Turkey for Energy Production: Part I.* Energy Sources, Part B: Economics, Planning, and Policy, 2010. **5**(3): p. 272-278.

[32] **Bilgen, S., et al.,** *Global warming and renewable energy sources for sustainable development: A case study in Turkey.* Renewable and Sustainable Energy Reviews, 2008. **12**(2): p. 372-396.

[33] **Toklu, E.**, *Overview of potential and utilization of renewable energy sources in Turkey.* Renewable Energy, 2013. **50**(0): p. 456-463.

[34] **UNDP**. 15.07.14]; Available from: http://www.tr.undp.org/content/dam/turkey/docs/Publications/EnvSust/Turkey.

[35] **TurkStat**, *Greenhouse gas inventory report 1990-2011, annual report submission under the "framework convention on climate change".* 2011.

[36] **Rosillo-Calle, F., et al.**, *Biomass Assessment Handbook: bioenergy for sustainable development*. 2006: Earthscan.

[37] **WGBN**. 28.06.2014]; Available from: http://www.wgbn.wisc.edu/key-concepts/grassland-biomass-sources/sources-biomass.

[38] **Mascia, P.N., J. Scheffran, and J.M. Widholm**, *Plant Biotechnology for Sustainable Production of Energy and Co-products*. Biotechnology in Agriculture and Forestry. Vol. 66. 2010, Heidelberg: Springer.

[39] *Biobased Industrial Products: Research and Commercialization Priorities*. 2000, Washington, DC: The National Academies Press. 162.

[40] **Donald, D.,** *Overview*, in *Lignin and Lignans*. 2010, CRC Press. p. 1-10.

[41] **Menon, V. and M. Rao**, *Recent Trends in Valorization of Lignocellulose to*

Biofuel. 2012: p. 381-409.

[42] **Bracmort, K.** *Biomass: Comparison of Definitions in Legislation Through the 112th Congress*. 2012 18.06.2014]; Available from: www.fas.org.

[43] **Wu, A., et al.**, *Breakdown of lignins, lignin model compounds, and hydroxy-aromatics, to C1 and C2 chemicals via metal-free oxidation with peroxide or persulfate under mild conditions.* RSC Advances, 2014. **4**(34): p. 17931.

[44] *Hemicelluloses and Lignin, Other Key Constituents of Biomass*, in *Lignocellulosic Biorefineries*. 2013, EFPL Press. p. 239-297.

[45] **Bajpai, P**., *Overview of Pulp and Papermaking Processes*, in *Environmentally Friendly Production of Pulp and Paper*. 2010, John Wiley & Sons, Inc. p. 8-45.

[46] **Hood, E.E., P. Nelson, and R. Powell**, *Plant Biomass Conversion*. 2011, West Sussex: John Wiley & Sons.

[47] **Aracri, E., C. Diaz Blanco, and T. Tzanov**, *An enzymatic approach to develop a lignin-based adhesive for wool floor coverings.* Green Chemistry, 2014. **16**(5): p. 2597-2603.

[48] **Sixta, H.,** *Introduction*, in *Handbook of Pulp*. 2008, Wiley-VCH Verlag GmbH. p. 2-19.

[49] **Lora, J.H.** *GreenValue*. 23.04.15]; Available from: http://www.bio-based.eu/iBIB/pdf/47.pdf.

[50] **Joffres, B., et al.,** *Catalytic hydroconversion of a wheat straw soda lignin: Characterization of the products and the lignin residue.* Applied Catalysis B: Environmental, 2014. **145**(0): p. 167-176.

[51] **BMELV**, *Biorefineries Roadmap*. 2012: Berlin.

[52] **Werpy, T.A., J.E. Holladay, and J.F. White**, *Top Value chemicals from biomass:*
1. Results of Screening for Potential Candidates from Sugars and Synthesis Gas. 2004.

[53] **Service,** U.F. *Woody Biomass Utilization*. 2008 18.06.14]; Available from: http://www.fs.fed.us/woodybiomass/whatis.shtml.

[54] **Kamm, B., P.R. Gruber, and M. Kamm,** *Biorefineries – Industrial Processes and Products*, in *Ullmann's Encyclopedia of Industrial Chemistry*. 2000, Wiley-VCH Verlag GmbH & Co. KGaA.

[55] **Kamm, B., M. Gerhardt, and Lei,** *Chapter 3 The Biorefinery Concept - Thermochemical Production of Building Blocks and Syngas*, in *Thermochemical Conversion of Biomass to Liquid Fuels and Chemicals*. 2010, The Royal Society of Chemistry. p. 46-66.

[56] **Apprich, S., et al.**, *Wheat bran-based biorefinery 2: Valorization of products.* LWT - Food Science and Technology, 2014. **56**(2): p. 222-231.

[57] **Hongbin, C. and W. Lei,** *Lignocelluloses Feedstock Biorefinery as Petrorefinery Substitutes*. Biomass Now - Sustainable Growth and Use. 2013.

[58] **Villegas, J.D. and E. Gnansounou,** *Techno-economic and environmental evalution of lignocellulosic biochemical refineries: need for a modular platform for integrated assessment (MPIA).* Journal of Scientific & Industrial Research, 2008. **67**: p. 927-940.

[59] **Bu, Q., et al.,** *Bio-based phenols and fuel production from catalytic microwave pyrolysis of lignin by activated carbons.* Bioresour Technol, 2014. **162**: p. 142-7.

[60] **Garver, M.P. and S. Liu,** *Chapter 27 - Development of Thermochemical and Biochemical Technologies for Biorefineries*, in *Bioenergy Research: Advances and Applications*, V.K. Gupta, M.G.T.P. Kubicek, and J.S. Xu, Editors. 2014, Elsevier: Amsterdam. p. 457-488.

[61] **Scott, F., et al.,** *Process design and sustainability in the production of bioethanol from lignocellulosic materials.* Electronic Journal of Biotechnology, 2013. **16**: p. 13-13.

[62] **Linger, J.G., et al.,** *Lignin valorization through integrated biological funneling and chemical catalysis.* Proceedings of the National Academy of Sciences, 2014. **111**(33): p. 12013-12018.

[63] **Ragauskas, A.J., et al.,** *Lignin valorization: improving lignin processing in the biorefinery.* Science, 2014. **344**(6185): p. 1246843.

[64] **Yuan, T.-Q., F. Xu, and R.-C. Sun**, *Role of lignin in a biorefinery: separation characterization and valorization.* Journal of Chemical Technology & Biotechnology, 2013. **88**(3): p. 346-352.

[65] **Pandey, M.P. and C.S. Kim,** *Lignin Depolymerization and Conversion: A Review of Thermochemical Methods.* Chemical Engineering & Technology, 2011. **34**(1): p. 29-41.

[66] **Yuan, T.Q., et al.,** *Synergistic benefits of ionic liquid and alkaline pretreatments of poplar wood. Part 2: characterization of lignin and hemicelluloses.* Bioresour Technol, 2013. **136**: p. 345-50.

[67] **Jongerius, A.L., P.C.A.** Bruijnincx, and B.M. Weckhuysen, *Liquid-phase reforming and hydrodeoxygenation as a two-step route to aromatics from lignin.* Green Chemistry, 2013. **15**(11): p. 3049-3056.

[68] **Wang, H., M. Tucker, and Y. Ji,** *Recent Development in Chemical Depolymerization of Lignin: A Review.* Journal of Applied Chemistry, **2013. 2013: p. 9.**

[69] **Basu, P.,** *Chapter 7 - Gasification Theory*, in *Biomass Gasification, Pyrolysis and Torrefaction (Second Edition)*, P. Basu, Editor. 2013, Academic Press: Boston. p. 199-248.

[70] **Zakzeski, J., et al.**, *The catalytic valorization of lignin for the production of renewable chemicals.* Chem Rev, 2010. **110**(6): p. 3552-99.

[71] **Gosselink, R.J.A.,** *Lignin as a renewable aromatic resource for the chemical industry*, in 2011, Wageningen University: Wageningen.

[72] **Ma, L., et al.,** *A review of thermal–chemical conversion of lignocellulosic biomass in China.* Biotechnology Advances, 2012. **30**(4): p. 859-873.

[73] **Basu, P.,** *Chapter 5 - Pyrolysis*, in *Biomass Gasification, Pyrolysis and Torrefaction (Second Edition)*, P. Basu, Editor. 2013, Academic Press: Boston. p. 147-176.

[74] **Werhan, H.,** *A process for the complete valorization of lignin into aromatic chemicals based on acidic oxidation*. 2013, ETH Zurich: Zurich.

[75] **Basu, P.,** *Chapter 9 - Hydrothermal Gasification of Biomass*, in *Biomass Gasification, Pyrolysis and Torrefaction (Second Edition)*, P. Basu, Editor. 2013, Academic Press: Boston. p. 315-352.

[76] **Joffres, B., et al.,** *Thermochemical Conversion of Lignin for Fuels and Chemicals: A Review.* Oil Gas Sci. Technol. – Rev. IFP Energies nouvelles, 2013. **68**(4): p. 753-763.

[77] **Cao, J., et al.,** *Study on carbonization of lignin by TG-FTIR and high-temperature carbonization reactor*. Fuel Processing Technology, 2013. **106**(0): p. 41-47.

[78] **Warner, G., et al.,** *Depolymerization of organosolv lignin using doped porous metal oxides in supercritical methanol.* Bioresour Technol, 2014. **161**: p. 78-83.

[79] **Kim, J.Y., et al.,** *Effects of various reaction parameters on solvolytical depolymerization of lignin in sub- and supercritical ethanol.* Chemosphere, 2013. **93**(9): p. 1755-64.

[80] **Holmelid, B., M. Kleinert, and T. Barth**, *Reactivity and reaction pathways in thermochemical treatment of selected lignin-like model compounds under hydrogen rich conditions.* Journal of Analytical and Applied Pyrolysis, 2012. **98**(0): p. 37-44.

[81] **Kleinert, M., J.R. Gasson, and T. Barth**, *Optimizing solvolysis conditions for integrated depolymerisation and hydrodeoxygenation of lignin to produce liquid biofuel.* Journal of Analytical and Applied Pyrolysis, 2009. **85**(1–2): p. 108-117.

[82] **Barta, K., et al.,** *Catalytic disassembly of an organosolv lignin via hydrogen transfer from supercritical methanol.* Green Chemistry, 2010. **12**(9): p. 1640-1647.

[83] **Effendi, A., H. Gerhauser, and A.V. Bridgwater,** *Production of renewable phenolic resins by thermochemical conversion of biomass: A review.* Renewable and Sustainable Energy Reviews, 2008. **12**(8): p. 2092-2116.

[84] **Beauchet, R., F. Monteil-Rivera, and J.M. Lavoie**, *Conversion of lignin to aromatic-based chemicals (L-chems) and biofuels (L-fuels).* Bioresour Technol, 2012. **121**: p. 328-34.

[85] **Wang, H., M. Tucker, and Y. Ji,** *Recent Development in Chemical Depolymerization of Lignin: A Review.* Journal of Applied Chemistry, 2013: p. 1-9.

[86] **Song, Q., et al.,** *Lignin depolymerization (LDP) in alcohol over nickel-based catalysts via a fragmentation–hydrogenolysis process.* Energy & Environmental Science, 2013. **6**(3): p. 994.

[87] **Güvenatam, B., et al.,** *Hydrodeoxygenation of mono- and dimeric lignin model compounds on noble metal catalysts.* Catalysis Today, 2014. **233**(0): p. 83-91.

[88] **Eriksson, K.E.L. and H. Bermek**, *Lignin, Lignocellulose, Ligninase*, in *Encyclopedia of Microbiology (Third Edition)*, M. Schaechter, Editor. 2009, Academic Press: Oxford. p. 373-384.

[89] **Latif, H., et al.,** *Trash to treasure: production of biofuels and commodity chemicals via syngas fermenting microorganisms.* Current Opinion in Biotechnology, 2014. **27**(0): p. 79-87.

[90] **Tuomela, M., et al.**, *Biodegradation of lignin in a compost environment: a review.* Bioresource Technology, 2000. **72**(2): p. 169-183.

[91] **Bugg, T.D., et al.,** *The emerging role for bacteria in lignin degradation and bio-product formation.* Curr Opin Biotechnol, 2011. **22**(3): p. 394-400.

[92] *Pines*, in *Forest Trees of Maine*. Maine Forest Service.

[93] **England, F.C.**, *Scots pine- pinus sylvestris*.

[94] *Scotch Pine*. 28.04.2015]; Available from: http://www.borealforest.org /world/trees/scotch_pine.htm.

[95] **Service**, U.F. *Scotch Pine*. 28.04.2015]; Available from: http://www.na.fs.fed. us/pubs/silvics_manual/Volume_1/pinus/sylvestris.htm.

[96] *Trees for Life*. 28.08.14]; Available from:

http://www.treesforlife.org.uk/tfl.scpine.html.
[97] **OGM**, *Forest Atlas*. 2013.
[98] **OGM**, *Forests of Turkey.* 2012.
[99] **Zhou,** C.H., et al., *Catalytic conversion of lignocellulosic biomass to fine chemicals and fuels.* Chem Soc Rev, 2011. **40**(11): p. 5588-617.
[100] **Stöcker, M.**, *Biofuels and Biomass-To-Liquid Fuels in the Biorefinery: Catalytic Conversion of Lignocellulosic Biomass using Porous Materials.* Angewandte Chemie International Edition, 2008. **47**(48): p. 9200-9211.
[101] **Lin, Y.-C. and G.W. Huber,** *The critical role of heterogeneous catalysis in lignocellulosic biomass conversion.* Energy & Environmental Science, 2009. **2**(1): p. 68-80.
[102] **Yin, W., et al.**, *Catalytic upgrading of sugar fractions from pyrolysis oils in supercritical mono-alcohols over Cu doped porous metal oxide.* Applied Catalysis B: Environmental, 2015. **166–167**(0): p. 56-65.
[103] **Li, R.-d., et al.,** *Liquefaction of rice stalk in sub- and supercritical ethanol.* Journal of Fuel Chemistry and Technology, 2013. **41**(12): p. 1459-1465.
[104] **Brand, S., et al.**, *Supercritical ethanol as an enhanced medium for lignocellulosic biomass liquefaction: Influence of physical process parameters.* Energy, 2013. **59**: p. 173-182.
[105] **Okajima, I. and T. Sako,** *Energy Conversion of Biomass and Recycling of Waste Plastics Using Supercritical Fluid, Subcritical Fluid and High-Pressure Superheated Steam.* 2014: p. 249-267.
[106] **Tang, S.-R., et al.,** *Molecular composition of soluble fraction from depolymerized cornstalk powder in supercritical methanol and ethanol.* Renewable Energy, 2010. **35**(5): p. 946-951.
[107] **Torri, C., et al.,** *Investigation on catalytic pyrolysis of pine sawdust: Catalyst screening by Py-GC-MIP-AED.* Journal of Analytical and Applied Pyrolysis, 2010. **88**(1): p. 7-13.
[108] **Matson, T.D., et al.,** *One-pot catalytic conversion of cellulose and of woody biomass solids to liquid fuels.* J Am Chem Soc, 2011. **133**(35): p. 14090-7.
[109] **Wu, Y., et al.,** *Hydrogenolysis of cellulose to C4-C7 alcohols over bi-functional CuO-MO/Al2O3 (M=Ce, Mg, Mn, Ni, Zn) catalysts coupled with methanol reforming reaction.* Bioresour Technol, 2013. **137**: p. 311-7.
[110] **Huang, X., et al.,** *Catalytic depolymerization of lignin in supercritical ethanol.* ChemSusChem, 2014. **7**(8): p. 2276-88.
[111] **Riittonen, T., et al.,** *One-Pot Liquid-Phase Catalytic Conversion of Ethanol to 1-Butanol over Aluminium Oxide—The Effect of the Active Metal on the Selectivity.* Catalysts, 2012. **2**(1): p. 68-84.
[112] **Ma, R., et al.,** *Catalytic Ethanolysis of Kraft Lignin into High-Value Small-Molecular Chemicals over a Nanostructured α-Molybdenum Carbide Catalyst.* Angewandte Chemie, 2014. **126**(28): p. 7438-7443.
[113] **Dutta, S., K.C.W. Wu, and B. Saha,** *Emerging strategies for breaking the 3D amorphous network of lignin.* Catal. Sci. Technol., 2014. **4**(11): p. 3785-3799.
[114] **Crivello, M., et al.,** *Characterization of AlCu and AlCuMg mixed oxides and their catalytic activity in dehydrogenation of 2-octanol.* Catalysis Today, 2005. **107-108**: p. 215-222.

[115] **Bravo-Suárez, J.J., B. Subramaniam, and R.V. Chaudhari,** *Vapor-phase methanol and ethanol coupling reactions on CuMgAl mixed metal oxides.* Applied Catalysis A: General, 2013. **455**: p. 234-246.

[116] **Marcu, I.-C., et al.,** *Catalytic valorization of bioethanol over Cu-Mg-Al mixed oxide catalysts.* Catalysis Today, 2009. **147**(3-4): p. 231-238.

[117] **Wu, J.-S., et al.,** *Synthesis and structural analysis of a regular Cu-Mg-Al hydrotalcite-like compound.* Turk J Chem, 2011. **35**: p. 881-891.

[118] *Applied Mineralogy*. 17.04.15]; Available from: http://tresen.vscht.cz/min/en/research-team-mineralogy.

[119] **Marcu, I.-C., et al.,** *Catalytic Conversion of Ethanol into Butanol over M–Mg–Al Mixed Oxide Catalysts (M = Pd, Ag, Mn, Fe, Cu, Sm, Yb) Obtained from LDH Precursors.* Catalysis Letters, 2012. **143**(1): p. 23-30.

[120] **Haider, P. and A. Baiker,** *Gold supported on Cu–Mg–Al-mixed oxides: Strong enhancement of activity in aerobic alcohol oxidation by concerted effect of copper and magnesium.* Journal of Catalysis, 2007. **248**(2): p. 175-187.

[121] **Yin, W., et al.,** *Catalytic upgrading of sugar fractions from pyrolysis oils in supercritical mono-alcohols over Cu doped porous metal oxide.* Applied Catalysis B: Environmental, 2015. **166-167**: p. 56-65.

[122] **Jones, W. and e. C. N. R. Rao,** *Supramolecular Organization and Materials Design*. 2001: Cambridge University Press.

[123] **Cavani, F., F. Trifirò, and A. Vaccari,** *Hydrotalcite-type anionic clays: Preparation, properties and applications.* Catalysis Today, 1991. **11**(2): p. 173-301.

[124] **Millange, F., R.I. Walton, and D. O'Hare,** *Time-resolved in situ X-ray diffraction study of the liquid-phase reconstruction of Mg-Al-carbonate hydrotalcite-like compounds.* Journal of Materials Chemistry, 2000. **10**(7): p. 1713-1720.

[125] **Liu, P., M. Derchi, and E.J.M. Hensen,** *Promotional effect of transition metal doping on the basicity and activity of calcined hydrotalcite catalysts for glycerol carbonate synthesis.* Applied Catalysis B: Environmental, 2014. **144**(0): p. 135-143.

[126] **Wise, L.E. and E.C. John,** *Wood Chemistry*. 1952, Reinhould Publishing Corporation: New York. p. 35-43.

[127] **Runkel, R.O. and K.D. Wilke,** *Holz Roh-Werkst*. 1951: Berlin. p. 260-270.

[128] **Karaca, F.,** *Molecular Mass Distribution and Structural Characterization of Liquefaction Products of a Biomass Waste Material.* Energy & Fuels, 2005. **20**(1): p. 383-387.

[129] **Long, J., et al.,** *Simultaneous delignification and selective catalytic transformation of agricultural lignocellulose in cooperative ionic liquid pairs.* Green Chemistry, 2012. **14**(7): p. 1935-1941.

[130] **Wang, K., F. Xu, and R. Sun,** *Molecular Characteristics of Kraft-AQ Pulping Lignin Fractionated by Sequential Organic Solvent Extraction.* International Journal of Molecular Sciences, 2010. **11**(8): p. 2988-3001.

[131] **Tekin, K., S. Karagöz, and S. Bektaş,** *Hydrothermal conversion of woody biomass with disodium octaborate tetrahydrate and boric acid.* Industrial Crops and Products, 2013. **49**(0): p. 334-340.

CURRICULUM VITAE

Name Surname: Ceylanpınar ATAY

Place and Date of Birth: Şanlıurfa, 04/08/1990

Address: Barış Mah. Adaçiftlik Cad. Öncü Apt. No: 30/45, Beylikdüzü, İstanbul-Turkey

E-Mail: atayce@itu.edu.tr; ceylanpinaratay@gmail.com

EDUCATION:

M.Sc.: Istanbul Technical University, Chemical Engineering Department (2015)

B.Sc.: Istanbul Technical University, Chemical Engineering Department (2013)

PROFESSIONAL EXPERIENCE AND REWARDS:

Erasmus Student Exchange Programme - 6 months Abroad Master Thesis Research, University of Eindhoven, Chemistry and Chemical Engineering Department, Molecular Catalysis Group, The Netherland, September 2014- February 2015.

NATIONAL AND INTERNATIONAL MEMBERSHIPS:

- Turkish Association for Energy Economics (TRAEE)
- International Association for Energy Economics (IAEE)
- Sustainable Production & Consumption Association (SPCA)

DUTIES FOR NATIONAL AND INTERNATIONAL ORGANIZATIONS:

- "38th International Association for Energy Economics (IAEE) International Conference: Economic, Environmental, Technological and Security Challenges for Energy", Antalya, May, 25-27, 2015.

  Member of Student Committee

- "II. Carbon Summit: Carbon Management, Technologies & Trade, Istanbul, April, 2-3, 2015.

  Member of Youth Commission

- "İstanbul Electrical & Electronics Waste Summit", Istanbul, March, 5-6, 2015.

  Member of Youth Commission